The role of myocardin-related transcription factors in proliferation and cell cycle regulation of fibroblast cells

Dissertation

zur Erlangung des akademischen Grades

doctor rerum naturalium (Dr. rer.nat.)

vorgelegt der

Naturwissenschaftlichen Fakultät I

- Biowissenschaften -

der Martin-Luther-Universität Halle-Wittenberg

von

Herrn Dmitry Shaposhnikov

geboren am 03.03.1984 in Kaliningrad

Gutachter:

Prof. Dr. Guido Posern

Prof. Dr. Elmar Wahle

Prof. Dr. Gunter Meister

Halle (Saale), April 2013

Max-Planck Institute for Biochemistry

Martin-luther universität halle-wittenberg

Doctoral thesis

The role of myocardin-related transcription factors in proliferation and cell cycle regulation of fibroblast cells

Dmitry Shaposhnikov

April 2013

Tag der mündlichen Prüfung	31.07.2013
Prüfungskommission:	Prof. Dr. Ingo Heilmann (Vorsitzender) Prof. Dr. Elmar Wahle Prof. Dr. Guido Posern Dr. habil. Hauke Lilie Dr. Ralph Golbik

TABLE OF CONTENT

Summary **1**

Introduction **3**

SRF 3

TCFs (Elk1, SAP-1, Net) 6

Myocardin family 9

Myocardin 9

MRTF-A/B 13

SRF-MRTFs in proliferation and cell cycle regulation 18

Practical methods to manipulate the SRF-MRTF pathway 19

Materials and Methods **20**

Materials 20

Equipment [selected items used in this study] 20

Chemicals and Reagents 21

Common buffers and solutions 25

Antibodies and staining reagents 26

Oligonucleotides 27

Plasmids 29

Cells 30

Culture media 31

Methods 32

Molecular cloning and DNA manipulation methods 32

Mammalian cell culture methods 33

Protein analytical methods. 35

Quantitative real-time PCR 36

Luciferase reporter assay 36

Cell cycle analysis 36

Immunofluorescence staining . . . 36
Chromatin immunoprecipitation . . . 37
Live cell microscopy . . . 37
Mass-spectrometry . . . 37
Results . . . 39
Novel targets of MRTF-SRF pathway: validation using chromatin immunoprecipitation. . . . 39
Identification of G-actin regulated genes: combination of actin-binding drugs and microarray analysis. . . . 39
Chromatin immunoprecipitation protocol . . . 40
Mig6/Errfi1 . . . 42
Eplin-alpha . . . 43
Plakophilin 2, Pai-1, Fhl1 . . . 44
Anti-proliferative effect of MRTF-A in NIH 3T3 cells: apoptosis connection? . . . 45
MRTF-A regulates expression of pro-apoptotic proteins Bok and Noxa. . . . 49
MRTF-A is sufficient and required for Bok and Noxa transcription . . . 49
The role of p53 in Bok and Noxa transcriptional regulation. . . . 52
Are SRF-MRTFs required for apoptosis induction? . . . 55
MRTFs and their role in the cell cycle regulation . . . 57
MRTF-A/B knockdown leads to increase in S and G2/M populations in the absence of growth factors. . . . 57
MRTF-A/B knockdown impairs proliferation of NIH 3T3 fibroblasts. . . . 59
MRTF-A/B knockdown changes the lengths of cell cycle phases. . . . 60
MRTF-A/B knockdown influences cel cycle protein levels. . . . 64
MRTF-A/B knockdown leads to defects in chromosomal stability. . . . 67
Identification of proteins competing with MRTFs for binding to G-actin. . . . 69
Fluorescently tagged MRTF-A: characterization of the fusion proteins. . . . 74
Discussion . . . 79
Binding of SRF and MRTFs to the promoters of target genes. . . . 79
MRTF activity and apoptosis. . . . 82
Pro-apoptotic genes Bok and Noxa are MRTF-A targets. . . . 85
Effects of MRTF depletion on cell cycle. . . . 86
Potential competition candidates for dissociation of G-actin-MRTF complex. . . . 89
Bibliography . . . 90
Abbreviation list . . . 104
List of Publications . . . 105
Acknowledgements . . . 106

I. SUMMARY

Serum response factor (SRF) regulates transcription of genes involved in a broad range of functional processes, ranging from cellular proliferation to muscle differentiation programs. The temporal and spatial fine tuning of SRF activity is achieved via its cooperation with a number of regulatory factors, most prominently, the ternary complex factors family and the myocardin-related transcription factors family (MRTFs). The latter includes proteins MRTF-A and MRTF-B, which are regulated by the changes in the monomeric actin dynamics in the cell. The repertoire of MRTF target genes ranges from cytoskeleton-associated proteins and muscle-specific genes to the components of signaling pathways, transcription factors and genes involved in cellular motility. Novel MRTF-controlled genes are still being actively discovered and validated.

In this work I first explored the regulation of two pro-apoptotic genes, Bok and Noxa, by the SRF-MRTF pathway and using chromatin immunoprecipitation and quantitative reat-time PCR have shown that Bok is a direct target of the pathway, while Noxa is likely to be regulated by MRTFs, although not via serum response elements in the proximal promoter.

Second, employing the combination of apoptosis detection assays, I investigated the anti-proliferative effects of the constitutively active MRTF-A in fibroblasts and conclude that MRTF-A-induced cell death can be explained at least in part by the activation of apoptosis.

Third, I have shown that in fibroblasts MRTFs are required for normal cell proliferation and cell cycle progression. Their siRNA-mediated depletion leads to the down-regulation of CIP/KIP family members and premature entry into the S phase coupled with slightly extended G2 phase, as established by quantification of live cell imaging of cell cycle stages. Additionally, I observed an increased formation of nuclear defects during mitosis, which ultimately leads to aneuploidisation.

Finally, I have performed a mass-spectrometry screen for the G-actin-interacting proteins that display differential binding to the actin before and after stimulation with serum. Results of this screen can be used to explore the potential competitors with MRTFs for binding to G-actin upon extracellular stimuli.

The results of this work demonstrate that MRTFs have an important role in the regulation of cell proliferation, since both constitutively increased MRTF activity and its absence, result in the impairment of growth, albeit to a different extent. Moreover, this study for the first time establishes the connection between MRTFs and the regulation of cell cycle progression.

ZUSAMMENFASSUNG

Der "Serum Response Factor" (SRF) reguliert die Transkription von Genen, die, angefangen bei Zellproliferation bis hin zu Muskeldifferenzierungsprogrammen, in vielen verschiedenen funktionellen Prozessen involviert sind. Die zeitliche und örtliche Feinregulation der Aktivität von SRF wird durch sein Zusammenspiel mit zahlreichen Faktoren erreicht, vor allem mit der "ternary complex factors" Familie und der Familie der Myocardin-ähnlichen Tranksriptionsfaktoren. Letztere beinhaltet MRTF-A und MRTF-B, die durch Änderungen in der Dynamik von monomerem Aktin in der Zelle reguliert werden. Das Repertoire an SRF-MRTF regulierten Genen reicht von Zytoskelett-assoziierten und muskelspezifischen Genen bis zu Komponenten von Signaltransduktionswegen und Genen, die für Zellmotilität verantwortlich sind.

In dieser Arbeit habe ich zuerst die SRF-MRTF –abhängige Regulation von zwei proapoptotischen Genen, Bok und Noxa, untersucht und konnte mittels Chromatinimmunopräzipitation und quantitativer Real-time PCR zeigen, dass Bok direkt durch SRF-MRTF reguliert wird, während Noxa wahrscheinlich durch MRTFs reguliert wird, aber nicht über die serum response elements im proximalen Promoter.

Zweitens habe ich mittels Tests zum Nachweis von Apoptose die antiproliferatorischen Effekte von konstitutiv aktivem MRTF-A in Fibroblasten analysiert und konnte nachweisen, dass MRTF-A induzierter Zelltod zumindest zum Teil durch die Aktivierung von Apoptose erklärt werden kann.

Drittens habe ich gezeigt, dass in Fibroblasten MRTFs für normale Zellproliferation und Ablauf des Zellzyklus benötigt werden. Deren siRNA vermittelte Depletion führt zu einer Herunterregulation von Mitgliedern der CIP/KIP Familie. Anhand Mikroskopie lebender, MRTF-depletierter Zellen und Quantifizierung derer Zellzyklusstadien konnte ein verfrühter Eintritt in die S-Phase, gekoppelt mit einer leicht verlängerten G2-Phase nachgewiesen werden. Des weiteren habe ich in diesen Zellen vermehrte Kerndefekte während der Mitose beobachtet, was letztendlich zu Aneuploidie führt.

Zuletzt habe ich mittels Massenspektrometrie Proteinen identifiziert, die vor und nach Serumstimulation unterschiedliches Bindungverhalten zu G-Aktin zeigen. Die Resultate dieses Screenings können verwendet werden, um mögliche Antagonisten von MRTFs bei der Bindung an G-Aktin nach extrazellulärer Stimulation zu finden.

Die Ergebnisse dieser Arbeit demonstrieren, dass MRTFs eine wichtige Rolle in der Regulation der Zellproliferation spielen, da sowohl konstitutiv erhöhte MRTF-Aktivität als auch Abwesenheit von MRTF zu Beeinträchtigung im Wachstum führt, wenn auch in unterschiedlichem Maß. Weiters konnte diese Arbeit zum ersten Mal eine Verbindung zwischen MRTFs und der Regulation des Zellzuklus herstellen.

II. INTRODUCTION

SRF

Back in 1984, the year I was born, Michael Greenberg and Edward Ziff from New York University Medical Center published a study describing an extremely rapid increase in *c-fos* proto-oncogene transcription in response to serum stimulation of quiescent BALB/c-3T3 A31 fibroblasts (Greenberg & Ziff, 1984). Two years later, Richard Treisman working at MRC LMB in Cambrigde showed that this transient transcriptional activation requires a conserved DNA element 300 base pairs upstream from the mRNA cap site and a nuclear protein factor that specifically binds this element (Treisman, 1985; Deschamps *et al.,* 1985; Prywes and Roeder, 1986; Treisman, 1986). For convenience, he referred to the binding site as Serum Response Element (SRE) and to the binding protein as Serum Response Factor (SRF). Since then, SRF has become one of the best understood DNA-binding protein in the human proteome with more than 60 co-factors that modulate its activity identified to date (Miano, 2003).

In the years following SRF identification, the protein itself and its binding site were extensively characterized. The serum response element in the *c-fos* gene was originally identified as a 23-bp sequence containing symmetric inverted repeats flanking a 6-bp core (Treisman, 1986). An independent study (Minty & Kedes, 1986) identified a 10-bp element in the promoter of the cardiac α-actin gene which was highly conserved between human, mouse and chicken species. They called this element CCArGG box (CC(A-rich)GG), which was later found to be interchangeable with the serum response element in the *c-fos* gene

(Phan-Dihn-Tuy *et al.,* 1988; Boxer *et al.,* 1989; Taylor *et al.,* 1989). Nowadays, the SRF-binding site is termed CArG-box. Its consensus sequence is $CC(A/T)_6GG$, while single base deviations, usually C or G substitutions in the AT-core, result in non-consensus CArG-like elements, which can also be functional SRF-binding sites. SRF binds to the CArG boxes as a homodimer.

The murine SRF gene consists of 7 exons interrupted by 6 introns, spanning around 11 kilobases of the chromosome 17 (6p21 in human). Its cDNA has an open reading frame of 508 amino acids and four isoforms were identified differing in their 3' untranslated region (Norman *et al.,* 1988; Kemp & Metcalfe, 2000). The promoter of the SRF gene contains two evolutionary conserved SRF-binding sites (Spenser and Misra, 1996), suggesting that its expression might be regulated by a positive autoregulatory loop, in addition to Sp1-dependent transcription. The fact that SRF itself is induced by growth factors, such as serum and this induction is independent of *de novo* protein synthesis, makes it a member of so-called immediate early genes family (IEGs) (Norman *et al.,* 1988; Almedral *et al.,* 1988). SRF protein has been defined as a founding member of MADS-box family of transcriptional factors (Shore & Sharrocks, 1995). MADS box (MCM1, Agamous, Deficiens, SRF) is a modular 56 amino acid DNA-binding domain conserved in evolution from plants to mammals (Pellegrini *et al.,* 1995). In SRF, MADS box is located approximately in the middle of the polypeptide and is responsible for homodimerization, binding to DNA and interaction with other proteins (Shore & Sharrocks, 1995). The N-terminal part of SRF contains phosphorylation sites that can influence its DNA-binding and transcriptional potential (Misra *et al.,* 1991; Iyer *et al.,* 2003; Iyer *et al.,* 2006). The C-terminal region contains transcriptional activation domain (Johansen and Prywes, 1993), which does not belong to any standard class of activation domains (Tjan & Manniatis, 1994).

SRF is a ubiquitously expressed protein; its mRNA can be detected in most mouse tissues, while *in vitro*, SRF DNA binding was demonstrated in virtually all cell types. The deletion of SRF is incompatible with development. SRF-null mouse embryos fail to develop mesoderm and stop developing at gastrulation (Arsenian, 1998). Nevertheless, it appears that SRF is dispensable for cell proliferation *per se*, as evidenced by the normal growth of SRF-*null* mouse embryos until day E6.0 (Arsenian et al., 1998), and seemingly normal proliferation rates of SRF-*null* mouse embryonic stem (ES) cells, although these cells lack serum-induced immediate-early gene (IEG) response and exhibit various defects in morphology and spreading (Schratt *et al.,* 2001). The precise role of SRF in the formation of mesoderm is not known, since $SRF^{-/-}$ ES cells can be differentiated into mesoderm marker-expressing cells *ex*

vivo and form mesodermal cell types when introduced into nude mice (*Weinhold et al.,* 2000). Studies of conditional SRF deletion using cell type specific promoters as *Cre* recombinase drivers, established multiple roles of SRF in development and maintenance of many vital systems, including cardiovascular system (Parlakian *et al.,* 2004), skin development (Verdoni *et al.,* 2010), skeletal muscle (Li *et al.,* 2005; Charvet *et al.,* 2006), liver development (Sun *et al.,* 2009) and central nervous system (Alberti *et al.,* 2005). An excellent in-depth summary of SRF knockout phenotypes and their implication in pathological processes has been published recently (Miano, 2010).

Ever since SRF was found to regulate diverse and sometimes opposing sets of genes, ranging from genes controlling IEG response and cellular proliferation to cardiac or smooth muscle differentiation, it has become clear that the regulation of SRF-mediated transcription is complex and is mainly based on co-operation of SRF with accessory proteins and other transcriptional factors, which confer temporal and spatial specificity to gene expression. For example, homeodomain proteins, such as Phox1 were shown to physically interact with SRF to increase its DNA-binding activity *in vitro* (Grueneberg *et al.,* 1992). Angiotensin II was able to induce homeodomain protein MHox in a way that this induction resulted in the increase in SRF-dependent smooth muscle (SM) α-actin promoter activity (Hautmann *et al.,* 1997). Another homeodomain protein, *tinman* homolog Nkx-2.5, was recruited by SRF to cardiac α-actin promoter to potentiate the transcription (Chen and Schwartz, 1996). SRF and the GATA-4 co-activator were found to co-regulate myogenic and smooth muscle α-actin promoters as well as the *c-fos* promoter *in vitro* via protein-protein association (Belaguli *et al.,* 2000). Separate studies defined a complex of SRF and GATA-4 over the adjacent SRE and GATA-binding sites in cardiac *ANF* promoter (Morin *et al.,* 2001) and in developing chick embryos (Sepulveda *et al.,* 2002). Further studies in chick embryos identified LIM-domain only proteins CRP1 and CRP2 together with GATA-6, as modulators of the smooth muscle differentiation program in early development (Chang *et al.,* 2003). Finally, very recently, it was discovered that SRF and cell type specific transcriptional factors co-occupy regulatory DNA elements in the distal inter- or intragenic regions of chromatin, taking control of SRF-driven transcription away from the proximal promoters (Sullivan *et al.,* 2010; He *et al.,* 2011).

The studies mentioned above, however, were essentially overshadowed by the tremendous research effort aimed to characterize two families of transcriptional co-activators that appeared to play a major role in SRF regulation. These families are the Ternary Complex Factors (TCFs) and the myocardin family of transcription factors and I will discuss both of them below.

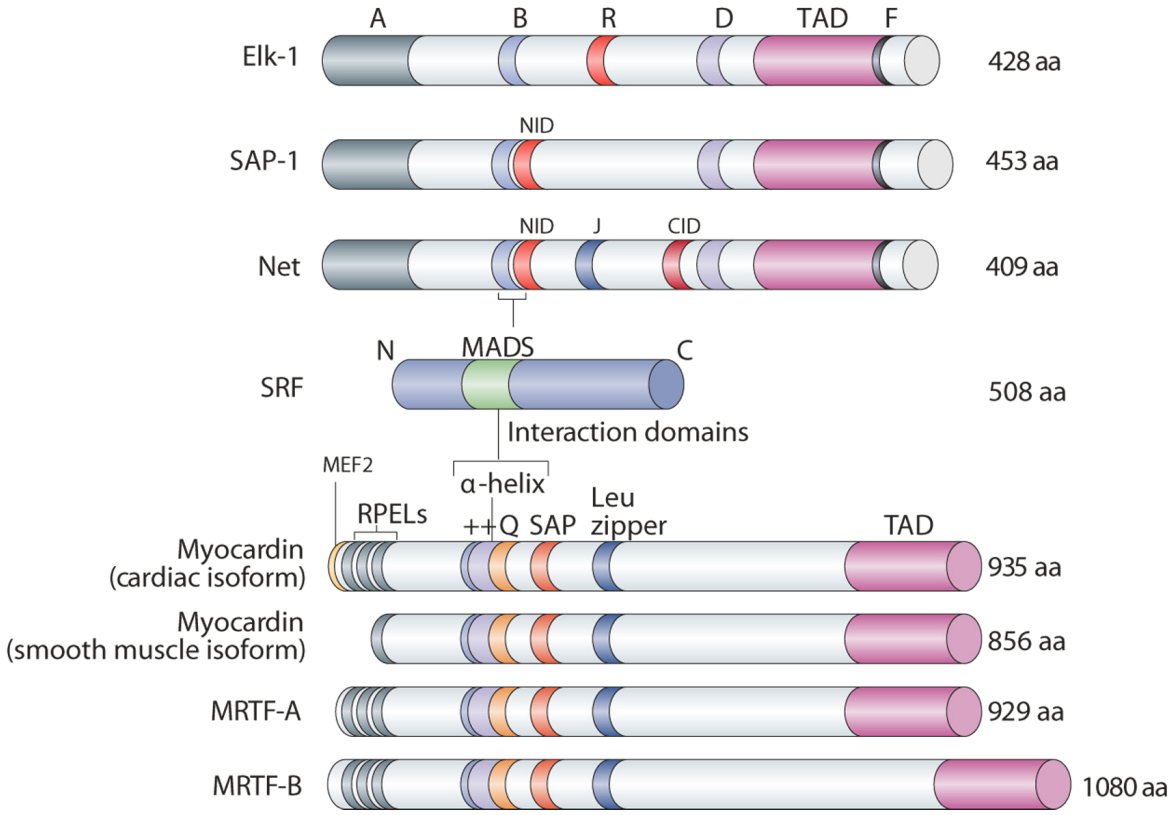

Figure II-1: *Schematic representations of SRF and its co-activators.* TCF family is shown on top. Conserved domains are represented as colored stripes. A-box is the Ets-DNA binding domain. B-box is the SRF-interaction domain. TAD is the transcactivation domain responsible for transcriptional activity. It contains MAPK pathway phosphorylation sites. D-box and F-box are docking sites for MAP kinases. Net also contains additional docking site for JNK kinase (J box). R, NID and CID are repression domains. MRTF family is at the bottom. RPEL domains are G-actin-binding sites. ++ (B-box) and Q-box are responsible for interaction with SRF. SAP domain is a putative DNA-binding element. Leucine zipper is necessary for dimerization. TAD - transactivation domain. Cardiac form of myocardin contains MEF2-binding site at the N-terminus. *Modified from* Olson & Nordheim, 2010 and Buchwalter *et. al,* 2004

TCFs (Elk1, SAP-1, Net)

Historically, the first ternary complex factor was identified as a fraction of HeLa nuclear lysate that forms a ternary complex with SRF on the c-fos promoter (Shaw *et al.,* 1989). This novel protein was termed p62TCF, because of its 62 kDa molecular weight. Later it was shown to be what is now known as Elk-1 (Ets-like transcription factor 1) (Hipskind *et al.,* 1991). Two other related proteins, SAP-1 (SRF accessory protein 1), also known as Elk-4, and Net (Erp/Sap-2/Elk-3) were also identified shortly thereafter (Dalton & Treisman, 1992; Giovane *et al.,* 1994). All three proteins comprise a sub-family of one of the largest family of transcription factors – Ets family, which contains approximately 30 members. All Ets fam-

ily members, including TCFs retain a highly conserved 85 amino acid DNA-binding motif, called Ets domain (Wasylyk *et al.,* 1998). It recognizes a core sequence GGA(A/T), referred to as EBS (Ets-binding sequence). EBS motifs located in the vicinity of CArG boxes are necessary for ternary complex formation between TCFs and SRF, although TCFs can weakly bind EBS-SRE even in the absence of SRF (Janknecht *et al.,* 1993). Promoters of immediate early genes, (*c-fos*, *egr-1*, *egr-2*, *junB*, *pip92*, *Srf*) are constitutively occupied by SRF, while TCFs are recruited to it in a stimulus-dependent manner. Formation of the ternary complex unmasks transactivation domain of SRF, allowing full activation of transcription (Johansen and Prywes, 1993). Ternary complex factors confer an immense versatility and specificity to the SRF-mediated transcription due to the following facts:

- Many different upstream pathways activate TCFs. The most prominent activation signaling pathway is the MAPK cascade. In the absence of MAPK activity in NIH 3T3 cells, Net is a powerful repressor of transcription (Giovane *et al.,* 1994), Elk-1 activates transcription to some extent, and SAP-1 is inactive (Giovane *et al.,* 1994; Maira *et al.,* 1996). Following extracellular stimuli, which rely on one of the three major MAP kinases (ERK, JNK and p38), Elk-1 is activated by all three of them (Janknecht *et al.,* 1994; Gille *et al.,* 1995), Net is phosphorylated by ERK and p38 through its D-box, and by JNK through so-called J-box (Ducret *et al.,* 2000) and SAP-1 is efficiently targeted only by ERK and p38 (Strahl *et al.,* 1996). In addition to MAPK pathway, SAP-1 was shown to be activated by colony stimulating factor-1 (CSF-1) in macrophages (Hipskind *et al.,* 1994). FGF signaling also leads to Elk-1 phosphorylation by kinases other than ERK1/2 (Chung *et al.,* 1998).

- TCFs are tightly regulated via post-translational modifications. While for SAP-1, only activating phosphorylation has been reported (Strahl *et al.,* 1996), Elk-1 is antagonistically regulated via SUMO (Small Ubiquitin-related Modifier) modification which repressed Elk-1-directed transcriptional activity (possibly through altered nucleo-cytoplasmic shuttling), and phosphorylation via MAPK pathway, which potentiates transcription (Yang *et al.,* 2003; Salinas *et al.,* 2004). Net exhibits an even more complex pattern of regulation. In the absence of modifications it is a potent transcriptional repressor, while SUMOylation increases the repressive potential further (Wasylyk *et al.,* 2005). ERK and p38 can bind the D-box of Net, inducing phosphorylation of its transactivation domain, thereby converting Net from a repressor to an activator of transcription (Giovane *et al.,* 1994; Ducret *et al.,* 2000). JNK, on the other hand, binds the J-box in the middle of the protein, which induces phosphorylation of the adjacent export motif. This

phosphorylation leads to the export of Net from the nucleus into the cytoplasm, leading to release from the transcriptional repression (Ducret *et al.,* 1999).

- TCFs cooperate with additional factors besides SRF to modulate gene expression.

One of the best known examples are p53-mediated inhibition of Net phosphorylation (Nakade *et al.,* 2004), and co-operation between transcriptional factors HIF-1α and HIF-2α with Elk-1 and Net to regulate transcription under hypoxic conditions (Yan *et al.,* 1999; Serchov *et al.,* 2010; Gross *et al.,* 2007; Gross *et al.,* 2008).

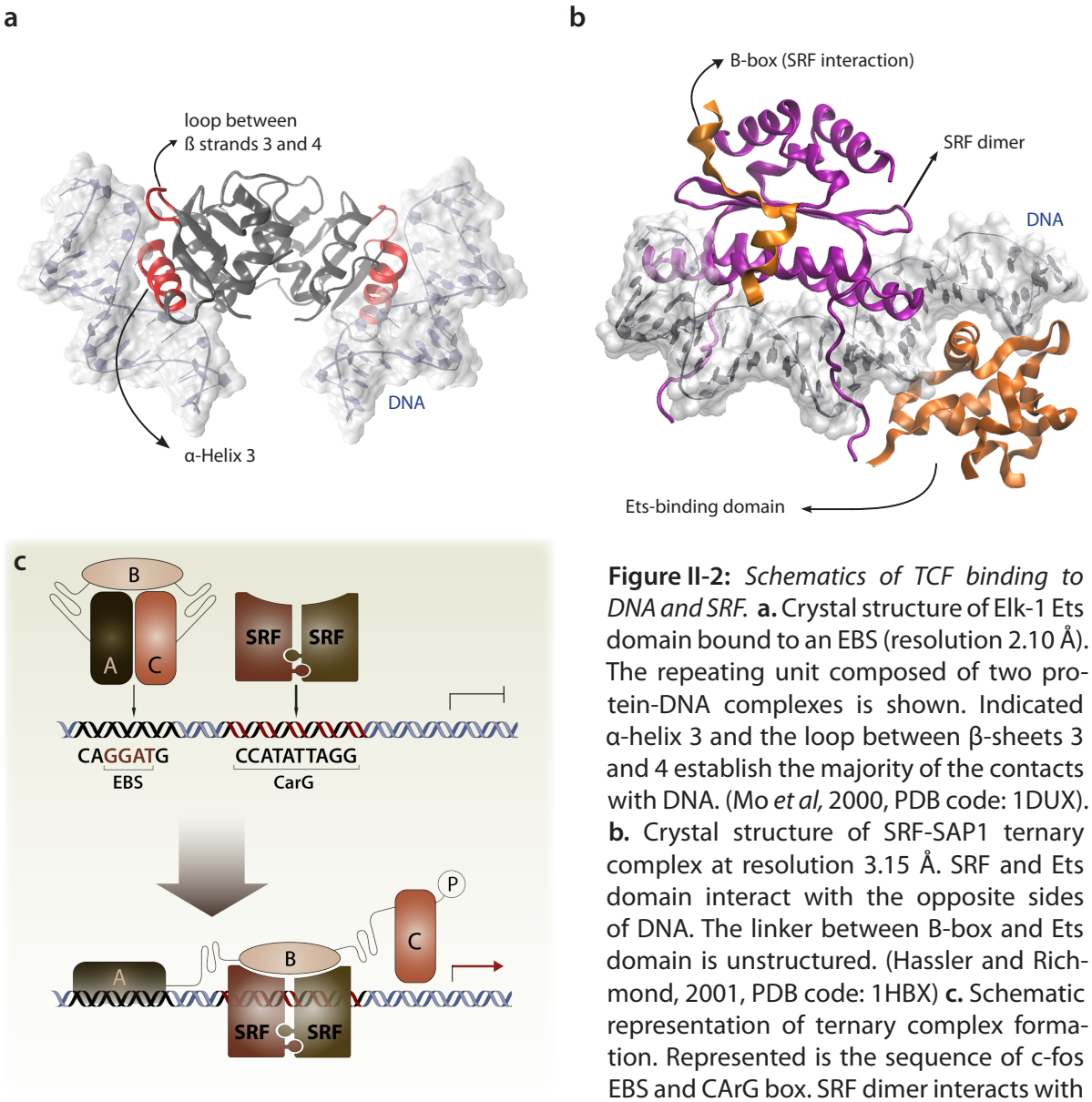

Figure II-2: *Schematics of TCF binding to DNA and SRF.* **a.** Crystal structure of Elk-1 Ets domain bound to an EBS (resolution 2.10 Å). The repeating unit composed of two protein-DNA complexes is shown. Indicated α-helix 3 and the loop between β-sheets 3 and 4 establish the majority of the contacts with DNA. (Mo *et al,* 2000, PDB code: 1DUX). **b.** Crystal structure of SRF-SAP1 ternary complex at resolution 3.15 Å. SRF and Ets domain interact with the opposite sides of DNA. The linker between B-box and Ets domain is unstructured. (Hassler and Richmond, 2001, PDB code: 1HBX) **c.** Schematic representation of ternary complex formation. Represented is the sequence of c-fos EBS and CArG box. SRF dimer interacts with CArG box. A-box of TCFs binds EBS. B-box contains the interface for interaction with SRF. Transactivation C-domain controls the transcription activity of the complex.

Despite the large number of studies on the regulation of ternary complex factors, their role *in vivo* remains incompletely understood. Studies using homologous recombination in mice are apparently hindered by the fact that there is a high degree of redundancy between TCFs. Net mutant mice seem to have a specific defect in the thoracic lymphatic vessels, which manifests in accumulation of chyle in lungs and death from respiratory failure (Ayadi *et al.,* 2001). Also, Net seems to be required for normal angiogenesis in adult (Zheng *et al.,* 2003). Phenotypes of Elk-1 and SAP-1 deficient mice display very few abnormalities. Further studies using combinational knockouts are necessary for delineating the roles of TCFs in embryonic development and maintenance of the adult organism.

Myocardin family

The myocardin family of transcription factors is the second most studied family of the SRF activity modulators. In mammals there are three members in the family – myocardin (MYOCD), MRTF-A (MAL/BSAC/Mkl1) and MRTF-B (Mkl2/MAL16). Structurally, they share homology in several functional domains and have been classified into the SAP family of proteins. The SAP domain comprises 35 amino acid helix-linker-helix stretch, named after SAF-A/B, Acinus and PIAS proteins. This domain has DNA-binding properties and was implicated in chromosomal dynamics, nuclear breakdown and apoptotic DNA fragmentation (Aravind & Koonin, 2000). The role of the SAP domain in MRTFs has not been clearly established, although it is known that its deletion abolishes the ability of myocardin to activate cardiac-specific *ANF* gene *in vitro* (Wang *et al.,* 2001). Functions of most of the other structural domains in MRTFs have been elucidated. N-terminal part is occupied by the RPEL motifs containing RPxxxEL core sequence which bind G-actin (Posern *et al.,* 2002; Miralles *et al.,* 2003). C-terminally from the RPEL motifs there is a B-box and glutamine-rich Q domain, which are required for interaction with SRF. A leuzine-zipper motif necessary for dimerization is approximately in the middle of the polypeptide and the C-terminal part harbors a transactivation domain which mediates transcriptional activity. Due to important differences between the founding member myocardin and MRTF-A/B, I will discuss these proteins separately, although they do display some degree of redundancy.

Myocardin

Myocardin was first identified in an *in silico* screen for genes expressed exclusively in the heart (Wang *et al.,* 2001) and since then has emerged as one of the most important regulators

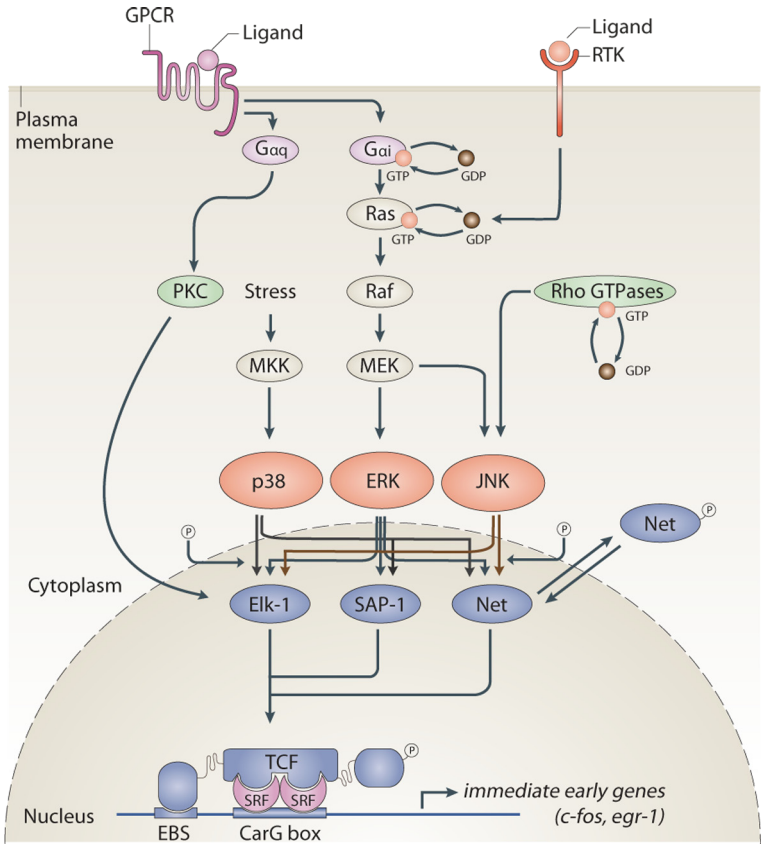

Figure II-3: Pathways leading to the activation of ternary complex factors. Only main TCFs (Elk-1, SAP-1 and Net) are shown. Extracellular stimuli that promote the activity of heterotrimeric G-protein (αi and αq subunits) and small GTPse Ras, activate downstream signaling pathways that result in phosphorylation of TCFs through their transactivation domain. The most prominent activation pathway is Raf-MEK-ERK. Elk-1 can be phosphorylated by p38, ERK and JNK, while SAP-1 is only efficiently activated by ERK and p38. Net is phosphorylated by ERK and p38 through D-box and by JNK through J-box. The latter phosphorylation leads to nuclear export of Net and supression of transcription. Represented pathways could be cell type specific.

of cardiac and smooth muscle differentiation programs (Wang *et al.*, 2001; Wang *et al.*, 2002; Wang *et al.*, 2003; Du *et al.*, 2003; Li *et al.,* 2003; Yoshida *et al.*, 2003; Chen *et al.*, 2002). During embryogenesis, its expression is first detected in cardiac precursor cells at ca. E7.5 and thereafter maintained in cardiac myocytes and smooth muscle cell lineages throughout adulthood (Wang *et al.*, 2001; Du *et al.*, 2003). Two alternatively spliced isoforms of myocardin have been identified – a longer, 935 amino acid form, has been primarily detected in the mouse heart, while a shorter, 856 aa form is expressed predominantly in smooth muscle cells (Creemers *et al.*, 2006b). The N-terminus of myocardin contains two RPEL motifs, but they have diverged from the consensus sequence to the point where myocardin does not bind G-actin and localizes exclusively in the nucleus (Miralles *et al.,* 2003). Myocardin binds SRF as a dimer (Wang *et al.,* 2003) and activates transcription of many cardiac and smooth muscle-restricted genes, including SM22α, smooth muscle myosin heavy chain (SM-MHC), SM myosin light chain (SM-MLC), SM-α-actin, cardiac α-actin and smoothelin-A. It is currently not known if any CArG-flanking DNA sequences are necessary for the myocardin binding. Myocardin is perhaps the only known smooth muscle-specific gene (also *HRCBP* (Anderson *et al.*, 2004)) that does not have SRF-responsive elements in the immediate promoter, although *in vitro* it does respond to SRF-mediated stimuli. Its expression has been explored in detail during mouse embryogenesis and

turned out to be rather unique. An enhancer 20-30 kb upstream of the myocardin gene has been shown to be a direct target of the transcriptional factors MEF2, Tead and Foxo, which drive its expression in early cardiac lineage during embryogenesis. Interestingly, the longer cardiac form of myocardin was found to interact and activate Mef2, which in turn activates transcription of myocardin itself in a positive autoregulatory loop. The shorter smooth muscle specific isoform does not have a Mef2 interaction site (Creemers *et al.*, 2006a). Also, this regulation appears to be SRF-independent.

Precise molecular mechanisms that govern myocardin-driven heart and smooth muscle programs are still poorly understood. Ectopical expression of myocardin in fibroblasts and ES cells triggers expression of smooth muscle, rather than cardiac genes (Yoshida *et al.*, 2003; Du *et al.*, 2003), while injecting myocardin mRNA into Xenopus embryos results in activation of cardiac genes (Small *et al.,* 2005). Myocardin-*null* mouse embryos survive only until day E10.5 due to block of vascular smooth muscle differentiation, especially in the aorta; the hearts of the embryos until then appear to be normal (Li *et al.*, 2003). To some extent this rather mild cardiac phenotype of myocardin-*null* mice could be explained by redundancy with MRTF-A/B which might be expressed in the early developing heart. In *Xenopus*, where MRTFs are not expressed at such early stages of development, expression of dominant negative version of myocardin led to the complete elimination of heart differentiation (Wang *et al*., 2001), while morpholino-directed knockdown of myocardin resulted in disruptions in heart tube formation but generally had much milder phenotype (Small *et al*., 2005).

Smooth muscle cells can modulate their phenotype in response to various external stimuli, such as injury. As a result, quiescent cells expressing high levels of contractile proteins switch to a proliferating type, expressing high levels of growth factors and extracellular matrix (Owens *et al.,* 2004). This phenomenon was explored in great detail to identify the mechanism used by SRF to differentiate between growth-promoting and muscle-restricted transcription. Apparently, many, but not all smooth muscle genes contain TCF binding sites in the vicinity of CArG boxes. In has been shown that in smooth muscle cells myocardin and TCFs associate with SRF in a mutually exclusive manner. External stimuli, for example PDGF, stimulate Elk-1 phosphorylation. Active Elk-1 is able to actively replace myocardin on the promoters of smooth muscle genes, which leads to the repression of their transcription. At the same time, direct TCF targets from IEG group of genes ensure that the cell starts proliferating (Miralles *et al*., 2003; Wang *et al*., 2004). Consistently with this, lowering endogenous

levels of Elk-1 in smooth muscle cells leads to an increase in expression of myocardin targets (Zhou *et al.,* 2005). Smooth muscle cells can also transdifferentiate with skeletal muscle (Odelberg *et al.*, 2000). It has been convincingly shown that myocardin play a crucial role in the conversion of skeletal muscle into smooth muscle via a complex chain of event, requiring inhibition of myogenin promoter via silencing by HDAC5 and physical contact of myocardin with MyoD transcriptional factor, which blocks DNA binding ability of MyoD and transcriprional synergy with MEF2, thereby inactivating all three master regulators of skeletal muscle differentiation (Long *et al.*, 2007).

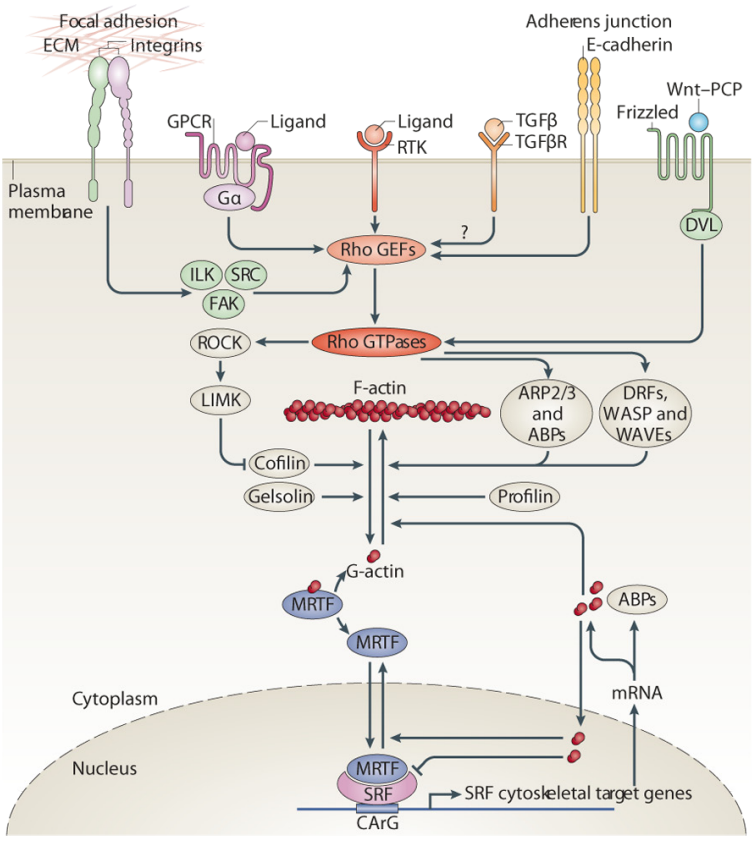

Figure II-4: *Pathways leading to the activation of MRTF-A/B.* Cytoskeletal actin filament dynamic is affected by a number of membrane receptors, including protein tyrosine kinases, G protein-coupled receptors (GPCR) with $G\alpha_{12/13}$ subunits, E-cadherins, integrins and other. Small GTPases from Rho family play a central role in regulating signals to G-actin-mediated activation and inactivation of MRTF-A/B. High levels of G-actin retain MRTF-A/B in the cytoplasm. Incorporation of G-actin into F-actin filaments depletes pool of free G-actin, allowing MRTF-A/B to escape from repressive complex, enter the nucleus and activate SRF-driven transcription of a MRTF-dependent subclass of SRF target genes. *From Olson and Nordheim, 2010*

In addition, myocardin activity is known to be regulated by a number of additional factors, such as GATA-4 (Oh *et al.*, 2004), homeodomain protein Nkx3.1 (Sun *et al.*, 2009), Tbx5 (Wang et al., 2011) and Smad3 (CArG-box independently) (Qui *et al.,* 2005). Since some of this cooperation partners have previously been reported for SRF itself, it would be important to determine if they represent real third layer of regulation above SRF-MYOCD, or some of these studies are interchangeable.

Recent studies have embarked on potentially novel mechanisms which can regulate myocardin activity, adding more complexity to the SRF-controlled network. Work from Chen *et al.*, 2001 has shown that myocardin can induce expression of micro-RNA-1 in smooth

muscle cells, which leads to inhibition of their proliferation. Similarly to Elk1, myocardin was found to be SUMOylated, but unlike Elk1, SUMO-1 modification enhanced myocardin's activity (Wang *et al.,* 2007). Another study discovered that acetylation is also required for myocardin to activate its target genes (Cao *et al.,* 2012).

MRTF-A/B

Early research on SRF cooperation with ternary complex factors has shown that inactivating TCFs does not fully abolish serum-induced activation of c-fos promoter, suggesting that at least two independent pathways activate SRF: TCF-dependent and TCF-independent (Johansen & Prywes, 1994; Hill *et al.,* 1994 and references therein). This TCF-independent pathway was shown to be responsive to the effectors of heterotrimeric G proteins lysophosphatidic acid (LPA) and aluminium fluoride ion (AlF4-) and required small GTPases from the Rho family: RhoA, Rac and Cdc42 (Hill *et al., 1995a;* Hill and Treisman, 1995b). Many details linking Rho signaling to the activation of SRF have emerged thereafter, finally leading to the realization that cytoskeletal actin dynamics is closely involved in this process (Sotiropoulos *et al.,* 1999). In mouse fibroblasts, RhoA activity coupled to the activation of Diaphanous-related formin-1 (mDia1) and downstream changes in actin threadmilling were necessary for activation of SRF-dependent transcription, while the activities of downstream RhoA targets ROCK kinase and LIM kinase were not required (Sahai *et al.,* 1998; Sotiropoulos *et al.,* 1999; Tominaga *et al.,* 2000; Copeland *et al.,* 2002). In contrast, in the aortic smooth muscle cells ROCK kinase activity was indispensable (Mack *et al.,* 2001) and in the neuronal cell line PC12 the presence of ROCK, LIMK and mDia1 (Geneste *et al.,* 2002). Actin mutants which cannot be polymerized were shown to have inhibitory effect on SRF-mediated transcription, while mutants which were stabilized in the polymerized form, activated SRF reporters (Posern *et al.,* 2002). Nevertheless, despite extensive research efforts unraveling upstream pathways leading to TCF-independent SRF activation, the SRF-interacting cofactor mediating this response was not known.

In 2001, two independent publications appeared describing the genetic defect behind a rare condition affecting infants and young children – acute megacaryoblastic leukemia (AMKL). Chromosomal translocation t(1;22)(p13;q13) associated exclusively with AMKL was found to result in a fusion protein, consisting of a fragment of unknown SAP domain-containing MKL1 polypeptide and RNA-binding motif protein 15 (RBM15, alternatively

OTT (from one-twenty-two)). Because it was involved in megakaryocytic acute leukemia, the MKL1 protein was named MAL. (Ma *et al.,* 2001; Mercher *et al.*, 2001). Almost two years later, in 2002, MAL was described again as a myocardin-related transcriptional factor A (MRTF-A), together with closely related MRTF-B. Both of them were found to be potent co-activators of SRF-mediated transcription and required SRF for their activity (Wang *et al.,* 2002). Another independent study has identified a mouse MRTF-A isoform, named BSAC, during the screen

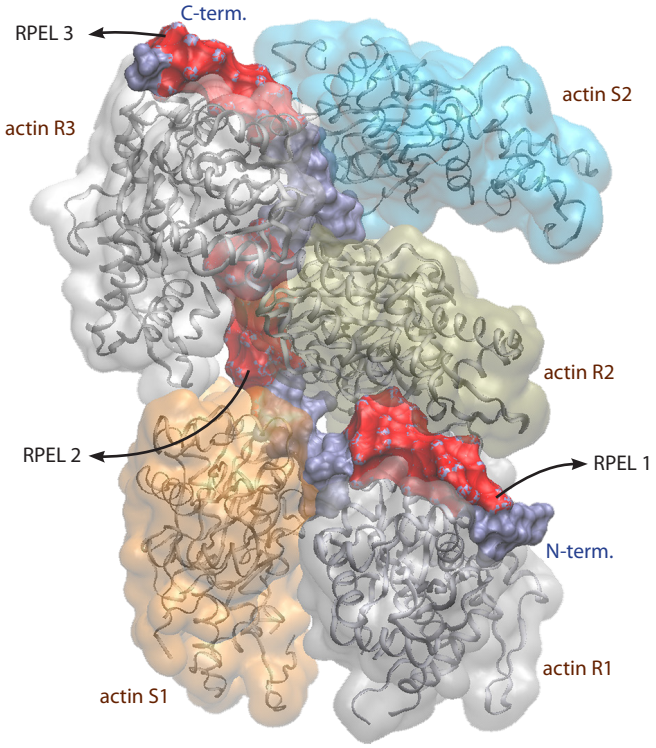

Figure II-5: *Crystal structure of MRTF-A RPEL domains bound to 5 G-actin molecules*. Complex of RPEL domains of MRTF-A (residues 67 to 199) with G-actin, ATP and latrunculin B was resolved at 3.5 Å resolution. Each RPEL motif engages a G-actin, designated here as actins R1-R2-R3. Helical N-terminal extensions of RPEL2 and RPEL3 recruit two other actins to the spacer elements - actins S1 and S2. RPEL-3 has considerably weaker affinity to actin, actins R3 and S2 can easily dissociate from MRTF-A, forming a trimeric complex. Residues involved in the interactions are mostly conserved between MRFT-A and MRTF-B. The cytoplasmic localisation of MRTF-A in unstimulated cells requires the integrity of both spacer sequences and binding of actin to spacer sequences is required for MRTF-A nuclear export. *Modified from* Mouilleiron *et al,* 2011. PDB code: 2YJF

for anti-apoptotic proteins (Sasazuki *et al.,* 2002). Shortly thereafter MRTF-A/B were defined as Rho-regulated SRF co-activators, connecting small GTPases from Rho family with the actin cytoskeleton and SRF-driven transcription.

MRTF-A/B unlike myocardin, are ubiquitously expressed in a broad range of cell types, including cardiac and smooth muscle cells. In non-stimulated NIH 3T3 cells MRTF-A/B are sequestered in the cytoplasm via interaction of their N-terminal RPEL motifs with monomeric G-actin (Miralles *et al.,* 2003, *Posern et al.,* 2004). Rho-mediated signaling (from LPA or serum) stimulates F-actin polymerization in the cytoplasm, depleting the G-actin pool and releasing MRTF-A/B from the inhibitory complex. Following importin α/β-mediated import, they bind SRF as a dimer and activate transcription of target genes (Miralles *et al.*, 2003; Posern *et al.*, 2004; Pawlowski *et al.*, 2010; Hirano *et al.,* 2011). It is not known if any of the

CArG-box flanking sequences are necessary for the binding, although MRTF-DNA contact has been reported and is necessary for efficient complex formation (Zaromytidou *et al.,* 2006). Nuclear G-actin also forms complexes with MRTF-A/B, facilitating its Crm1-dependent export into the cytoplasm and thus inhibiting transcriptional activity (Vartiainen *et al.,* 2007). Since the β-actin gene is one of the MRTF-SRF targets, ongoing rise in G-actin levels ensures downregulation of SRF response and retention of MRTFs in the cytoplasm. This regulatory mechanism was mostly studied in mouse fibroblasts and muscle cells. In contrast, in primary neurons and breast cancer epithelial cells MRTF-A is constitutively nuclear, suggesting existence of additional regulatory mechanisms (Kalita *et al.,* 2006; Medjkane *et al.,* 2009).

MRTF-A/B bind the same surface on SRF as TCFs. Similarly to the myocardin and Elk1 competition, mutually exclusive binding of MRTF-A/B and TCFs has been postulated (Murai *et al.,* 2002; Zaromytidou *et al.,* 2006). Moreover, the ability of MRTF-A/B to heterodimerize with myocardin in muscle cells has been found to direct some transcriptional targets (Wang *et al.*, 2003). With respect to the co-activator families, SRF target genes were proposed to be divided into two types – MRTF-dependent actin-regulated genes (*vinculin*, *actin*, *Srf*, *Cyr61* etc.) and TCF-dependent MAPK-regulated genes (IEGs). This division was based on the studies of upstream stimuli on the SRF-driven transcription in NIH 3T3 cells (Gineitis and Treisman, 2001). However, how exactly this level of separation is achieved *in vivo* and what is the role of MRTF-TCF competition/redundancy still remains elusive.

Similarly to myocardin and TCFs, MRTF-A/B were found to be additionaly regulated by interacting with other factors as well as by post-translational modifications. Stimulation of NIH 3T3 cells with serum or TPA (phorbol ester 12-O-tetradecanoyl-13-acetate) promotes not only nuclear translocation of MRTFs followed by transcriptional activation, but also Erk-dependent phosphorylation of MRTF-A on serine 454. This phosphorylation appears to act as an additional off-switch for MRTF-SRF activity, since it promotes binding of MRTFs to G-actin and nuclear export (Muehlich *et al.,* 2008). A number of other phosphorylation sites in MRTF-A/B were identified in a high-throughput mass spectrometry screen (Olsen *et al.*, 2006), but their functional importance has not been elucidated. SUMOylation has also been reported for MRTF-A. Like in Elk1, but unlike in myocardin, this modification correlated with decreased activation potential of MRTF-A (Nakagawa and Kuzumaki, 2005).

A few reports have established that MRTF-A/B might also act in an SRF-independent manner. During epithelial-mesenchymal transition of MDCK cells, MRTF-A/B were found to physically interact with Smad3 (previously seen for myocardin) upon exposure

to TGF-β, and direct transcription of another transcription factor – Slug, which, in turn directly repressed E-cadherin expression, leading to dissociation of cell contacts (Morita *et al.,* 2007). Intriguingly, dissociation of cell-cell contacts, in particular adherens junctions, is sufficient to activate MRTF-SRF pathway and transcription of target genes in the same MDCK cells (Busche *et al.,* 2008, Busche *et al.,* 2010). In C2C12 skeletal muscle cells, MRTF-A was found to be in complex with Smad 1/4. This complex was actively transcribing Id3 gene, whose product is a potent inhibitor of myogenic differentiation. Upon differentiation, one of the forkhead family transcription factors, Foxo1, translocated into the nucleus, forming inhibitory complex with MRTF-A/Smad 1/4 and suppressing Id3 transcription (Iwasaki *et al.,* 2008). Of note, this study opposing findings of others indicating that MRTF-A/B is necessary for skeletal muscle differentiation because MRTF-A knockdown in C2C12 cells blocks their ability to differentiate (Selvaraj and Prywes, 2003). Another study showed mechanical stress-induced, MRTF-A dependent transcription of extracellular matrix protein tenascin-C (Asparuhova et al., 2011). Interestingly, this regulation appeared to be completely SRF-independent.

A protein named SCAI (suppressor of cancer cell invasion) has been described as a negative regulator of MRTF-A (Brandt *et al.,* 2009). It binds to the RPEL motifs/B-box of MRTF-A and myocardin and suppresses their transcriptional activity without affecting MRTF-SRF binding. Finally, the LIM-only protein Fhl2 which is a direct transcriptional target of SRF was shown to compete with MRTF-A for SRF binding on the promoters of smooth muscle, but not immediate early or cardiac genes (Phillipar *et al.*, 2004).

Single MRTF-A or MRTF-B knockout phenotypes do not phenocopy SRF knockout, consistent with the idea that there is a significant degree of redundancy between them. To date, two MRTF-A null phenotypes are described. One is viable and does not exhibit any obvious abnormalities, except that MRTF-A mutant females are unable to productively nurse their offspring due to a very specific defects in mammary myoepithelial cells, which are required for ejection of milk from the mammary gland during lactation (Li *et al.,* 2006). This defect manifests in severely attenuated genes coding for smooth muscle restricted contractile proteins, such as SM-α-actin, SM-MHC, calponin 1 and tropomyosin 2. These mice were also found to have defective hypertrophic responses to chronic pressure overload in heart, as determined by angiotensin-II treatment (Kuwahara *et al.,* 2010). Second MRTF-A null phenotype was essentially similar to the one described before in respect to mammary gland dysfunction. In addition to this, around 40% of MRTF-A null embryos suffered lethal cardiac cell

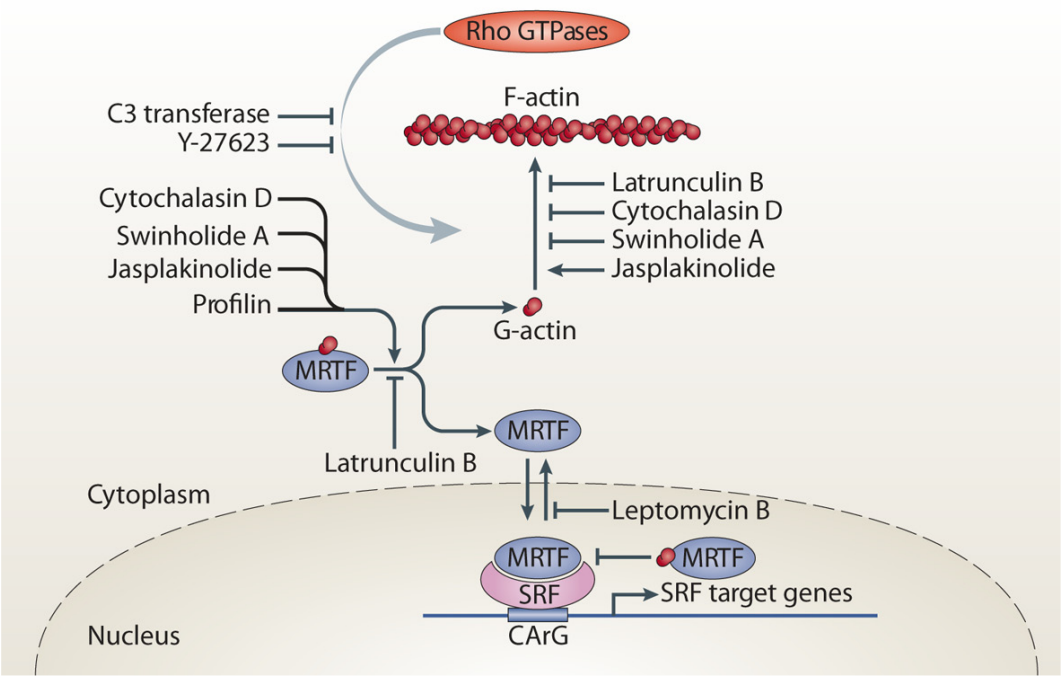

Figure II-6: *In vitro modulators of MRTF-SRF pathway.* For explanations see text. *From Olson and Nordheim, 2010*

necrosis at day E10.5 (Sun *et al.,* 2006b). Reasons for this discrepancy between phenotypes have not been established.

Global MRTF-B knockout was reported in three studies. Li *et al.*, 2005 used gene trap strategy to generate functionally null MRTF-B mutant protein. Homozygous embryos died between E17.5 and P1, exhibiting a spectrum of cardiac outflow tract defects (interrupted aortic arch, double-outlet right ventricle and others). Observed defects apparently stemmed from the cell autonomous flaw in differentiation of smooth muscle cells from the cardiac neural crest. Oh *et al.*, 2005 used gene targeting strategy to generate MRTF-B null phenotype. These mice died at E13.5-E14.5 with nearly identical spectrum of cardiac outflow tract defects. Wei *et al.*, 2007 generated yet another gene trap-targeted MRTF-B mutant with *null* phenotype. In addition to cardiac defects, hemorrhages in liver and dilations of vitelline veins that connect the embryo to the yolk sac, were observed. Targeted deletion of both MRTF-A and MRTF-B in the heart was also reported. While double cardiac knockout mice were born at Mendelian ratios, 75% of them died at P1, while the rest 25% gradually between weeks 2 and 13 (M. Mokalled, doctoral dissertation). Reported cardiac defects ranged from endocardial fibrosis and cardiac dilation to disarrangement of cardiomyocytes. Targeted deletion of both MRTF-A/B in megakaryocyte lineage has led to macrothrombocytopenia, platelet cytoskeletal abnormalities and severely impaired platelet activation (Smith *et al.,* 2012). Finally, conditional deletion of MRTF-A and –B in the brain results in lethality at

P16-P21. Mutant mice display morphological abnormalities in the hippocampus, cerebral cortex and subventricular zone (Mokkaled *et al.,* 2010). Interestingly, a single copy of MRTF-A or –B is sufficient to support normal brain development, while the double knockout mimics the phenotype observed upon brain-specific SRF ablation (Knöll *et al.,* 2006).

SRF-MRTFs in proliferation and cell cycle regulation

The role of SRF in the G1-S phase transition of cultured cells, especially fibroblasts, via cooperation with ternary complex factors and induction of immediate early genes is very well established (see above). The yeast SRF homolog MCM1 is necessary for G2-M phase transition (Althoefer *et al.,* 1995). However, the multitude of *in vivo* and *in vitro* studies suggests that the effects of SRF and its co-activators on cell proliferation are very likely to be context and cell type-specific. Murine ES cells are able to proliferate at normal rates (Schratt *et al.,* 2001), however, differentiating ES cells *in vitro* and epiblasts *in vivo* require SRF-mediated anti-apoptotic Bcl-2 expression for survival (Schratt *et al.*, 2004; Niu *et al.,* 2005). Conditional SRF depletion in liver showed impaired regeneration of tissue after partial hepatectomy, associated with blunted IEG response. SRF, however, was not strictly required for the regeneration process, although in normal mice its levels were acutely upregulated in response to injury (Latasa *et al.,* 2007). In the neuronal system, constitutively active SRF has been shown to be beneficial for survival of motoneurons upon nerve fiber injury (Stern *et al.,* 2012) and SRF-deficient neurons displayed signs of neurogeneration (Beck *et al.,* 2012). In contrast, Ramanan *et al.*, reported that SRF-deficient neurons did not show decrease in viability or defects in morphology (Ramanan *et. al.*, 2005). Also, brain-specific SRF ablation led to severe impairments in neuronal migration, but did not affect survival (Alberti *et al.,* 2005).

Myocardin was shown to inhibit proliferation of cardiomyocytes and aortic smooth muscle cells at least in part via antagonizing NF-kB-dependent cell proliferation (Tang *et al.,* 2008) and its knockdown using siRNA led to an increase in proliferation of fibroblasts (Milyavsky *et al.,* 2007). MRTF-A has been shown to confer anti-proliferative effects on fibroblasts, partly via induction of the negative regulator of EGFR signaling – Mig6 (Descot *et al.,* 2009). In contrast, MRTF-A was also shown to possess anti-apoptotic effects in Traf2/Traf5 double knockout mouse embryonic fibroblasts (Sasazuki *et al.,* 2002).

Practical methods to manipulate the SRF-MRTF pathway

Research in the field of SRF-MRTF-mediated transcription has been greatly facilitated by the use of agents that modulate MRTF function directly or change the state of actin equilibrium in a cell. The actin-targeting natural compounds cytochalasin D, jasplakinolide and swinholide A disrupt the MRTF-G-actin inhibitory complex, thereby liberating MRTFs and activating target gene transcription. Latrunculin B, on the other hand inhibits dissociation of MRTF-G-actin, preventing the activation of transcription (Miralles *et al*, 2003; Posern *et al,* 2004; Vartiainen *et al*, 2007). Three of this compounds, cytochalasin D, swinholide A and latrunculin B impair actin polymerization, while jasplakinolide stabilizes F-actin structures (Allingham *et al,* 2006). Effects of the upstream Rho-mediated signaling can be efficiently inhibited with either clostridial toxin C3 transferase (RhoA inhibitor), or with the ROCK-inhibiting agent Y-27623. Because nuclear MRTF-G-actin complexes also inhibit activation of SRF and stimulate MRTF export into the cytoplasm, ectopic expression of actin fused to a nuclear localization signal will have a strong inhibitory effect on MRTF-SRF transcription. Over-expression of actin mutants has also been useful in studying MRTF-dependent regulation of SRF. Non-polymerizable variants G13R and R62D can inhibit MRTF activity, while S14C and V159N stimulate F-actin formation and activate MRTF-driven transcription (Posern *et al,* 2002). MRTF variants lacking RPEL motifs and SRF-interacting domain (B1-box) (ΔNΔB) or RPEL motifs and C-terminal transactivation domain (ΔNΔC) act in a dominant-negative manner, suppressing activity of endogenous MRTFs.

III. MATERIALS AND METHODS

Materials

III.1.1. Equipment [selected items used in this study]

Agarose gel equipment	Horizontal Elpho	Workshop of MPI of Biochemistry (Martinsried)
Balances	Kern 572 and Kern ABS 120-4 Mettler AE200	Kern & Sohn GmbH (Balingen) Mettler Toledo (Giessen)
Centrifuges	Microcentrifuge 5417R Microcentrifuge 5417C Allegra 6KR Sorvall Evolution RC Universal 16	Eppendorf AG (Wesseling-Berzdorf) Beckman Coulter (Krefeld) Thermo Scientific (USA) Hettich (Kirchlengern)
PAGE equipment	Mini-PROTEAN 3 Elpho B100 XCell SureLock® Mini-Cell	Bio-Rad (Munich) Workshop of MPI of Biochemistry (Martinsried) Invitrogen (Darmstadt)
Western blotting	Mini Trans-Blot® electrophoretic transfer cell	Bio-Rad (Munich)
Power supplies	Consort/Peqlab EV261	distributed by Peqlab (Erlangen)
Microplate reader	Labsystems Multiscan RC model 351	Thermo Scientific (USA)
Luminometer	Microlumat Plus LB 96V Labsystems Fluoroscan Ascent FL type 374	EG&G Berthold (Schwerzenbach, CH) Thermo Scientific (USA)

Spectro-photometer	BioPhotometer™ Nanodrop, ND1000 and 2000c	Eppendorf AG (Wesseling-Berzdorf) Thermo Scientific (USA)
Electroporation	Genepulser XCell™	Bio-Rad (Munich)
Gel documentation	IDA gel documentation system LAS-1000 gel documentation system ChemiDoc™ XRS gel documentation system	Raytest (Straubenhardt) FujiFilm (Düsseldorf) Bio-rad (Munich)
PCR equipment	Thermocycler T3000 StepOnePlus™ real-time PCR system LightCycler® 480 II real-time PCR system	Biometra (Göttingen) Applied Biosystems (Darmstadt) Roche (Mannheim)
Microscopes	Axio Observer.A1 Axioplan 2 Axio Observer.Z1	Zeiss (Jena)
FACS machines	FACSCalibur flow cytometer FACSAria II cell sorter Accuri C6 flow cytometer	BD Biosciences (USA)
Mass spectrometry	LTQ-Orbitrap mass spectrometer Agilent 1100 nanoflow HPLC system	Thermo Scientific (USA) Agilent Technologies (USA)
Sonication	HD3100 sonicator	Bandelin (Berlin)
Incubation	HERAcell® 150i CO2 incubator XL S1 incubator equipped with TempModule S, CO2 module S and heating unit XL S	Thermo Scientific (USA) Pecon GmbH (Erbach)

III.1.2. Chemicals and Reagents

General laboratory chemicals

2-Mercaptoethanol ..... Merck (Darmstadt)
2-Propanol, absolute ..... Carl Roth GmbH (Carlsruhe)
Acetic acid, glacial, 100% ..... Merck (Darmstadt)
Acetonitrile ..... Sigma-Aldrich (Steinheim)
Acrylamide/Bis solution [37.5:1 (30% w/v), 2.6% C] ..... Serva (Heidelberg)
Agar-Agar, bacteriological grade ..... Carl Roth GmbH (Carlsruhe)
Agarose, for routine use ..... Sigma-Aldrich (Steinheim)
Albumin from bovine serum ..... Sigma-Aldrich (Steinheim)
Ammonium bicarbonate (NH_4HCO_3) ..... Sigma-Aldrich (Steinheim)
Ammonium persulfate (APS) ..... Bio-Rad (Munich)
BES (N,N-Bis(2-hydroxyethyl)-2-aminoethanesulfonic acid) ..... Carl Roth GmbH (Carlsruhe)
Boric acid (H_2BO_3) ..... Sigma-Aldrich (Steinheim)
Calcium chloride (CaCl2) ..... Carl Roth GmbH (Carlsruhe)

Chelex® 100 ion exchange resin ..... Bio-Rad (Munich)
Chloroquine ..... Sigma-Aldrich (Steinheim)
Dimethyl sulfoxide (DMSO) ..... Sigma-Aldrich (Steinheim)
DL-Dithiothreitol, for molecular biology ..... Sigma-Aldrich (Steinheim)
Ethidium bromide, 1% solution ..... Carl Roth GmbH (Carlsruhe)
Ethyl alcohol, absolute ..... Sigma-Aldrich (Steinheim)
Ethylenediaminetetraacetic acid (EDTA) ..... Carl Roth GmbH (Carlsruhe)
Formaldehyde, 16% solution ..... Pierce (Sankt Augustin)
Gelatin, from cold water fish skin, 45% ..... Sigma-Aldrich (Steinheim)
Glycerol, 87% for molecular biology ..... Merck (Darmstadt)
Glycine, molecular biology grade ..... Sigma-Aldrich (Steinheim)
HEPES (4-(2-hydroxyethyl)-1-piperazineethanesulfonic acid) ..... Sigma-Aldrich (Steinheim)
Hydrochloric acid (HCl), 37% ..... Sigma-Aldrich (Steinheim)
Lithium chloride ..... Sigma-Aldrich (Steinheim)
Magnesium chloride ($MgCl_2$) ..... Carl Roth GmbH (Carlsruhe)
Methyl alcohol, absolute ..... Carl Roth GmbH (Carlsruhe)
Monopotassium phosphate (KH_2PO_4) ..... Sigma-Aldrich (Steinheim)
Moviol 4-88 ..... Sigma-Aldrich (Steinheim)
Non-fat milk powder, blotting grade ..... Carl Roth GmbH (Carlsruhe)
Paraformaldehyde (PFA) ..... Sigma-Aldrich (Steinheim)
Polybrene (hexadimethrine bromide) ..... Sigma-Aldrich (Steinheim)
Ponceau-S [0.1% (w/v) solution in 5% acetic acid] ..... Sigma-Aldrich (Steinheim)
Potassium chloride (KCl) ..... Sigma-Aldrich (Steinheim)
Propidium iodide ..... Sigma-Aldrich (Steinheim)
Sodium acetate (CH_3COONa) ..... Sigma-Aldrich (Steinheim)
Sodium bicarbonate ($NaHCO_3$) ..... Sigma-Aldrich (Steinheim)
Sodium chloride (NaCl) ..... Sigma-Aldrich (Steinheim)
Sodium hydroxide (NaOH) ..... Calbiochem (Nottingham, UK)
Sodium phosphate dibasic (Na_2HPO_4) ..... Sigma-Aldrich (Steinheim)
TEMED (N,N,N',N'-Tetramethylethylenediamine) ..... Serva (Heidelberg)
Theazolyl blue tetrazolium bromide (MTT) ..... Sigma-Aldrich (Steinheim)
Trifluoroacetic acid (TFA) ..... Sigma-Aldrich (Steinheim)
Tris base (Trisma®) ..... Sigma-Aldrich (Steinheim)
Tryptone/Peptone ..... Carl Roth GmbH (Carlsruhe)
Yeast extract, bacteriological grade ..... Carl Roth GmbH (Carlsruhe)

Detergents

Nonidet® P-40 Substitute (NP-40) ..... Fluka (Buchs, CH)
Sodium deoxycholate, powder ..... Sigma-Aldrich (Steinheim)
Sodium dodecyl sulfate (SDS), powder ..... Carl Roth GmbH (Carlsruhe)
Triton X-100 ..... Serva (Heidelberg)
Tween 20 ..... Sigma-Aldrich (Steinheim)

Antibiotics

Ampicillin ..... Roche (Mannheim)
Blasticidine S hydrochloride ..... Sigma-Aldrich (Steinheim)
G418 disulfate salt (*Geneticin*) ..... PAA (Cölbe)
Kanamycin sulphate ..... Invitrogen (Karlsruhe)
Puromycin dichloride ..... Calbiochem (Nottingham,GB)
Zeocin™ [100 mg/ml solution] ..... Invitrogen (Karlsruhe)

Composite reagents and kits

100 bp ladder ..... NEB (Frankfurt am Main)
2-log DNA ladder (0.1-10 kb) ..... NEB (Frankfurt am Main)
Annexin V-FITC apoptosis detection kit I ..... BD Biosciences (Heidelberg)
ANTI-FLAG® M2 magnetic beads ..... Sigma-Aldrich (Steinheim)
Colloidal Blue staining kit ..... Invitrogen (Karsruhe)
Complete™ protease inhibitor cocktail ..... Roche (Mannheim)
Dual-Glo™ Luciferase Assay Kit ..... Promega (Madison, USA)
Dynabeads® Protein G ..... Invitrogen (Karsruhe)
Fast SYBR® Green master mix ..... Applied Biosystems (Darmstadt)
FITC BrdU Flow Kit ..... BD Biosciences (Heidelberg)
Gel loading dye, blue (6X) ..... NEB (Frankfurt am Main)
Immobilon-P PVDF membrane ..... Millipore (Billerica, USA)
Micro BCA™ protein assay kit ..... Pierce (Sankt Augustin)
NuPAGE® LDS sample buffer (4X) ..... Invitrogen (Karsruhe)
PCR marker ..... NEB (Frankfurt am Main)
PE Caspase-3 active apoptosis kit I ..... BD Biosciences (Heidelberg)
PhoSTOP™ phospatase inhibitor coctail ..... Roche (Mannheim)
Precision Plus Protein™ dual color standards ..... Bio-Rad (Munich)
QIAGEN Plasmid Maxi Kit ..... Qiagen (Hilden)
QIAGEN Plasmid Mini Kit ..... Qiagen (Hilden)
QIAGEN RNeasy Mini Kit ..... Qiagen (Hilden)
QIAquick Gel Extraction Kit ..... Qiagen (Hilden)
QIAquick MinElute Gel Extraction Kit ..... Qiagen (Hilden)
QIAquick MinElute PCR Purification Kit ..... Qiagen (Hilden)
QIAquick PCR Purification Kit ..... Qiagen (Hilden)
Restore™ Western blot stripping buffer ..... Pierce (Sankt Augustin)
Verso™ cDNA kit ..... Thermo Scientific (Schwerte)
Western Lightning®-ECL ..... PerkinElmer (Boston, USA)

Enzymes and reagents used in molecular cloning

All restriction endonucleases purchased from ..... NEB (Frankfurt am Main)
Alkaline phosphatase, calf intestinal (CIP) ..... NEB (Frankfurt am Main)
Deoxynucleotide (dNTP) solution mix, 10 mM each ..... NEB (Frankfurt am Main)

DNA polymerase I, large (Klenow) fragment ..... NEB (Frankfurt am Main)
Phusion® high-fidelity DNA polymerase ..... Thermo Scientific (Schwerte)
Proteinase K, 20 mg/ml ..... NEB (Frankfurt am Main)
Ribonuclease A (RNAse A) from bovine pancreas ..... Sigma-Aldrich (Steinheim)
T4 DNA ligase ..... NEB (Frankfurt am Main)
Taq DNA polymerase ..... NEB (Frankfurt am Main)
Trypsin, sequencing grade ..... Promega (Madison, USA)

Transfection reagents

Lipofectamine™ reagent ..... Invitrogen (Karsruhe)
Lipofectamine™ 2000 reagent ..... Invitrogen (Karsruhe)
Lipofectamine™ RNAiMAX reagent ..... Invitrogen (Karsruhe)

Cell culture reagents

DMEM, high glucose, no Glu, no Lys, no Arg (Gibco®) ..... Invitrogen (Karsruhe)
DMEM, high glucose, without phenol red (Gibco®) ..... Invitrogen (Karsruhe)
Dulbecco's modified Eagle medium (Gibco® DMEM), high glucose (4.5g/L) ..... Invitrogen (Karsruhe)
Fetal bovine serum ..... Invitrogen (Karsruhe)
Fetal bovine serum, dialysed ..... Invitrogen (Karsruhe)
L-[U-$^{13}C_6$, $^{14}N_2$]lysine (Lys8) ..... Sigma-Aldrich (Steinheim)
L-[U-$^{13}C_6$, $^{15}N_4$]arginine (Arg10) ..... Sigma-Aldrich (Steinheim)
L-arginine (Arg0) ..... Sigma-Aldrich (Steinheim)
L-glutamine, 200 mM (100X) ..... PAA (Cölbe)
L-lysine (Lys0) ..... Sigma-Aldrich (Steinheim)
Opti-MEM® reduced serum medium (Gibco®) ..... Invitrogen (Karsruhe)
Penicillin-Streptomycin, liquid, 100X ..... PAA (Cölbe)
Sodium pyruvate, 100 mM (100X) ..... PAA (Cölbe)
Trypsin-EDTA solution, 10X ..... PAA (Cölbe)

Inhibitors and inducers

Cycloheximide ..... Sigma-Aldrich (Steinheim)
Cytochalasin D ..... Calbiochem (Nottingham,GB)
Doxorubicine ..... Sigma-Aldrich (Steinheim)
Doxycyclin, Hyclate ..... Calbiochem (Nottingham,GB)
Etoposide ..... Calbiochem (Nottingham,GB)
Jasplakinolide ..... Calbiochem (Nottingham,GB)
Latrunculin B ..... Calbiochem (Nottingham,GB)
Staurosporine ..... Sigma-Aldrich (Steinheim)
TNF alpha ..... Sigma-Aldrich (Steinheim)
z-VAD-FMK ..... Biomol (Hamburg)

III.1.3. Common buffers and solutions

Most of single component solutions were made at 1M concentration. pH was adjusted when necessary. Following autoclaving, solutions were stored at room temperature. Exceptions are 3M KCl, 5M NaCl, 0.5M EDTA, 10% SDS, 10% Na-deoxycholate. Below are universally used buffers. For protocol-specific recipes, see Methods section.

TE buffer (1x)	
Tris-HCl, pH 8.0	10 mM
EDTA	1 mM

BBS buffer (2x)	
BES	50 mM
NaCl	280 mM
Na_2HPO_4	1.5 mM
pH	6.96

RIPA buffer	
Tris-HCl, pH 8.0	20 mM
NaCl	150 mM
Glycerol	5% (v/v)
Triton X-100	1% (v/v)
Na deoxycholate	0.5%
SDS	0.1%

Running gel (PAGE)	
Acrylamide/Bis	8-14%
Tris-HCl pH 6.8	375 mM
SDS	0.1%
APS	0.1%
TEMED	0.1%

TBS buffer (1x)	
Tris-HCl, pH 7.5	20 mM
NaCl	150 mM

PBS	pH 7.4
KCl	2.7 mM
NaCl	137 mM
Na_2HPO_4	10 mM
KH_2PO_4	1.8 mM

Running buffer (PAGE)	
Tris base	25 mM
Glycine	192 mM
SDS	0.1% (w/v)

Blocking (IF)	
FBS	10% (v/v)
Gelatine	1% (v/v)
Triton X-100 in PBS	0.05%

Blocking (PAGE)	
non-fat milk in TBS/T	5 % (w/v)

TBS/T buffer (1x)	
Tris-HCl, pH 7.5	20 mM
NaCl	150 mM
Tween 20	0.1% (v/v)

TBE buffer (1x)	
Tris-HCl, pH 8.0	90 mM
Boric acid	90 mM
EDTA	3 mM

Transfer buffer (PAGE)	
Tris base	25 mM
Glycine	192 mM
Methanol	20% (v/v)
SDS	0.05%

Stacking gel (PAGE)	
Acrylamide/Bis	5%
Tris-HCl pH 6.8	127 mM
Glycerol	4.5%
SDS	0.1%
APS	0.1%
TEMED	0.1%

III.1.4. Antibodies and staining reagents

Primary reagents

Reagent	Description	Sourse	Used in
anti-FLAG M2 Peroxidase	Mouse monoclonal IgG_1 conjugated to horseradish peroxidase (HRP)	Sigma-Aldrich cat. A8592	WB 1:2000
anti-MRTF-A/B	Rabbit polyclonal serum	Homemade (Sina Pleiner)	WB 1:1000 IF: 1:500 ChIP: 300 µl
anti-SRF	Rabbit polyclonal, clone G-20	Santa Cruz Biotechnology cat. sc-335	ChIP: 5 µg
anti-NF2	Rabbit polyclonal, clone A-19	Santa Cruz Biotechnology cat. sc-331	ChIP: 5 µg
anti-α-tubulin	Mouse monoclonal IgG_1, clone DM1A	Sigma-Aldrich cat. T9026	WB 1:10000
anti-p21Waf1	Mouse monoclonal IgG_1, clone 65	Calbiochem cat. OP76	WB 1:1000
anti-p27Kip1	Mouse monoclonal IgG_1	BD Biosciences cat. 610242	WB 1:1000
anti-p53	Mouse monoclonal IgG_1, clone 1C12	Cell Signaling cat. 2524	WB 1:1000
anti-cyclin D1	Mouse monoclonal IgG_1, clone D1-72-13G-11	Millipore cat. 05-815	WB 1:1000
anti-Rb (total)	Rabbit polyclonal, clone C-15	Santa Cruz Biotechnology cat. sc-50	WB 1:100
anti-phospho-Rb (Ser^{780})	Rabbit monoclonal IgG, clone C84F6	Cell Signaling cat. 3590	WB 1:1000
anti-GFP	Mouse monoclonal, clone GFP-20	Sigma-Aldrich cat. G6539	WB 1:2000
DAPI, Molecular Probes®	4',6-Diamidino-2-Phenylindole, Dihydrochloride	Invitrogen cat. D1306	IF 1:5000
Hoechst 33258	Pentahydrate (bis-Benzimide)	Invitrogen cat. H-3569	IF 1:5000
Phalloidin-Atto 488	Marker for F-actin	Sigma-Aldrich cat. 49409	IF 1:100

Secondary reagents

Reagent	Sourse	Used in
Alexa Fluor® 546 goat anti-rabbit	Molecular Probes (Eugene, USA)	IF 1:1000
Polyclonal goat anti-mouse-HRP	DakoCytomation (Glostrup, Denmark)	WB 1:5000
Polyclonal swine anti-rabbit-HRP	DakoCytomation (Glostrup, Denmark)	WB 1:2000

III.1.5. Oligonucleotides

Cloning primers

Amplicon		Name	Sequence, 5'-3'	Enzyme
MRTF-A f.l. $^{no\ ATG}$ (pEGFP-N1)	Forward	DS.MAL f.l.for	CGCGCTCGAGCTGCCCCCTTCCGTCATT	XhoI
	Reverse	DS.MAL f.l.rev	CGCGAAGCTTCAAGCAGGAATCCCAGTG	Hind III
MRTF-A f.l. ^{ATG} (pEGFP-N1)	Forward	DS.MAL f.l.ATG.for	CGCGCTCGAGATGCTGCCCCCTTCCGTCATT	XhoI
	Reverse	DS.MAL f.l.rev	CGCGAAGCTTCAAGCAGGAATCCCAGTG	Hind III
MRTF-A $^{ATG+Kozak}$ (pEGFP-N1)	Forward	DS.MAL.fl.Koz.F	CGCTCGAGGCCACCATGCCCCCTTCCGTCATT	XhoI
	Reverse	DS.MAL f.l.rev	CGCGAAGCTTCAAGCAGGAATCCCAGTG	Hind III
ΔN MRTF-A (pEGFP-N1)	Forward	DS.dN.MAL.Xho.F	CCGGCTCGAGATGGAGCTGGTGGAGA	XhoI
	Reverse	DS.MAL f.l.rev	CGCGAAGCTTCAAGCAGGAATCCCAGTG	Hind III
ΔN MRTF-A (pEGFP-C1)	Forward	DS.dN.AML.C1.F	CGCGCTCGAGCCATGGAGCTGGTGGAG	XhoI
	Reverse	DS.dN.MAL.C1.R	CGCGAAGCTTCTACAAGCAGGAATCCCAGTG	Hind III
TagRFP	Forward	DS.TagRFP.Nhe.F	GCGCACCGGTATGGTGTCTAAGGGCGAA	Age I
	Reverse	DS.TagRFP.mod.R	GCGCCTCGAGGATTAAGTTTGTGCCCCAGTT	Xho I

Detection Primers

Amplicon		Name	Sequence, 5'-3'	Source
HPRT	Forward	ADM1 HPRT1 F	TCA GTC AAC GGG GGA CAT AAA	A.Descot
	Reverse	ADM1 HPRT1 R	GGGGCTGTACTGCTTAACCAG	
MRTF-A	Forward	MRTFA FW 195	CCA GGA CCG AGG ACT ATT TG	L.Leitner
	Reverse	MRTFA RV 196	CGA AGG AGG AAC TGT CTG CTA	
MRTF-B	Forward	MRTFB FW 213	CCC ACC CCA GCA GTT TGT TGT T	L.Leitner
	Reverse	MRTFB RV 214	TGC TGG CTG TCA CTG GTT TCA TC	
Bok	Forward	ADM1 BokF	GGC AAG GTA GTG TCC CTG TA	A.Descot
	Reverse	ADM1 BokR	GCT CAT CTC TCT GGC AAC AAC	
Noxa	Forward	ADM1 NoxaF	CGC CAG TGA ACC CAA CG	A.Descot
	Reverse	ADM1 NoxaR	GGC TCC TCA TCC TGC TCT TT	
Acta2	Forward	ADM1 SMA2 F	GGG AGT AAT GGT TGG AAT GG	A.Descot
	Reverse	ADM1 SMA2 R	CAG TGT CGG ATG CTC TTC AG	
SRF	Forward	ADM1 SRF F	GGC CGC GTG AAG ATC AAG AT	A.Descot
	Reverse	ADM1 SRF R	CAC ATG GCC TGT CTC ACT GG	
Vinculin	Forward	ADM2 Vinculin F	GGC CGG ACC AAC ATC AGT G	A.Descot
	Reverse	ADM2 Vinculin R	ATG TAC CAG CCA GAT TTG ACG	
P18^{Ink4c}	Forward	DS.Q.p18INK4c.F	GCT GCA GGT TAT GAA ACT TGG	This study
	Reverse	DS.Q.p18INK4c.R	GTT AAC ATC AGC CTG GAA CTC	
P19^{Ink4d}	Forward	DS.Q.p19INK4d.F	CTT GCA GGT CAT GAT GTT TGG	This study
	Reverse	DS.Q.p19INK4d.R	GTC CAG GGC ATT GAC ATC AG	
P21^{Waf1}	Forward	DS.Q.p21WAF1.F	ACA AGA GGC CCA GTA CTT CC	This study
	Reverse	DS.Q.p21WAF1.R	TGG AGT GAT AGA AAT CTG TCA GG	
P27^{Kip1}	Forward	DS.Q.p27KIP1.F	TAA TTG GGT CTC AGG CAA ACT C	This study
	Reverse	DS.Q.p27KIP1.R	AGA ATC TTC TGC AGC AGG TC	

ChiP primers

Amplicon		Sequence, 5′-3′	Source
GAPDH promoter (-ve control)	forward reverse	TCT TGT GCA GTC CCA GCC T CAA TAT GGC CAA ATC CGT TCA	Vartiainen *et al.*, 2007
SRF	forward reverse	TTC CCG TCC GAG GAA ACA T GGC TCT TTT GAC CCA GAC CAT	Vartiainen *et al.*, 2007
Vinculin	forward reverse	AGC CCA GAT GCT TCA GTC AGA GGT CAG ATG TGC CAG AAA GGA	Vartiainen *et al.*, 2007
Mig-6 (CarG -260)	forward reverse	GCT CCC TGA GTT TCT TGG ATC ATG CCG CTA CCG AAG AGT TT	A.Descot
Mig-6 (intron +3160)	forward reverse	AGT TCC AGT TCC TGT CAT TGC CCC ACT CCT CCT TTC TAT CG	A.Descot
Cyr61	forward reverse	AAT CGC AAT TGG AAA AGG CA TGA AAA GAA CTC GCG GTT CG	Vartiainen *et al.*, 2007
Eplin-alpha (CarG -124)	forward reverse	AAA AAG TCT CTC CCT TCC AAT GT GTT ACT GCC CTG CCA CAA G	L.Leitner
Pkp2 (CarG-like +2894)	forward reverse	TTG TTG ACA TAC CAG AAA GGA TGA GG TTC CAG GGA AAC CAT ACA CCG TAA GA	L.Leitner
Bok (CarG-like -99)	forward reverse	GAA CTT GTG CTG GCC TTT CT GTC CAC ACC CGA GCT GAA	A.Descot

Small hairpin RNA

Name	Sequence, 5′-3′	Source
MRTF-A/B	GATCCCCGCATGGAGCTGGTGGAGAAGAA TTCAAGAGA AAAGGTTTTGTACCTCGACCACCTCTTCTT	Vartiainen *et al.*, 2007 L. Leitner

Small interfering RNAs

Name		Sequence, 5′-3′	Source
Silencer® negative control #1 siRNA	Sense Antisense	Proprietary Proprietary	Ambion cat. AM4635
MRTF-A/B	Sense Antisense	UGGAGCUGGUGGAGAAGAATT UUCUUCUCCACCAGCUCCAUG	Medjkane *et al.*, 2009
MRTF-A/B cy5-labeled	Sense Antisense	UGGAGCUGGUGGAGAAGAA[dT][dT][cy5] UUCUUCUCCACCAGCUCCA [dT][dT]	Medjkane *et al.*, 2009

III.1.6. Plasmids

Pre-existing

Plasmid name	Description	Source
pEF-MAL f.l.	Full length murine MRTF-A under EF1α promoter, HA-tagged	G. Posern (Sotiropoulos *et al.*, 1999)
pLPCX	Expression vector for use in retroviral infections	Clontech (Mountain View, USA)
pLPCX-eGFP	Ehnanced GFP under CMV promoter	G. Posern (Descot *et al.*, 2009)
pLPCX-MAL f.l.	Full length murine MRTF-A under CMV promoter	G. Posern (Descot *et al.*, 2009)
pLPCX-MAL met	Murine MRTF-A without first 92 aa, under CMV promoter	G. Posern (Descot *et al.*, 2009)
pLPCX ΔNMAL	Murine MRTF-A without first 173 aa, under CMV promoter	G. Posern (Descot *et al.*, 2009)
pEGFP-N1	Expression vector for creating C-terminal eGFP fusions	Clontech (Mountain View, USA)
pEGFP-C1	Expression vector for creating N-terminal eGFP fusions	Clontech (Mountain View, USA)
p3E-TagRFP	3'-entry plasmid from Gateway cloning system	Sergey Prikhozhij, MPI for Molecular Genetics, Berlin
pGIC	Expression vector for FUCCI markers	Christian Kuffer, MPI for Biochemistry, Martinsried
pBOS-H2B-GFP	Histone H2B fused to eGFP	Christian Kuffer, MPI for Biochemistry, Martinsried
pSuper.retro.puro-MAL_sh	shRNA against MRTF-A and MRTF-B	L.Leitner (Leitner *et al.*, 2011)
P3D.A-Luc	Three fos-derived SRF binding sites in front of Xenopus laevis type 5 actin TATA-box in pGL3-basic vector, driving expression of Firefly luciferase	G.Posern (Geneste *et al.*, 2002)
ptkRL	Internal control reporter for pGL3, thymidine kinase promoter from herpes simplex virus driving Renilla reniformis luciferase expression	Promega (Madison, USA)
pEF-HA	Mammalian expression vector based on pUC12 backbone. EF1α enhancer/promoter. 5'-terminal HA-tag	G. Posern (Sotiropoulos *et al.*, 1999)

Created

Plasmid name	Description	Source
pEGFP-N1-MAL f.l [noATG]	C-terminal full length murine MRTF-A-eGFP fusion without start ATG codon, under CMV promoter	this study
pEGFP-N1-MAL f.l [ATG]	C-terminal full length murine MRTF-A-eGFP fusion with start ATG codon, under CMV promoter	this study

Plasmid name	Description	Source
pEGFP-N1-MAL f.l [ATG/Koz]	C-terminal full length murine MRTF-A-eGFP fusion with start ATG codon and Kozak sequence, under CMV promoter	this study
pEGFP-N1-ΔMAL	Murine MRTF-A-without first 173 aa C-terminally fused to eGFP , under CMV promoter	this study
pEGFP-C1-ΔMAL	murine MRTF-A-without first 173 aa N-terminally fused to eGFP , under CMV promoter	this study
pC1-TagRFP	pEGFP-C1 vector with TagRFP instead of eGFP	this study
pC1-TagRFP-ΔMAL	Murine MRTF-A-without first 173 aa N-terminally fused to TagRFP, under CMV promoter	this study
pC1-TagRFP-MAL f.l.	Full length murine MRTF-A N-terminally fused to TagRFP, under CMV promoter	this study

III.1.7. Cells

Bacterial strains

Name	Description	Source
E. coli DH5α	F- φ80/*lac*Z ΔM15 Δ(*lac*ZYA-*arg*F) U169 *deo*R *rec*A1 endA1 endA1 *hsd*R17(rK-, mK+) *pho*A *sup*E44 thi-1 *gyr*A96 *rel*A1 λ-	Invitrogen (Karlsruhe)

Mammalian cells

Name	Description	Source
NIH 3T3	Spontaneously immortalized mouse embryonic fibroblasts	R.Treisman, CRUK (London, UK), Godaro & Green, 1963
NIH 3T3 - FUCCI	NIH 3T3 line stably expressing FUCCI markers, G418-resistant.	This study
NIH 3T3 –H2BGFP	NIH 3T3 line stably expressing histone H2B-GFP fusion	This study
NIH 3T3 –TR.TO e.v.	NIH 3T3 line with incorporated pcDNA6.TR and pcDNA4.TO empty vectors.	A.Descot
NIH 3T3 –TR.TO actin^{wt}	Tet-inducible NIH 3T3 line stably expressing wild type β-actin (from pcDNA4.TO vector)	A.Descot
MEF^{wt}	Wild type mouse embryonic fibroblasts immortalised with large T antigen of SV40	A.Descot
MEF E6i	SV40 large T antigen-immortalised wilt type MEFs. Wild type control for E8i MEFs	Marc Schmidt-Supprian, MPI for Biochemistry, Martinsried
MEF E8i	SV40 large T antigen-immortalised MEFs from NEMO$^{-/-}$ mouse embryos	Marc Schmidt-Supprian, MPI for Biochemistry, Martinsried

Name	Description	Source
MEF $p53^{-/-}$	SV40 large T antigen-immortalised MEFs from $p53^{-/-}$ mouse embryos	A.Descot
Phoenix E	Second generation retrovirus producer cell line, based on 293T cells (human embryonic kidney cells transformed with adenovirus E1a and carrying temperature-sensitive T antigen co-selected with neomycin)	Created by G.P.Nolan (Stanford, USA) Provided by A.Ullrich (MPI for Biochemistry, Martinsried)
NIH 3T3- shMAL	NIH 3T3 cells stably expressing shRNA against MRTF-A/B from pSUPER.retro.puro plasmid	This study
NIH 3T3 –pSUPER. retro.puro empty vector	NIH 3T3 cells with incorporated pSUPER.retro.puro vector. Used as negative control for NIH 3T3-shMAL cell line	This study

III.1.8. Culture media

Bacterial media

Lysogeny broth (LB) was used for propagation of bacterial cultures. It contained the following components per 1L: 10g Tryptone/peptone; 5g yeast extract; 10g NaCl. If necessary, supplemented with 100 µg/mL ampicillin, or 30 µg/mL kanamycin. Solid medium produced by adding 1.5% agar-agar.

Mammalian cell culture medium

All cell lines were routinely maintained in **full DMEM**: high glucose (4.5 g/L) + 1X L-glutamine,+ 1X sodium pyruvate,+ 1X penicillin-streptomycin + 10% FBS.

F**reezing medium**..... full DMEM with 20% FBS (instead of 10%) + 10% DMSO
S**erum starvation medium** ..... full DMEM with 0.5% FBS or 0.2% BSA (instead of 10% FBS)
L**ive microscopy medium**..... full DMEM (10% FBS) without phenol red.
S**ILAC labeling medium** ..... full DMEM (10% dialyzed FBS) without Arginine and Lysine, supplemented with Arg0 and Lys0 (light medium) or Arg10 and Lys8 (heavy medium).

Methods

III.2.1. Molecular cloning and DNA manipulation methods

Preparation of electrocompetent bacteria

Single colony of DH5α cells, grown on LB-agar plate, was inoculated into 5 mL of LB broth and incubated overnight (37°C, 180 RPM) to generate starter culture. Starter culture was diluted 1:100 in fresh LB broth and grown until OD_{600}= 0.5-0.6. Cells harvested by centrifugation (1200xg, 10 min, 4°C). Pellet was re-suspended in equal to the original volume of ice-cold 10% glycerol and incubated for 20 min at 4°C. Cells centrifuged as before and re-suspended in 10% of the original volume of ice-cold 10% glycerol followed by incubation for 20 min at 4°C. Cells were pelleted again and re-suspended in 2 ml of 10% glycerol, aliquoted in eppendorf tubes (40 µL each) and shock-frozen in liquid nitrogen. Aliquots stored at -80°C. Every new preparation routinely tested for transformation efficiency by electroporating 1 ng of pUC18 plasmid. Batches with efficiencies less than $5x10^7$ colonies per µg of DNA were discarded.

Electroporation of competent bacteria

40 µL aliquots of electrocompetent bacteria were thawed on ice. DNA (ligation reactions – no more than 5 µL, purified DNA – 5-15 ng) was added and misture was transferred into an ice-cold electroporation cuvette (0.2 cm, Bio-Rad). Electroporated using Genepulcer XCell™ with the following settings: 2.5 kV, 25 µF and 200 Ohm. After zapping, 500 µL of pre-warmed LB medium was added and cells were incubated at 37°C with shaking for 60 minutes. 20 and 200 µL aliquots were plated onto LB-agar plates containing appropriate antibiotics and incubated at 37°C overnight.

Preparation of plasmid DNA.

Plasmids were purified from bacterial cultures using either QIAGEN Plasmid Mini Kit or QIAGEN Plasmid Maxi Kit according to manufacturer's instructions.

DNA manipulation

Restriction digests carried out in 20 µL (analytical) or 50 µL (preparative) volumes. Amounts of DNA were 0.5-3 µg. Single and double digests were done according to recommendations from restriction enzyme supplier using provided buffers (New England Biolabs). Incubation times – 1-2 hours. Where necessary, overhangs were blunted using large (Klenow) fragment of DNA polymerase I, according to manufacturer's instructions (NEB). To prevent self-circularization of digested plasmid DNA, 5'-termini were de-phosphorylated using calf intestinal alkaline phosphatase according to manufacturer's instructions (NEB). Directly after all necessary DNA manipulations were finished, fragments were purified from agarose gels using QIAquick PCR Purification Kit or QIAquick MinElute PCR Purification Kit. Purified fragments were used at 1:3 (sticky ends) or 1:10 (blunt ends) molar vector:insert ratios for ligation in 10 µL, using 1 µL of T4 DNA ligase and supplied buffer (NEB). Self-ligation control (ligation without insert) was set up in parallel using the same amount of vector as in test reaction. Ligation was routinely carried out overnight at 16°C followed by inactivation at 70°C for 15 minutes. 1-2 µL of ligation mix was used to electroporate competent cells.

High fidelity PCR

DNA fragments for cloning purposes were amplified using Phusion® High Fidelity polymerase, using HF reaction buffer. Reactions carried out in presence of 0.25 µM primers, according to manufacturer's recommendations. Routinely, 36 cycles of amplification were used, while annealing temperature and time varied with melting temperature of primers. PCR products were run on agarose gels and purified either using QIAquick PCR Purification Kit or QIAquick MinElute PCR Purification Kit.

Colony PCR

Screening for insert-containing clones was done using either restriction digest or colony PCR. The latter was carried out as follows: master mix, consisting of 2U Taq polymerase, 1X Thermopol buffer (NEB), 250 µM dNTPs, 0.5 µM primers, and 8.25 µL H2O per reaction was dispensed in 0.2 mL PCR tubes. Well isolated colony was picked with pipette tip and first streaked onto fresh LB-agar plate and then dipped into PCR tube. PCR was carried out for 36 cycles, annealing temperature varied for different primer pairs

Agarose gel electrophoresis

Agarose solutions (0.8% - 2.5%) were prepared by boiling agarose powder in TBE buffer. Ethidium bromide (0.01%, v/v) was added to the solution before polymerization. Gels were polymerized at room temperature for a minimum of 40 minutes. DNA samples mixed with 6X loading dye were loaded into wells and separated at 100-120V until Orange G dye reached the bottom of the gel. DNA visualized and documented using 302 nm UV light. For excision of fragments, DNA was visualized using 460 nm blue light (Dark Reader™, Clare Chemical Research).

Sequencing of DNA fragments

was done by the core facility of the MPI of Biochemistry, Martinsried

III.2.2. Mammalian cell culture methods

General procedures

All mammalian cells were incubated at 37°C, 10% CO_2. Cell work was carried out in a biosafety level S1 laboratory using sterile laminar flow cabinets. For cell counting, improved Neubauer chamber (hemacytometer) was used. For freezing, cells were re-suspended in freezing medium, aliquoted into CryoTube™ vials and deposited at -80°C in isopropanol chambers. 24-48 hours later vial were transferred to liquid nitrogen for long term storage. Thawing of cells was done in water bath set at 37°C for 2-3 minutes.

Introduction of nucleic acids into the cells

Lipofection

Transient transfections for reporter assays (luciferase assay) were done using Lipofectamine® reagent as described previously (Posern, 2004). 35000 cells in every well of a 12-well plate were seeded the day before transfections. 100 µL complexes were prepared using OPTI-MEM medium with 2 µL of lipofectamine reagent and 500 ng of DNA (20 ng p3D.A reporter, 50 ng ptkRL reporter, plus co-transfected construct or empty vector up to 500 ng). Following 20 minutes incubation at room temperature, complexes were added to wells with 0.5 mL OPTI-MEM. 5 hours later, medium was changed to starvation medium for 16-24 hours. Stimulations were done with 15% FBS for 7 hours.

Other transient transfections were done using Lipofectamine® 2000 according to manufacturer's instructions.

Transient transfections of siRNAs were carried out using Lipofectamine® RNAiMAX, according to manufacturer's protocol. Briefly, 40000 cells were seeded in 12-well plates, 250000 cells seeded into 6-cm dishes. For 12-well plates, 30 pmol siRNA and 3 µL Lipofectamine were used to make complexes. For 6-cm dishes, 80 pmol and 10 µL Lipofectamine were used.

Retroviral transfections

First, packaging line Phoenix E was transiently transfected with pLPCX plasmids using calcium phosphate method (Sambrook, 2001). Briefly, $15x10^6$ cells were seeded into 15-cm dishes 24 hours before transfection. One hour before transfection, medium was replaced with 15 ml fresh medium containing 25 µM chloroquine. For each transfection, 1 mL 250 mM $CaCl_2$ was mixed with 40 µg of plasmid DNA. To the mix, 1 mL of 2X BBS solution was added dropwise while vortexing. Mixture incubated for 20 minutes at room temperature and added to the dishes. Packaging cells incubated at 3% CO2, 37°C for 24 hours. Next day, medium changed to fresh medium without antibiotics and cells incubated for another 24 hours at 7% CO2, 32°C to produce viruses.

One 15-cm dish of virus-producing packaging line was used to infect NIH 3T3 cells in 6-cm dish. $1.5x10^5$ NIH 3T3 cells were seeded one day before infection and medium was changed to fresh DMEM supplemented with 8 µg/mL polybrene just before infections. Supernatant from transfected packaging cells was concentrated using Vivaspin 20 centrifugal concentrators (Sartorius, Göttingen) down to 1 -2 mL and used to infect NIH 3T3 cells. Packaging line was supplemented with fresh medium again and second round of infections repeated 8 hours later.

Generation of stable cell lines

Cells stably expressing FUCCI markers and H2B-GFP were generated following transfection with Lipofectamine® 2000. NIH-3T3-FUCCI cells were FACS-sorted as follows: first two sorts – mAG-positive cells only, next 4 times – mAG- and mKO2-double positive cells. Between sorts and afterwards cells were maintained in medium supplemented with 250 µg/mL of G418. NIH 3T3-H2BGFP cells were sorted 2 times for GFP-positive cells. Between sorts and afterwards maintained in 0.2 µg/mL puromycin. NIH 3T3-shMAL and NIH 3T3 pSUPER empty vector cell lines were generated following retroviral transfection with pSUPER.retro.puro-shMAL or pSUPER.retro.puro empty vector and selection with 1µg/mL puromycin for 3 weeks. These cell lines were further sub-cloned to produce monoclonal cell lines by re-seeding cells at 1:30 dilution and expanding individual clones after 2 weeks of selection. Both polyclonal pool and clones were afterwards maintained in medium supplemented with 0.2 µg/mL of puromycin. Stable NIH 3T3 cell lines expressing Tet-inducible $actin^{wt}$ or pcDNA.TO empty vector were maintained in medium supplemented with 2.5 µg/mL blasticidin and 150 µg/mL zeocin.

Proliferation assays

For MTT assay, cell were seeded into 96-well plates in quadruplicates 18 hours post-transfection and incubated for further 15 hours before the first time point. 1 hour before the time point, 40 µL of MTT solution (5 mg/mL in PBS) was added to the well and cell incubated for 1 hour. Medium was removed and MTT Formazan crystals dissolved in 150 µL of DMSO. Absorbance at 560 nm measured using Labsystems Multiscan RC (Thermo Scientific).

For cell counting, cells were seeded into 12-well plates in duplicates (10000 for 10% FBS-containing medium, 35000 for 0.5% FBS-containing medium). At the indicated time points, cells were trypsinized and counted using improved Neubauer chamber. 9 quadrants counted per sample.

III.2.3. Protein analytical methods.

Cell lysis for Western blotting

Cells were washed with ice-cold PBS in plates and ice-cold RIPA buffer, supplemented with 1X Complete™ protease inhibitor cocktail, added to the cell monolayer. Lysate scraped with rubber policeman and transferred into Eppendorf tubes. Before measuring concentration, lysate were pre-cleared by centrifugation at 14000 RPM for 10 minutes at 4°C.

Co-immunoprecipitation

For mass-spectrometry analysis of G-actin interacting proteins, Tet-inducible cell lines were stimulated with 1 µg/mL doxycycline for 24 hours and then serum starved in starvation medium (0.5% FBS) supplemented with doxycycline for another 18 hours. For every co-IP sample 2 15-cm dishes of ca. 70% confluent cells were used. After stimulation with 15% FBS for 30 minutes, cells were scraped from the dishes in 1 ml of PBS and pellets lysed in 1 mL of RIPA buffer supplemented with protease inhibitor cocktail. After centrifugation at 14000 RPM, 4°C for 20 minutes, 950 µL of lysates were incubated with 25 µL packed volume of anti-FLAG® M2 magnetic beads for 3 hours at 4°C. Beads were washed 3 times with 700 µL of lysis buffer and immunoprecipitated proteins eluted from the beads with 25 µL of 4x SDS-PAGE sample loading buffer (Invitrogen). Eluates from appropriate samples were mixed and separated on the gradient acrylamide gels.

Determination of protein concentration

Protein concentration measured using Micro BCA™ protein assay kit (Pierce) according to manufacturer's instructions using 96-well plate format. Briefly, for every measurement, standard curve was set up using provided BSA solution. In parallel, 2 µL of protein lysates were added to 100 µL of BCA reagent in triplicates and incubated for 30 minutes at 37°C. Absorption was measured at 595 nm using microplate reader. Protein concentration was calculated from standard curve using 2nd power polynomial equation.

SDS-polyacrylamide gel electrophoresis

Proteins were separated using PAGE according to Laemmli, 1970 with minor modifications. Stacking gel was 5% acrylamide-bis (37.5:1) solution in 127 mM Tris-HCl pH 6.8, 0.1% (w/v) SDS, 4.5% (v/v) glycerol and 0.1% (w/v) APS. Separating gel contained 8-12% acrylamide in 377 mM Tris-HCl pH 8.8, 0.1% (w/v) SDS and 0.1% (w/v) APS. 0.1% (v/v) TEMED was used for polymerization. Equalized amounts of lysates were mixed with 4X sample loading buffer, boiled at 95°C for 5 minutes and separated at 100-150V until bromphenol blue dye front reached the bottom of the gel. For mass-spectrometry analysis, pre-cast gradient (4-12%) NuPAGE® gels were used (Invitrogen). Following separation, gels were either stained with Coomassie using Colloidal Blue staining kit (Invitrogen) or used for western blotting.

Western blotting

Proteins were transferred to PVDF membrane using Mini Trans-Blot Cell (Bio-Rad) according to manufacturer's recommendations. Transfer was done at constant 100V for 1.5 hours. To monitor transfer efficiency, membranes were stained with Poceau to visualize proteins.

Immunoblot detection

After the transfer, membranes were blocked with 5% non-fat milk in TBS/T for 1 hour at room temperature. After blocking, membranes were incubated with primary antibodies in blocking solution overnight at 4°C. Next day, membranes were washed 3 times (5 minutes each) with TBS/T and

incubated with secondary antibodies in blocking solution for 1 hour at room temperature. For HRP-conjugated primary antibodies incubation was 1 hour at room temperature. After washing 3 times (10 minutes each) with TBS/T, membranes were incubated with Western Lightning ECL reagent for 1 minute. Signal was captured using cooled CCD-cameras on gel documentation systems (FujiFilm of Bio-Rad). When necessary, membranes were stripped using Restore Western Blot stripping buffer and the whole procedure from the blocking step onward was repeated.

III.2.4. Quantitative real-time PCR

Total RNA was isolated using QIAGEN RNeasy Mini Kit according to manufacturer's instructions. cDNA was synthesized from 1 µg of RNA and oligo-dT primer using Verso™ cDNA kit according to manufacturer's protocol. For qRT-PCR, cDNA was diluted 1:5. Reaction setup was as follows: 7.5 µL of SYBR Green Master mix, 0.25 µM gene-specific primers and H2O to 12.5 µL. 2.5 µl of diluted cDNA added to the mix to complete 15 µL reaction volumes. PCR reaction was carried out on either StepOnePlus or LightCycler 480 II instruments. Cycling conditions were 95°C for 10 seconds, 60°C for 30 seconds. Melting curves were routinely generated from every reaction to access the specificity of PCR. Relative concentrations were calculated using ΔΔCt method in qBase software (Hellemans, 2007).

III.2.5. Luciferase reporter assay

The luciferase reporter assay was carried out using Dual-Glo™ Luciferase Assay Kit (Promega). Cells were washed twice with ice-cold PBS and lysed by incubation in 100 µL of Passive Lysis Buffer (PLB) per one well of 12-well plate for 15 minutes. Lysates were transferred in eppendorf tubes and cleared by centrifugation at 13000 RPM for 5 minutes. 20 µL of the supernatant was transferred into a well of a white-walled 96 well microtiter plate and mixed with 45 µL LARII solution. Luminescence readings were collected and 45 µL of Stop & Glow reagent supplemented with Stop & Glow substrate was added to the well to stop the Firefly reaction and start Renilla luminescence emission. Luminescence was read again. Reporter activity was calculated by normalizing Firefly luminescence values with Renilla luminescence values

III.2.6. Cell cycle analysis

Propidium iodide staining was done according to Riccardi, 2006. Briefly, 18 hours post-transfection, cells were split into 6-cm plates and grown for indicated periods of time. Cells were collected by trypsinization and fixed with 70% ethanol. After washing with PBS, cells were stained for 30 min with 50 µg/mL propidium iodide in PBS, supplemented with 200 µg/mL RNase A. BD FACSCalibur or BD Accuri C6 (BD Biosciences) were employed to measure fluorescence from 20000 cells per sample. Data was analysed using FlowJo software v7 (TreeStar, USA). DNA histograms were generated by gating on single cell events and cell cycle phases de-convoluted using built-in Dean-Jet-Fox algorithm. BrdU staining was carried out using FITC BrdU Flow kit (BD Pharmigen) according to manufacturer's protocol. Briefly, cells were pulse-labeled with 10 µM BrdU for 20 minutes in medium, trypsinized and fixed. After DNA digestion, cells were stained with FITC-labeled anti-BrdU antibody for 20 min, co-stained with 7-AAD and analyzed with FACSCalibur or Accuri C6 flow cytometers. 50000 events collected per sample and dot plots of single events generated with FlowJo software.

III.2.7. Immunofluorescence staining

Cells were grown on uncoated glass coverslips in 12-well dishes. Prior to fixation, the cells were washed twice in PBS on ice. Then fixed in 4% PFA for 10 – 15 minutes at RT and permeabilized for 10 minutes in 0.2% Triton X-100 in PBS. Unspecific epitopes were blocked by incubation for 1 hour in blocking solution. Coverslips incubated with primary antibodies in blocking solution for 1 hour at room temperature, with phalloidin or nuclear dyes in PBS for 20 minutes at room temperature. Secondary antibodies in blocking buffer were applied for 1 hour at room temperature. Afterwards coverslips were washed 2 times with PBS, once with bi-distilled water and mounted onto glass slides with Mowiol reagent supplemented with 2.5% DABCO. Pictures acquired in MetaMorph of AxioVi-

sion software using either Zeiss Observer.A1 or Z1 microscopes with Plan-Apochromat 20x/0.8 or Plan-Apochromat 63x/1.40 Oil objectives.

III.2.8. Chromatin immunoprecipitation

$2x10^7$ NIH 3T3 cells for each immunoprecipitation reaction were fixed with 1% formaldehyde in growth medium for 10 minutes at room temperature. Cross-linking was stopped with 125 mM glycine for 5 minutes. Cells were washed twice with PBS and scraped in 3 ml of PBS into eppendorf tubes. Cell pellets were lysed with 3 mL Farnham lysis buffer (20 mM Tris-HCl, pH 8.0, 85 mM KCl, 0.5% Triton X-100) for 5 minutes on ice and nuclei pelleted by centrifugation at 500xg, 4°C, 5 minutes. Nuclear pellet was lysed using 1 mL of ChIP RIPA buffer (1% Triton X-100, 0.5% Na-deoxycholate, and 0.1% SDS in 1 X PBS) for 20 minutes on ice. Lysates were sonicated on Bandelin HD3100 sonicator equipped with MS72 tip with the following settings: 80% amplitude, 10 sec pulce, 30 sec pause. Every sample was sonicated for a total of 24 cycles (4 minutes of sonication). Sheared chromatin was pre-cleared by centrifugation at 14000 RPM, 4°C for 10 minutes. 40 µL of Dynabeads Protein G were pre-coupled with anti-MAL antibody (#79, 300 µl), anti-SRF antibody (G-20, 5 µg) or anti-NF2 antibody (5 µg) by incubating beads and antibodies in total volume of 500 µL (PBS) for 6 hours. 850 µL of sheared chromatin was mixed with antibody-coupled Dynabeads and incubated overnight on a rotating wheel at 4°C. After incubation, beads were washed 5 times with LiCl buffer (100 mM Tris-HCl, pH 7.5, 500 mM LiCl, 1% Tritox X-100, 1% Na-deoxycholate) and once with TE buffer. Complexes eluted with 100 µL of elution buffer (0.2% SDS, 0.1M NaHCO3) at 65°C for 30 minutes. Eluates and separately collected input chromatin samples were subjected to the cross-link reversal by supplementing 100 µL of sample with 5 µL of 5M NaCl, 1 µL of Proteinase K and 1 µL of RNase A. Samples were first incubated at 37°C for 1 hour and then at 65°C overnight. DNA purified using QIAGEN PCR purification kit according to manufacturer's instructions. Eluted in 100 µL of EB buffer and used for qualitative real-time PCR according to standard protocol. Results were calculated as percent of input chromatin according to the formula $2\%x2(Ct^{INPUT}-Ct^{IPsample})$, where 2% is the percentage of chromatin purified as input sample (for example, for 850 µL of chromatin used in IP, 17 µL of input chromatin is needed to make up 2%).

III.2.9. Live cell microscopy

Cells were seeded into non-coated, 4-chambered Cellview™ glass bottom dishes (Greiner Bio-One) 18 hours post-transfection and incubated for 6 hours before live imaging was started. During live imaging, cells were maintained at 37°C, 10% CO_2 in a Carl Zeiss Observer.Z1 microscope equipped with incubator XL S1 (Pecon), TempModule S, CO_2 module S and heating unit XL S. Images captured every 5 min for 48 to 65 hours with AxioCam MRm camera and Plan-Apochromat 10x/0.45 objective (FUCCI markers) or Plan-Apochromat 20x/0.8 objective (H2BGFP). GFP and mAG fluorescence imaged using Zeiss Filter Set 38HE (BP470/40, FT 495, BP 525/50), mKO2 fluorescence imaged using Zeiss Filter Set 43HE (BP 545/25, FT570, BP 605/70). Exposures were 200 ms for mAG, 400 ms for mKO2 and 90 ms for GFP. Images were saved with AxioVision 4.7 software. For analysis, TIFFs were exported to ImageJ software and manually analyzed for individual cell phase duration, total cell cycle length, duration of mitosis.

III.2.10. Mass-spectrometry

SILAC-based mass-spectrometry analysis was done according to Ong, 2007. Briefly, cells were labeled with heavy and light amino acids (see above) for at least 6 generations. After determining that the labeling efficiency was greater than 99%, cells were serum-starved, stimulated and subjected to co-immunoprecipitation. coIP samples were separated using PAGE and protein samples for analysis prepared using in-gel digestion protocol. Briefly, every lane of the gel was cut into 6 slices and each slice was further cut into small cubes, with the side of approximately 1mm. Gel cubes were washed with 50 mM ammonium bicarbonate (ABC), 50% acetonitrile until fully de-stained. Gel cubes were further dehydrated with acetonitrile and re-hydrated with 50 mM ABC with 10 mM DTT.

Proteins were reduced at 56°C for 1 hour. Resulting thiol groups were alkylated by adding 55 mM iodoacetamide in 50 mM ABC for 1 hour at 25°C in the dark. After washing, gel cubes were dehydrated in acetonitrile and dried in vacuum concentrator. Each sample was re-hydrated using 50 mM ABC solution containing 0.4 µg trypsin. Digestion was carried out at 37°C overnight. Peptides were extracted from the gel cubes 2 times with 30% acetonitrile-3% trifluoroacetic acid (TFA) and 2 times with 100% acetonitrile. All extracts were combined and acetonitrile was evaporated in a vacuum concentrator. Samples were de-salted using home-made reverse phase C18 STAGE Tips (Rappsilber, 2003) and eluted peptides were used for mass-spectrometry analysis. All peptides were separated by on-line reverse phase nano-liquid chromatography (nano-LC) using Agilent 1100 nanoflow system connected to LTQ-Orbitrap mass spectrometer, equipped with nano-electrospray ion source (Proxeon Biosystems). Loaded peptides were eluted with 140-min gradients from 5-40% acetonitrile in 0.5% acetic acid. Data acquisition performed using Xcalibur 2.0 software in positive ion mode. Identification of peptides and downstream analysis was done using MASCOT search engine, MSQuant software and custom R scripts. All analysis performed by collaborators.

IV. RESULTS

Novel targets of MRTF-SRF pathway: validation using chromatin immunoprecipitation.

IV.1.1. Identification of G-actin regulated genes: combination of actin-binding drugs and microarray analysis.

Transcription via MRTF-SRF pathway is regulated through direct physical interaction between MRTF co-activators and monomeric G-actin and therefore depends on the availability of G-actin pool in a cell. Interfering with actin polymerization dynamics by using cytochalasin D and latrunculin B have antagonistic effects on the MRTF-SRF pathway. Used at certain concentrations, cytochalasin D potently activates MRTF-mediated transcription, while pre-treatment with latrunculin B quenches the effect of cytochalasin D and represses the pathway further, past the level of background transcription (Descot *et al.*, 2009). Our group previously employed this phenomenon to identify genes transcriptionally regulated by G-actin dynamics on a whole-genome scale. RNA isolated from NIH 3T3 cells that were treated with cytochalasin D alone or in combination with latrunculin B, was analyzed using Affimetrix Gene Chip arrays. Genes up-regulated by cytochalasin D, but repressed by double treatment with cytochalasin D and latrunculin B were considered as putative G-actin-regulated targets and analyzed further. For detailed description of the screening approach and full list of identified targets, see (Descot *et al.*, 2009) and GEO dataset GSE17105.

IV.1.2. Chromatin immunoprecipitation protocol

The focus of several projects in our group was to characterize certain target genes from the microarray screen as direct MRTF-SRF targets. The most conclusive approach to show direct physical recruitment of a transcriptional co-activator to the promoter of a target gene is to employ chromatin immunoprecipitation (ChIP). My very first task was to establish a reliable ChIP protocol and use it to confirm the binding of MRTFs and SRF to the promoter elements of putative target genes. Various parameters of the protocol have been tested: initial cell number, sonication versus micrococcal nuclease digestion, sonication duration, immunoprecipitation conditions, various MRTF antibodies, washing conditions and DNA purification methods. Optimized protocol used $1.5x10^7$ NIH 3T3 cells, sonication of the genomic DNA in 1 ml of lysis buffer to the fragment sized between 300 and 1000 bp (Figure IV-1) and home-made anti-MRTF antibody #79. These conditions allowed for effective DNA shearing for better ChIP resolution and, at the same time, MRTF protein integrity was not compromised (Figure IV-2). Immunoprecipitation efficiency was adequate when using anti-MRTF antibody #79 (Figure IV-3), while other antibodies tested either did not work with the protocol or gave inferior results in qPCR (data not shown). Antibody #79 is polyclonal rabbit serum which recognized both MRTF-A and MRTF-B. Therefore, in ChIP experiments presented here it is technically not possible to discriminate between the two isoforms. Promoters of the known MRTF-SRF targets Cyr61 and SRF itself were used as positive controls to monitor the efficiency of the procedure. In control NIH 3T3 cells I consistently observed strong inducible recruitment of MRTFs to the promoters of Cyr61 and SRF upon stimulation with cytochalasin D. At the same time, in cells stably expressing shRNA against MRTFs this recruitment was strongly impaired (Figure IV-4). I employed this established ChIP method to probe the recruitment of SRF and MRTFs to certain genes that scored positively on Affimetrix microarray.

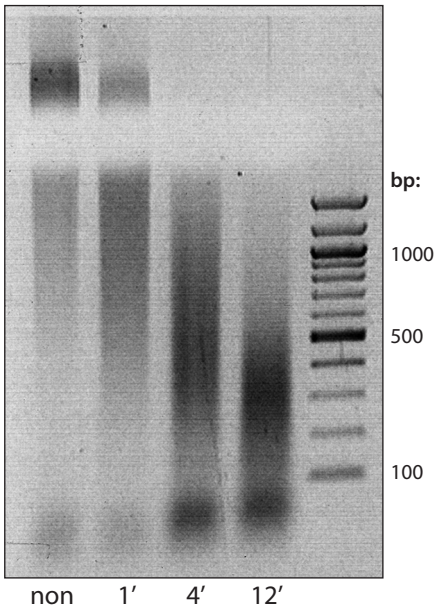

Figure IV-1: *Optimisation of chromatin shearing for ChIP.* NIH 3T3 cell lysates were sonicated for 0, 1, 4 or 12 minutes. 5 µg of total DNA was separated on 1% agarose gel. 4 minutes was used for subsequent experiments. Marker - log 2 ladder (NEB)

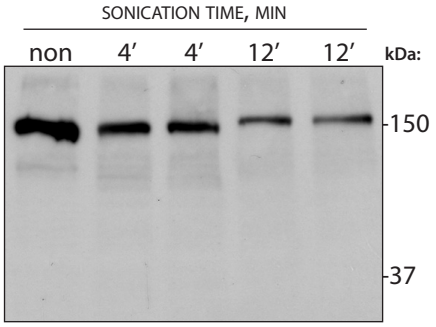

Figure IV-2: *MRTF-A/B protein integrity check following sonication.* Western blot showing MRTF-A/B in NIH 3T3 lysates after chromatin shearing for indicated times. Sonication to some extent reduces amount of protein in lysates, but the integrity is not compromised.

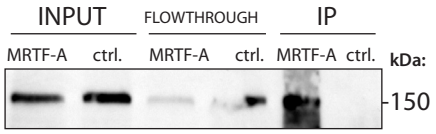

Figure IV-3: *Immunoprecipitationefficiency of MRTF-A/B using antibody #79 and ChIP protocol.* Western blot showing MRTF-A/B IP'd using ant-MRTF-A/B #79 antibody and nonsprecific control antibody. IP efficiency is greater than 90%. Control Ab does not precipitate MRTF-A/B

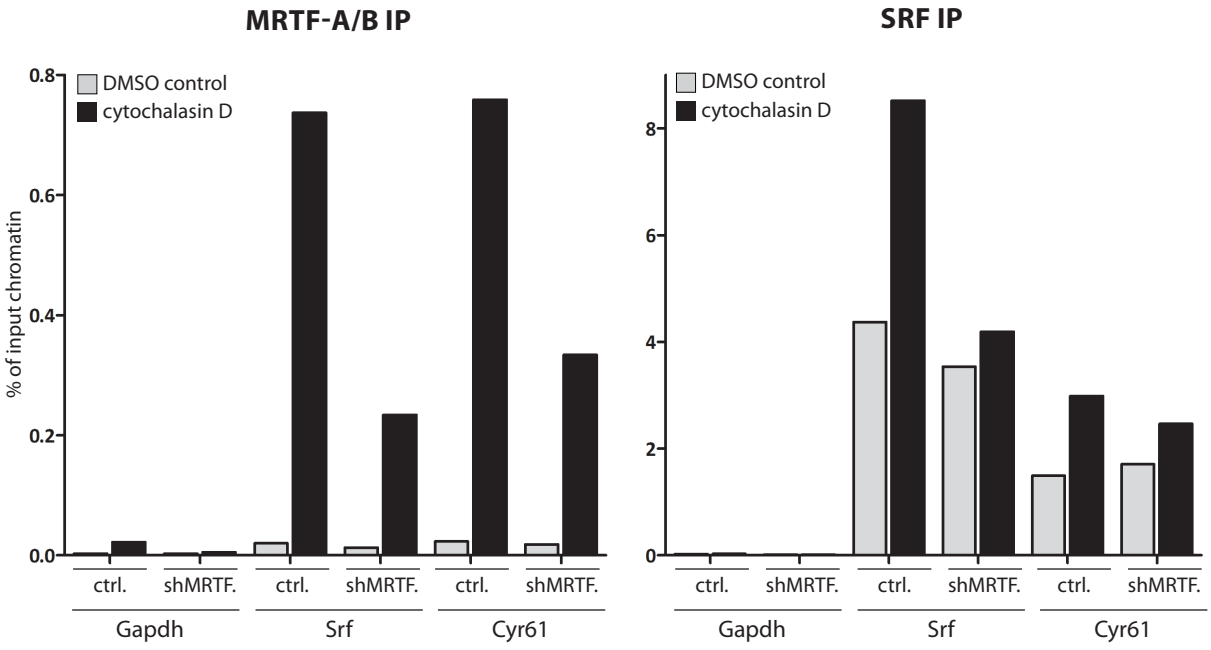

Figure IV-4: *Chromatin immunoprecipitation efficiency and specificity.* NIH 3T3 cells stably expressing empty pSuper.retro.puro (ctrl.) or shRNA against MRTF-A/B were serum starved for 24 hours and either stimulated with 2 μM cytochalasin D or left untreated (DMSO control). Following 30 min of stimulation, cells were subjected to chromatin immunoprecipitation using optimised protocol. Promoter fragments from known SRF target genes Srf and Cyr61 were amplified using real-time PCR. Gapdh promoter region served as negative control. MRTF-A/B knockdown cells display decreased enrichment of MRTFs on the promoters. Background binding of SRF is not affected by the knockdown. *n=1*

IV.1.3. Mig6/Errfi1

Mig6 is a negative regulator of EGFR signaling. It prevents EGFR dimer formation, thereby blocking the downstream signaling events (Zhang *et al.*, 2007). Promoter analysis done previously (Descot *et al.*, 2009), identified a putative SRF binding site at position -260 from the transcription start site. The sequence of this CarG-like element – CCTT***C***TAAGG – deviates from the consensus by the presence of base C in the A/T-rich core of the motif. Nevertheless, luciferase assays have established that a deletion of this CarG-like element leads to the complete block of transcription from the promoter fragment -392..-96. qPCR primers for amplification of the promoter fragment around the position -260 have been designed previously. ChIP experiments have established that, indeed, SRF is bound to this particular CarG-like element in serum-starved condition as well as upon stimulation with 15% fetal bovine serum. MRTFs, on the other hand, were only marginally bound to the same locus in the absence of stimulus, but were recruited to the promoter upon stimulation (Figure IV-5). Of note, the absolute recruitment levels of SRF and MRTFs to the Mig6 promoter were lower than those for the control SRF promoter, which potentially reflects the non-consensus nature of the CarG-like element in Mig6 promoter.

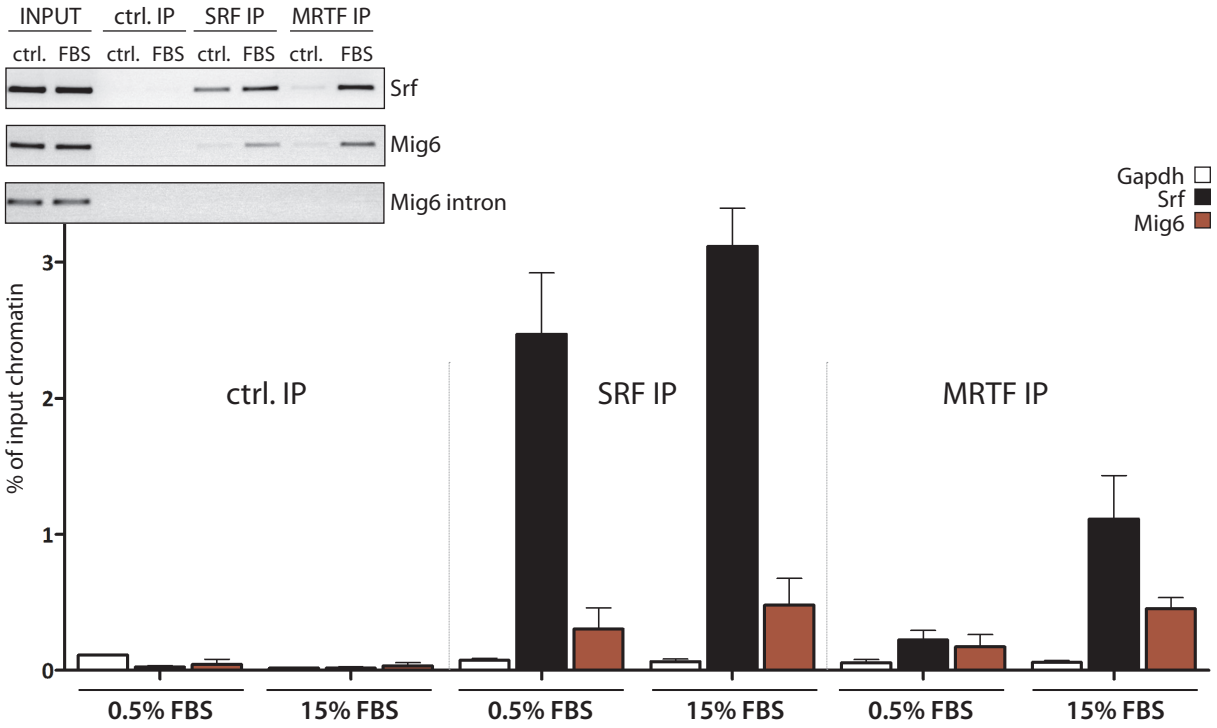

Figure IV-5: *Mig6 chromatin immunoprecipitation.* CarG-like element in Mig6 promoter (-260) is bound by SRF with ot without stimulation with 15% FBS for 30 min. MRTF-A/B are recruited to Mig6 promoter upon serum stimulation. Positive control Srf demonstrates similar behavior, although enrichment is stronger. Inset shows representative agarose gels with an additional negative control - intronic region of Mig6 gene. Real-time PCR, *n=3, bars - SEM.*

IV.1.4. Eplin-alpha

Epithelial Protein Lost in Neoplasm alpha has been recently established as an important component of adherens junctions in epithelial and endothelial cells with the suggested role in stabilizing capillary structures. It was proposed to act as a tether between VE-cadherin-catenin complexes and actin cytoskeleton, providing a link between the adherens junctions and intracellular cytoskeletal network (Chervin-Pétinot *et al.*, 2012). Analysis of the eplin-alpha promoter was done previously (Leitner *et al.*, 2010). In the first 2000 bp upstream from the transcription start site there are 2 potential SRF-binding sites, one of them is a consensus CarG box at -124 bp, and the second is a CarG-like element at position -1050. Luciferase assays have established that the 2000 bp long fragment of the immediate promoter was responsive to the serum and cytochalasin D stimulation, while latrunculin B had a repressing effect on the reporter. Deletion of the CarG-like element at position -1050 did not have an effect on the transcription, indicating that the consensus CarG box at position -124 is responsible for the transcription. For ChIP experiments I used qPCR primers amplify-

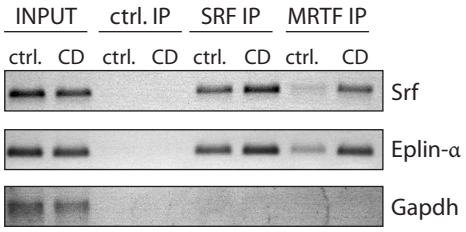

Figure IV-6: *Eplin-α chromatin immunoprecipitation.* Consensus CarG box at position -124 in Eplin-α promoter is bound by SRF. MRTF-A/B are recruited to this element upon stimulation with 2 μM cytochalasin D (30 min time point). Positive control, promoter region of Srf gene demonstrates similar behavior. Immunoprecipitation with non-specific antibody is shown only on the representative agarose gels. Real-time PCR, *n=3, bars - SEM.*

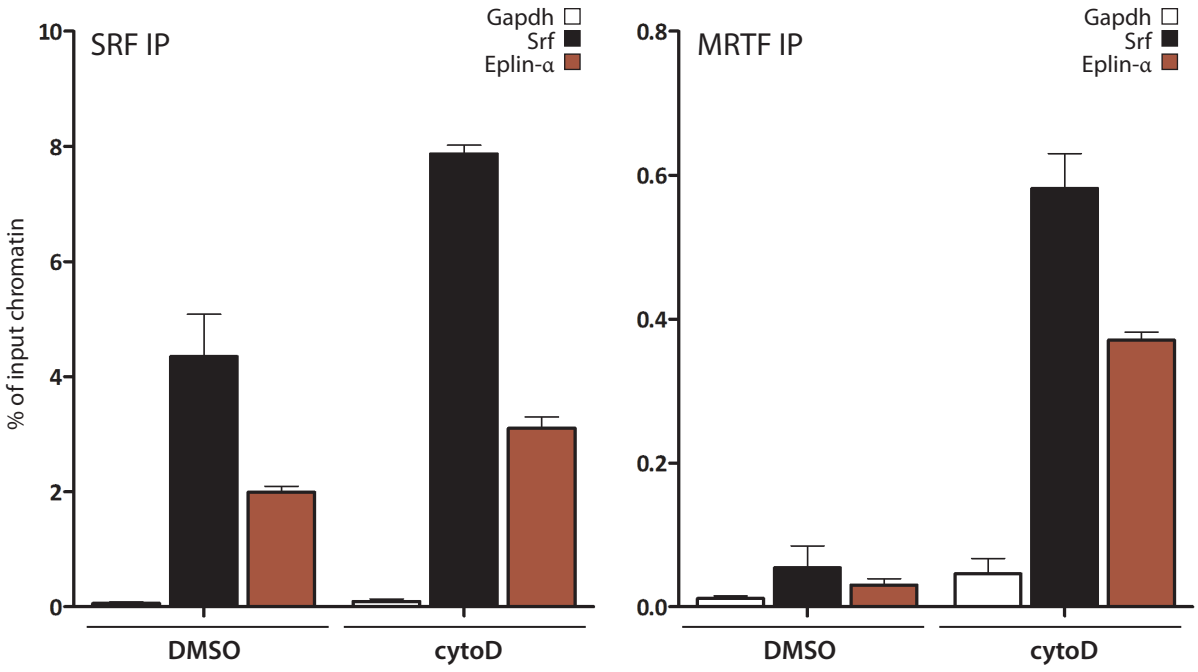

ing bases -178..-15 of the immediate promoter region of eplin-alpha gene and stimulation with cytochalasin D. Results (Figure IV-6) unequivocally place eplin-alpha into the cluster of SRF-MRTF-regulated genes. Recruitment pattern was similar for MRTFs, but I notice that SRF binds eplin-alpha promoter to a lesser extent with almost no observable increase in binding upon stimulation with cytochalasin D.

IV.1.5. Plakophilin 2, Pai-1, Fhl1

Plakophilin 2 is a member of the large armadillo plague proteins family. Is it localized to desmosomes of all proliferating epithelial cells and their derivative (e.g. tumors) (Bass-Zubek *et al.* 2009) and in the junctions connecting cardiomyocytes (Franke *et al.*, 2006). It has a critical role in heart development, since its knockout in mice and zebrafish results in lethality due to defects in heart formation (Grossmann *et al.*, 2004, Moriarty *et al.*, 2012).

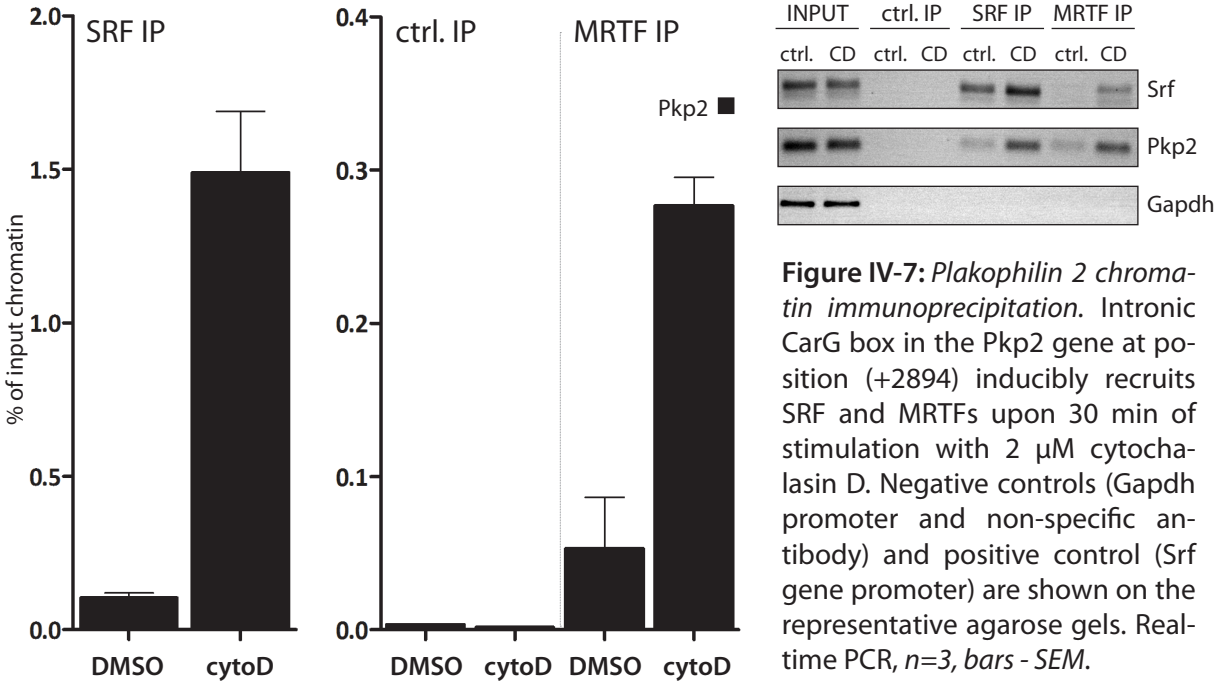

Figure IV-7: *Plakophilin 2 chromatin immunoprecipitation.* Intronic CarG box in the Pkp2 gene at position (+2894) inducibly recruits SRF and MRTFs upon 30 min of stimulation with 2 μM cytochalasin D. Negative controls (Gapdh promoter and non-specific antibody) and positive control (Srf gene promoter) are shown on the representative agarose gels. Real-time PCR, *n=3, bars - SEM.*

Surprisingly, pkp2 gene does not contain consensus CarG boxes in the immediate promoter up to 2000 bp upstream from the transcription start site. Several CarG-like elements found in this area did not recruit SRF or MRTFs to the corresponding promoter regions (data not shown). Further analysis (performed by Laura Leitner) has identified a consensus CarG box in the first intron of the gene at the position +2894 downstream from the transcription start site. ChiP using primers amplifying this region have confirmed an inducible binding of both SRF and MAL to the intronic CarG box (Figure IV-7) Intriguingly, unlike in control SRF promoter, where SRF is constantly bound to the DNA even in the absence of stimulus, SRF did not

occupy pkp2 promoter in the serum-starved cells, but got recruited upon serum stimulation.

Additional G-actin regulated genes that have been characterized as SRF-MRTF targets – plasminogen activator inhibitor 1(Pai-1) and four and a half LIM domains protein 1 (Fhl1) – were subjected to promoter analysis using chromatin immunoprecipitation. None of the tested CarG boxes or CarG-like elements within 2000 bp immediate promoters of both genes could show binding of SRF or MRTFs (data not shown), indicating that other binding sites might exist.

Anti-proliferative effect of MRTF-A in NIH 3T3 cells: apoptosis connection?

The fact that over-expression of constitutively active MRTF-A causes extensive cell death and is incompatible with clonal selection has been previously established by our group (Descot *et al.*, 2009). Moreover, this toxic effect positively correlated with the form of MRTF-A being over-expressed, i.e. full length protein with three intact RPEL motifs had almost negligible effect in retroviral transfections, while MRTF-A lacking first RPEL motif (MALmet), or constitutively active MRTF-A, which have all three RPEL motifs deleted (ΔN MAL), evoked gross enlargement of cells (Figure IV-8) accompanied by drastically increased cytotoxicity (Figure IV-9). Additionally, MRTF-A form that lack both C-terminal transactivation domain (which is indispensable for transcription) and three RPEL motifs had no adverse effects on cell proliferation (*Shaposhnikov et al.*, 2012), supporting the hypothesis that MRTF-A-mediated transcriptional activity is required for the observed effects.

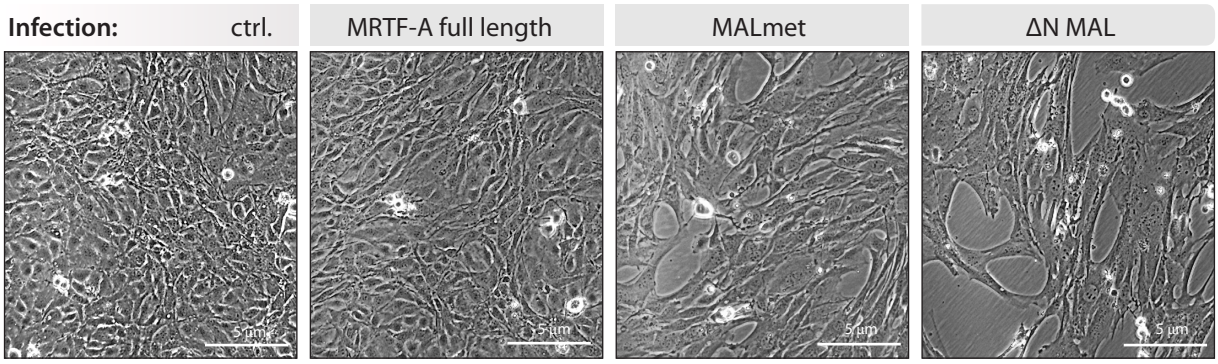

Figure IV-8: *Morphological changes in NIH 3T3 cells following MRTF-A over-expression.* Cells were infected with MRTF-A constructs using retroviral particles. ctrl. - pLPCX empty vector, MALmet - MRTF-A lacking first RPEL domain, ΔNMAL - MRTF-A lacking all three RPEL domains. Phase contrast pictures of live cells were taken 72 hours post-infection. *10x magnification*.

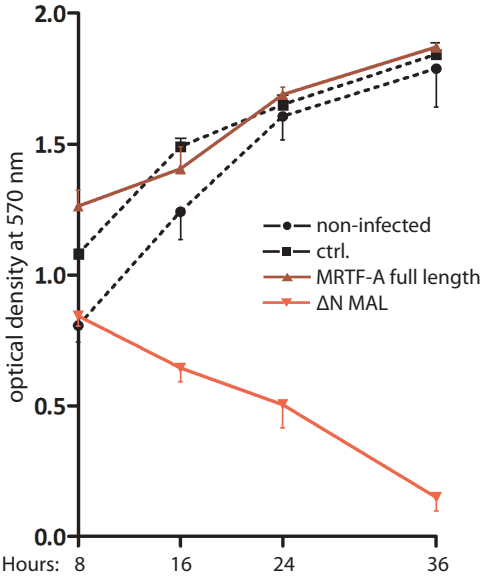

Figure IV-9: *Cytotoxic effect of constitutively active MRTF-A.* NIH 3T3 cells were infected with the indicated constructs and subjected to MTT assay at the time points shown. ctrl. - empty pLPCX vector. *n=1, bars - SEM of 3 technical triplicates*

Previous experiments with propidium iodide staining have identified an elevated sub-G1 population in MRTF-A over-expressing NIH 3T3 cells (Shaposhnikov *et al.*, 2012), pointing to the activation of classical apoptosis pathway. In order to pinpoint the involvement of apoptosis pathway in MRTF-A induced cell death, I have initially investigated one of the indicator events in the course of apoptosis execution – translocation of phosphatidylserine from the inner side of plasma membrane to the outer layer (Fadok *et al.,* 1992). Annexin V coupled to FITC (Vermes *et al.,* 1995) was used to detect PS in non-permeabilized NIH 3T3 cells transiently over-experssing either full length MRTF-A, or constitutively active MRTF-A (ΔN MAL). Time-course experiments have established that ΔN MAL, but not full length MRTF-A expressing cells display time-dependent increase in annexin V-positive staining (from 11 to 37%), characteristic of apoptotic cells (Figure IV-10). Importantly, a significant population of cells positive for both annexin V and propidium iodide was also detected, signifying the presence of cells with compromised plasma membrane integrity, which could represent either primary or secondary necrosis (Savill *et al.,* 2002, see Box 1). Therefore, these experiments do not eliminate the possibility of apoptosis-independent cell death occurring in parallel with true apoptosis.

Probably the most important hallmark of the classical apoptosis pathway is the activation of caspases (Salvesen & Dixit, 1997, Thornberry & Labeznik, 1998). Both extrinsic and intrinsic apoptosis pathways converge at the step of effector caspase activation: caspase-3 and 7 (reviewed in Tait and Green, 2010). Therefore, I set out to detect active form of the caspase-3 upon overexpression of constitutively active form of MRTF-A in NIH 3T3 cells. Staining with anti-active caspase-3 antibody coupled to phycoerytrin, followed by FACS analysis, have demonstrated that, indeed, a large percentage of MALmet and ΔN MAL overexpressing cells – 41.5% and 56.4% correspondingly – display positive staining for active caspase-3 (Figure IV-11). Of note, weak intensity of the FACS staining prompts to suggest that the activation of caspase-3 in these conditions happens only to a minor extent. Confirming this hypothesis, western blot analysis of total caspase-3 showed that only a small fraction of

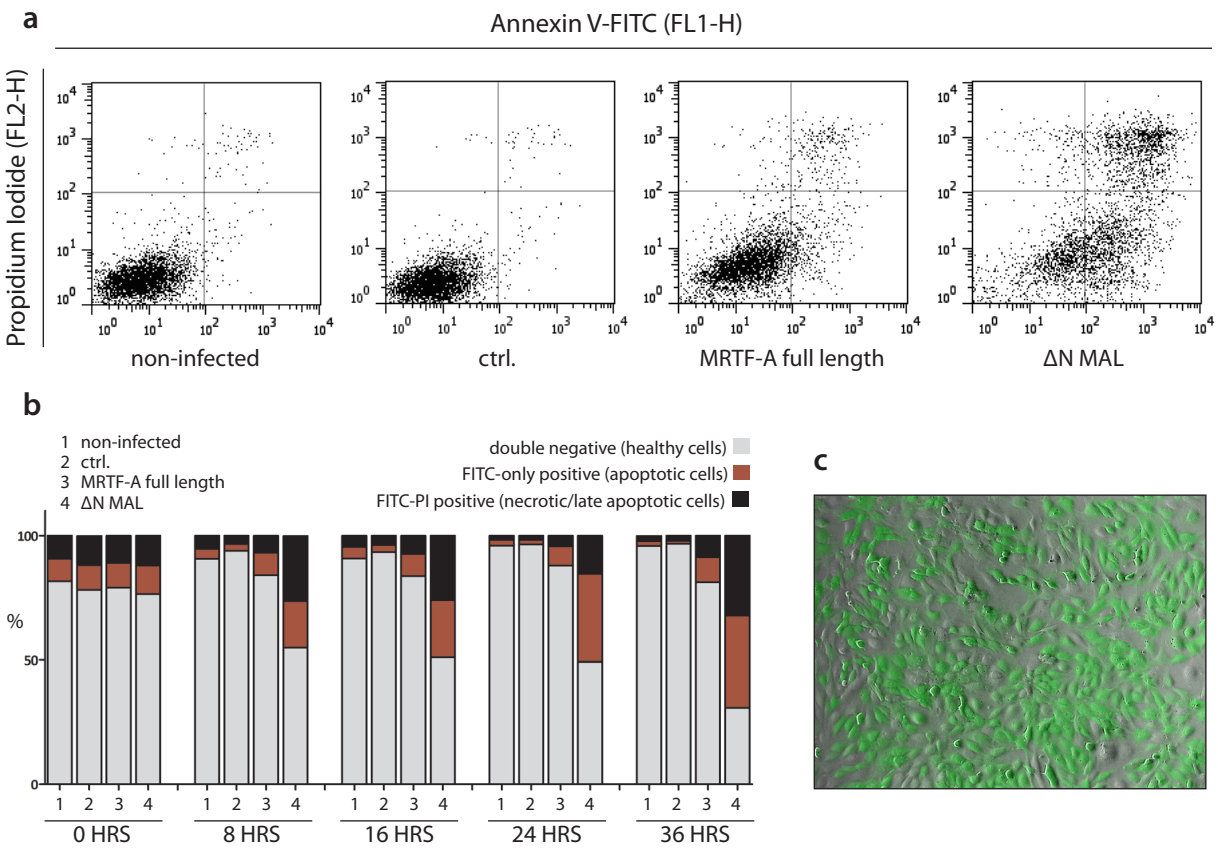

Figure IV-10: *Phosphatidylserine switch following MRTF-A over-expression.* NIH 3T3 cells were retrovirally infected with MRTF constructs and subjected to annexin V staining. **a.** Representative FACS scatter plots at 36 hours time point. 10000 cells per sample were analysed. Lower right quandrant contains apoptotic cells. **b.** Quantification of a time course of annexin V assay. Gray bars correspond to the lower left quadrant on scatter plot. Red bars - lower right quadrant, black bars - upper right and left quadrants. *n=1, representative experiment.* **c.** Infection efficiency. NIH 3T3 cells retrovirally infected with pLPCX-eGFP in parallel. Picture taken 36 hours post-infection. Overlay of phase contrast and eGFP fluorescence. Infection efficiency >95%.

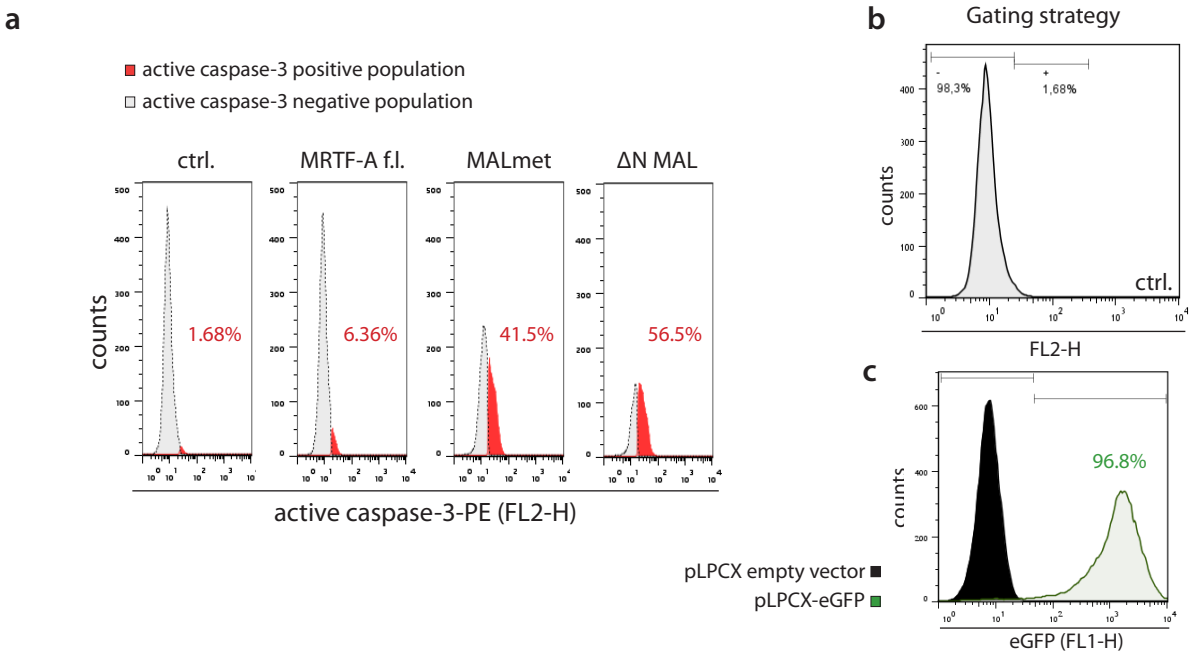

Figure IV-11: *Activation of caspase-3 following MRTF-A over-expression.* NIH 3T3 cells were retrovirally infected with MRTF-A constructs and subjected for active caspase-3 staining at 36 hours time point. **a.** Histograms showing caspase-3-positive and -negative populations in samples. Percentages of positive cells in each sample are indicated. Median FL2-H fluorescence was 8.98 for ctrl. (pLPCX empty vector), 9.31 for MRTF-A full length, 17.15 for MALmet (MRTF-A lacking first RPEL motif) and 21.67 for ΔN MAL. 10000 cells collected per sample. **b.** Gating strategy for histograms shown in a. **c.** Infection efficiency of pLPCX-eGFP vector at 36 hours time point. 96.8% of cells were infected.

caspase-3 is cleaved into the active form (Descot *et al.*, 2009 and data not shown).

To assess the extent to which caspases are responsible for the MRTF-A mediated cell death, I used a broad pan-caspase inhibitor zVAD-FMK (Slee *et al.*, 1996) alongside MRTF-A overexpression. Cells grown for 102 hours after retroviral infections with or without caspase inhibitor showed comparable levels of cytotoxicity (Figure IV-12), giving yet another indication that the role of the caspases (and classical apoptosis in general) in MRTF-mediated cell death might not be central. Alternatively, unidentified caspase-independent mechanisms could play a primary role here (see Dicussion). In summary, over-expression of active, but not full length MRTF-A could be directly linked to the activation of classical markers of apoptosis. This activation, however, occurs on a relatively minor scale and unlikely to be solely responsible for the extensive cell death observed in the experiments.

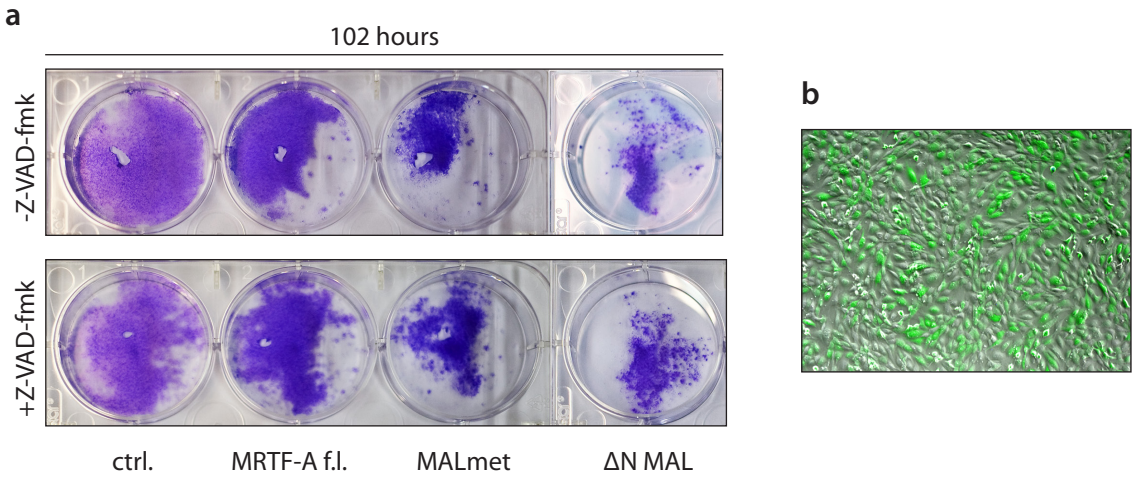

Figure IV-12: *Inhibition of caspases following MRTF-A over-expression.* **a.** NIH 3T3 cells were retrovirally infected with the indicated constructs and 20 μM Z-VAD-fmk was added at time point 0 hours. Fresh caspase inhibitor was re-added every 12 hours for a total of 102 hours. Afterwards cells were fixed with 4% PFA and stained with crystal violet. **b.** Infection efficiency of pLPCX-eGFP vector 36 hours post-infection. Overlay of phase contrast and eGFP fluorescence. 10x magnification. >90% of cells are infected.

MRTF-A regulates expression of pro-apoptotic proteins Bok and Noxa.

IV.3.1. MRTF-A is sufficient and required for Bok and Noxa transcription

Having observed a strong anti-proliferative effect of MRTF-A on NIH 3T3 cells, it was intriguing to discover that the microarray screen for G-actin-regulated genes described in Section IV.1.1, have identified several putative SRF-MRTF targets with the known function in apoptosis execution. Among them, Pmaip/Noxa and Bok were found to be up-regulated by cytochalasin D (6.04- and 2.92-fold, respectively). This activation was partially blocked by pre-treatment with latrunculin B (to 1.26- and 2.38-fold respectively) (Table IV-1). We hypothesized that MRTF-A-dependent transcription of Bok and Noxa plays a role in the anti-proliferative effect seen in over-expression studies and potentially contributes to the apoptosis induced by other stimuli. Therefore, initial microarray validation and promoter characterization studies were done by Arnaud Descot, and I joined this project with the goal to investigate the role of MRTFs in the regulation of Bok and Noxa in more detail.

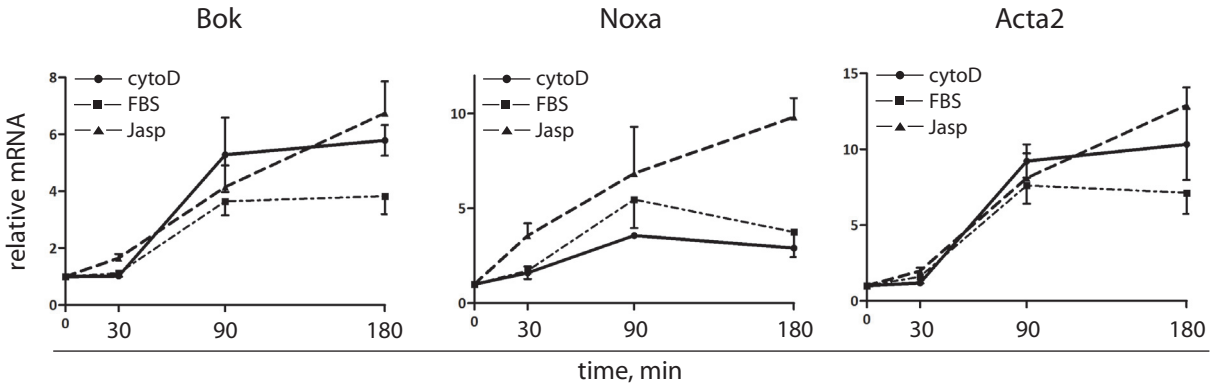

Figure IV-13: *Bok and Noxa mRNA temporal dynamics.* NIH 3T3 cells were treated with 2 μM cytochalasin D (CytoD), 15% FBS or 0.5 μM jasplakinolide (Jasp) for indicated periods of time. mRNA levels were quantified using real-time PCR and normalised to Hprt housekeeping control. Acta2 is a known SRF-MRTF target and served as a positive control. *n=3, bars - SEM.*

First, I examined the temporal dynamics of the Bok and Noxa mRNA following stimulation of NIH 3T3 cells with cytochalasin D, fetal bovine serum and F-actin stabilizing agent jasplakinolide, which is also able to activate SRF-MRTF signaling (Sotiropoulos *et al.*, 1999; Miralles *et al.*, 2003). Both Bok and Noxa mRNA levels were up-regulated at time points later than 30 minutes of stimulation (Figure IV-13). Induction profile of the Bok mRNA was similar to the control gene, smooth muscle α-actin, which is a well-characterized SRF-MRTF target.

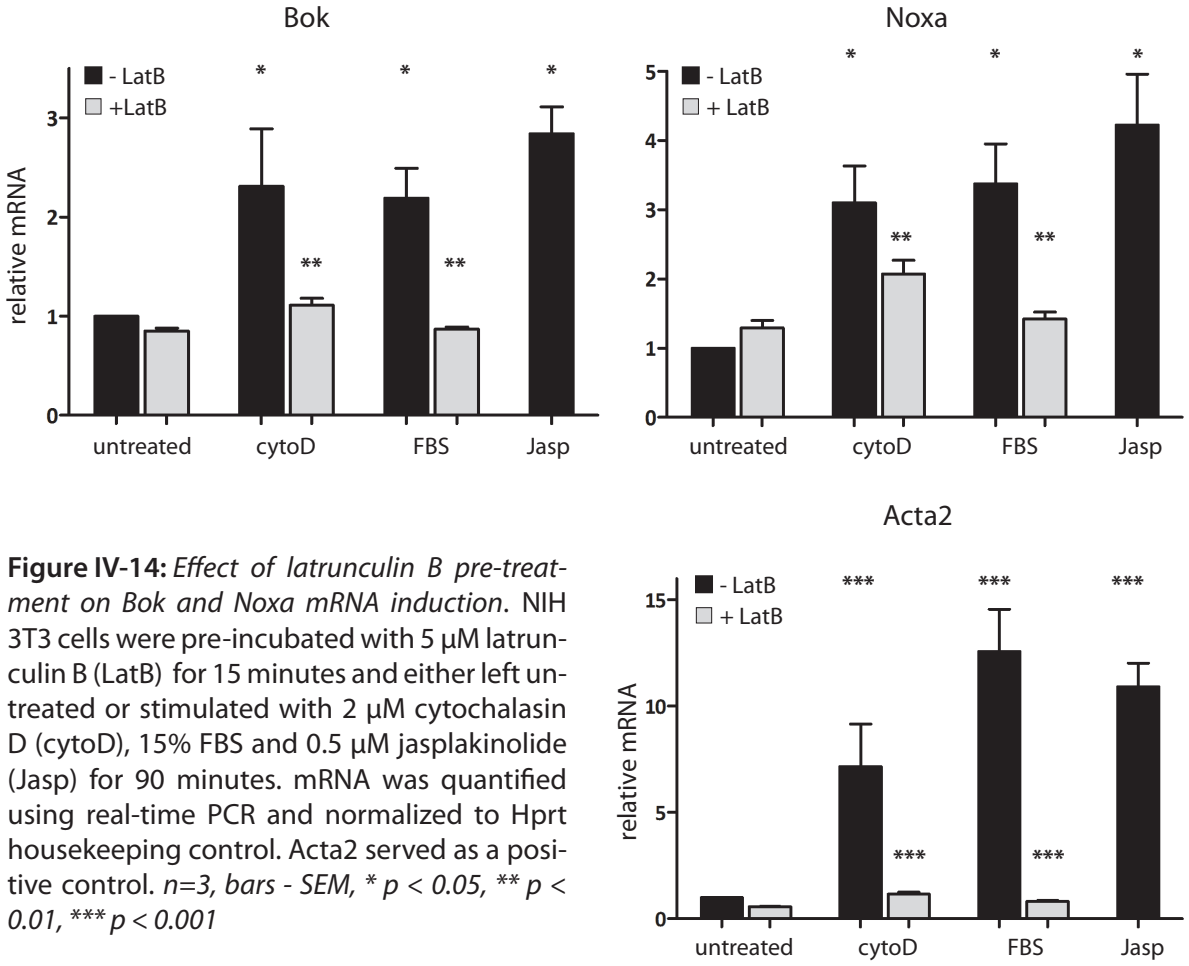

Figure IV-14: *Effect of latrunculin B pre-treatment on Bok and Noxa mRNA induction*. NIH 3T3 cells were pre-incubated with 5 µM latrunculin B (LatB) for 15 minutes and either left untreated or stimulated with 2 µM cytochalasin D (cytoD), 15% FBS and 0.5 µM jasplakinolide (Jasp) for 90 minutes. mRNA was quantified using real-time PCR and normalized to Hprt housekeeping control. Acta2 served as a positive control. *n=3, bars - SEM, * p < 0.05, ** p < 0.01, *** p < 0.001*

Noxa mRNA, on the other hand, displayed more transient activation pattern, dropping to the resting levels after 90 minutes of stimulation. To reproduce the conditions from the microarray screen, I used the same stimuli alone or in combination with 15 minutes of latrunculin B pre-treatment. After 90 minutes of stimulation, latrunculin B pre-treatment has efficiently suppressed cytochalasin D and serum-induced mRNA up-regulation (Figure IV-14). Additionally, over-expression of constitutively active MRTF-A in NIH 3T3 cells led to approximately 10-fold increase in relative mRNA abundance of both Bok and Noxa (Shaposhnikov *et al.*, 2012).

Table IV-1: Bok and Noxa probe sets from the Affimetrix microarray (Descot *et al.*, 2009)

			Induction		
Probe set ID	**Gene ID**	**Name**	**CytoD**	**CytoD+LatB**	**q-value**
1417040_a_at	Bok	Bcl-2-related ovarian killer	2.92	1.26	0.00
1418203_at	Pmaip1	TPA-induced protein 1	6.04	2.38	1.14

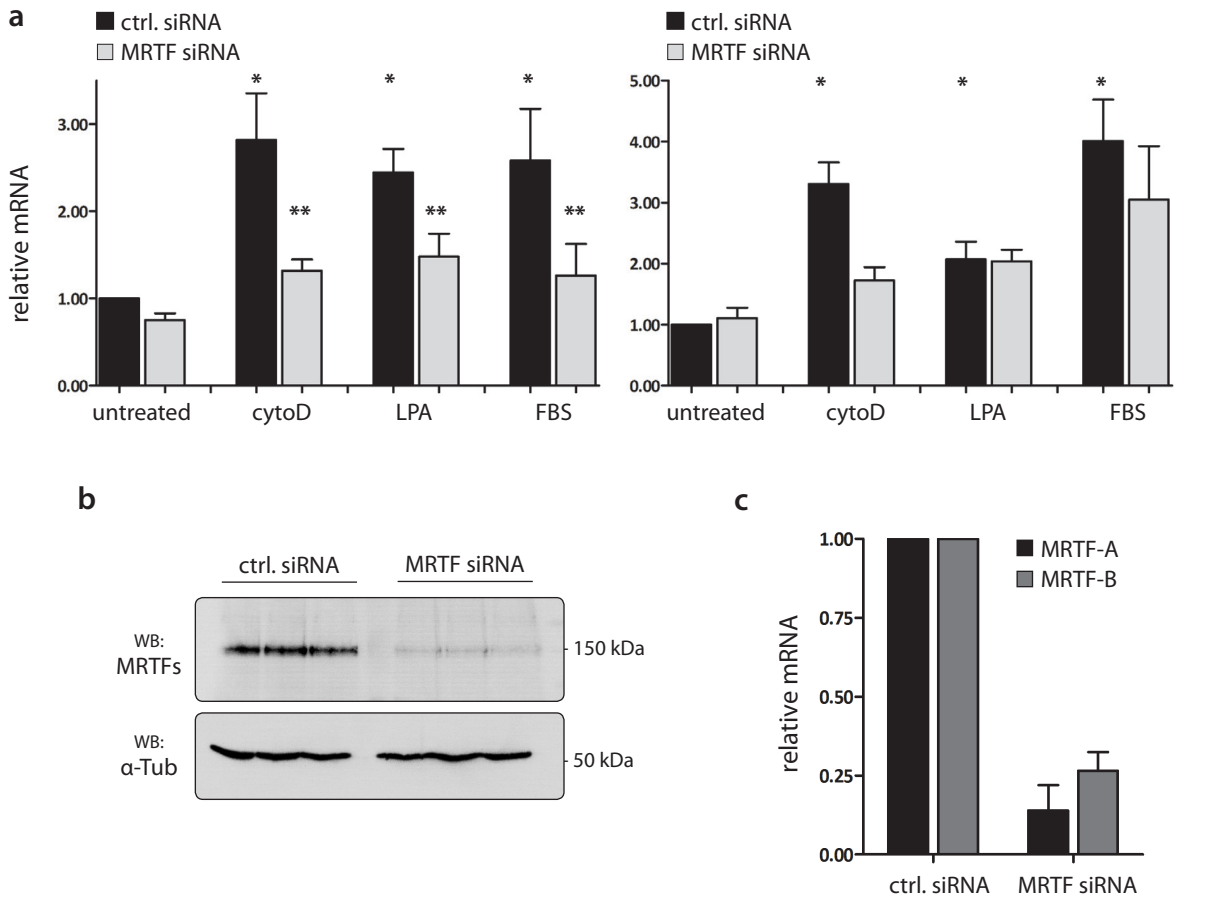

Figure IV-15: *Stimulation-dependent accumulation of Bok/Noxa mRNA following MRTF knock-down.* **a.** NIH 3T3 cells were transiently transfected with either control siRNA or siRNA against MRTFs. 12 hours post-transfection cells were serum starved for 24 hours and then either left untreated or stimulated with 2 μM cytochalasin D, 10 μM LPA or 15% FBS for 90 minutes. mRNA was quantified using real-time PCR and normalized to Hprt housekeeping control. *n=3, bars - SEM, * p<0.05, ** p<0.01.* **b.** Knockdown efficiency estimated by Western blotting and qPCR.

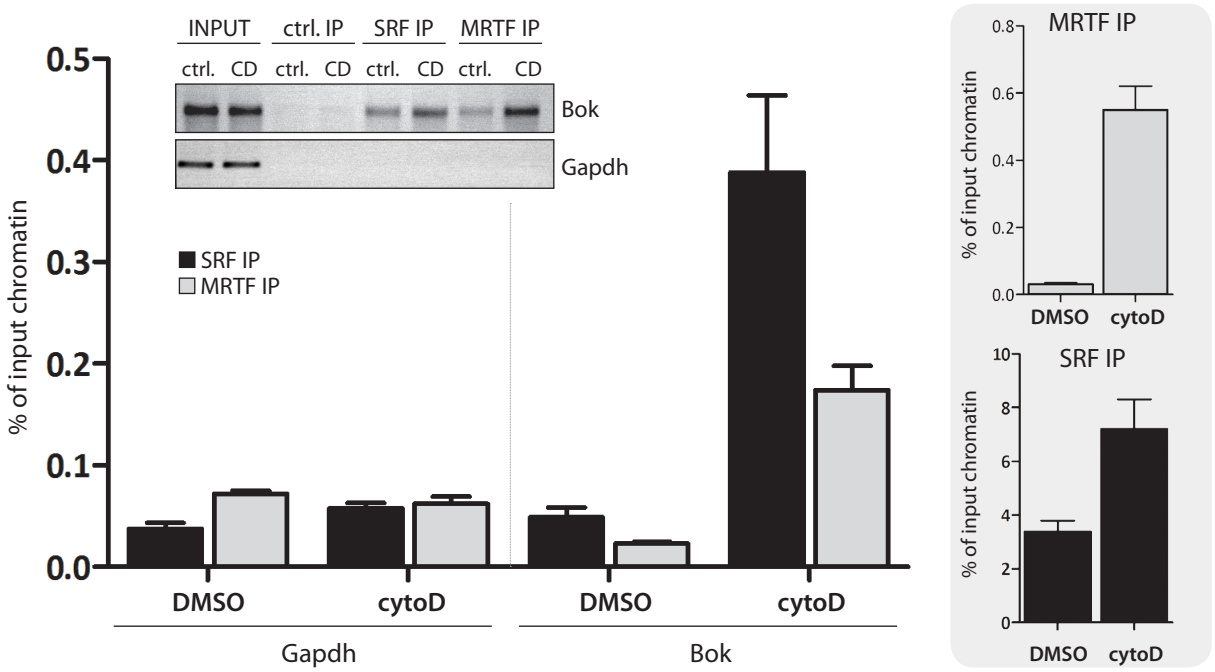

Figure IV-16: *Bok chromatin immunoprecipitation.* CarG-like element at position -99 in the proximal Bok promoter recriuts SRF and MRTF-A/B after stimulation with 2 μM cytochalasin D (30 minutes time point). Grey inset shows recruitment of SRF and MRTFs to a positive control promoter - Srf itself. *n=3, bars - SEM.*

Next I performed MRTF knockdown in the same cells to evaluate whether MRTFs are required for up-regulation of Bok and Noxa mRNA. In transient siRNA-mediated knockdown followed by stimulation with cytochalasin D, lysophosphatidic acid (LPA) and serum, Bok mRNA induction was severely impaired, while Noxa mRNA was affected less strongly (Figure IV-15A). In contrast, transient retroviral infections with shRNA of the same sequence have shown complete abrogation of induction for both genes (Shaposhnikov *et al.*, 2012). This discrepancy might a result of varying transfection/knockdown efficiencies between two knockdown methods, although siRNA-mediated knockdown was acceptably efficient (Figure IV-15B). Together, this data provided evidence that Bok and Noxa genes could be directly regulated by SRF-MRTF signaling pathway.

To identify SRF-MRTF responsive element in the promoters of Bok and Noxa, *in silico* analysis of proximal promoter regions was performed by Arnaud Descot. Immediate promoter of the Noxa gene (-2000..+1) contains one CArG-like element carrying a single mismatch from the consensus CArG box. Additional consensus CArG box was identified in the first intron of the gene. Similarly to the results obtained for some other target genes (Pai-1, Fhl1), ChIP experiments failed to show any significant binding of SRF or MRTFs to these cis-regulatory elements. We conclude, therefore, that Noxa regulation via SRF-MRTF pathway is unlikely to occur via proximal promoter or the first intronic region. On the other hand, a single CArG-like element at position -99 in the immediate promoter of the Bok gene was solely responsible for the promoter activity in luciferase reporter assays (Shaposhnikov *et al.*, 2012). Using stimulation with cytochalasin D followed by chromatin immunoprecipitation, I was able to show an inducible recruitment of both SRF and MRTFs to this CArG box (Figure IV-16). Similarly to the Plakophilin 2 promoter, SRF was not constitutively bound to the Bok promoter, like in classical SRF targets (*acta2*, *Srf*), but was inducibly recruited to the CArG box upon stimulation.

IV.3.2. The role of p53 in Bok and Noxa transcriptional regulation.

To date both Bok and Noxa genes have been thought as primarily regulated by p53 transcriptional factor. Direct p53 binding to the Noxa promoter has been shown previously (Oda *et al.*, 2000) and Noxa-deficient mouse embryonic fibroblasts were insensitive to p53-

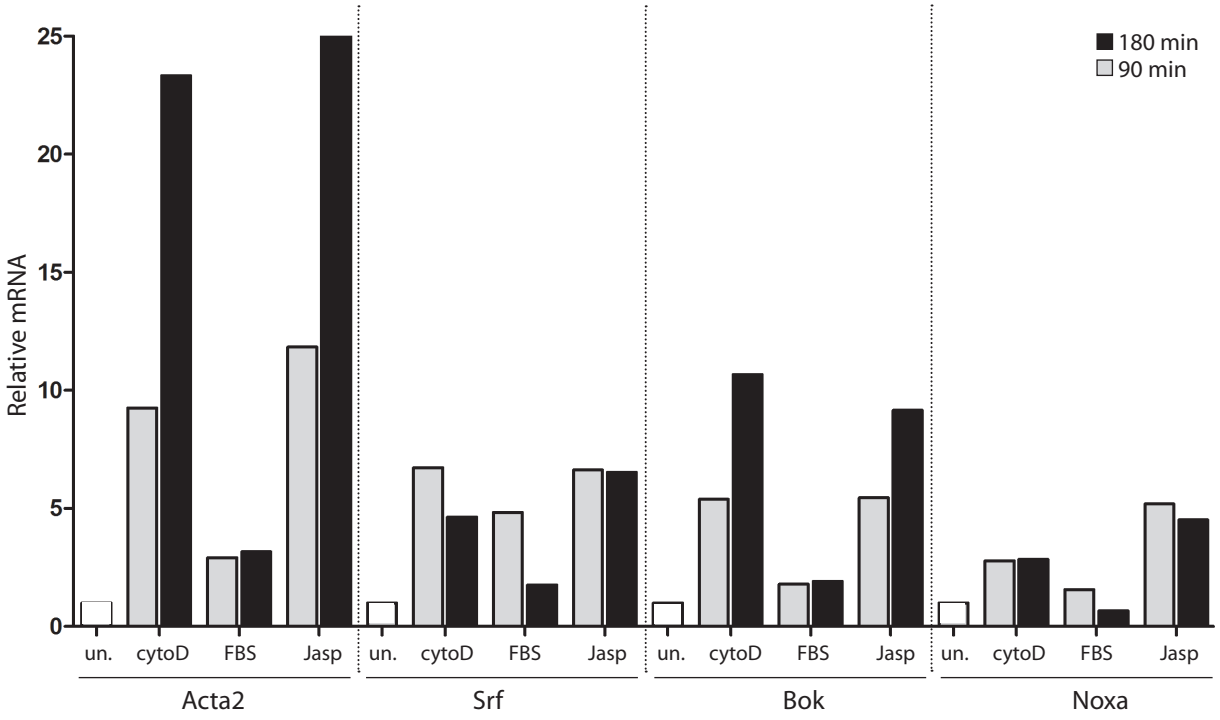

Figure IV-17: *Stimulation-dependent induction of Bok and Noxa in wild type MEFs.* MEF^{wt} were serum starved for 24 hours and either left untreated (un.) or stimulated with 2µM cytochalasin D (CytoD), 15% FBS or 0.5 µM jasplakinolide (Jasp) for 90 and 180 minutes. mRNA was quantified using real-time PCR and normalized to Hprt housekeeping control. *n=1*.

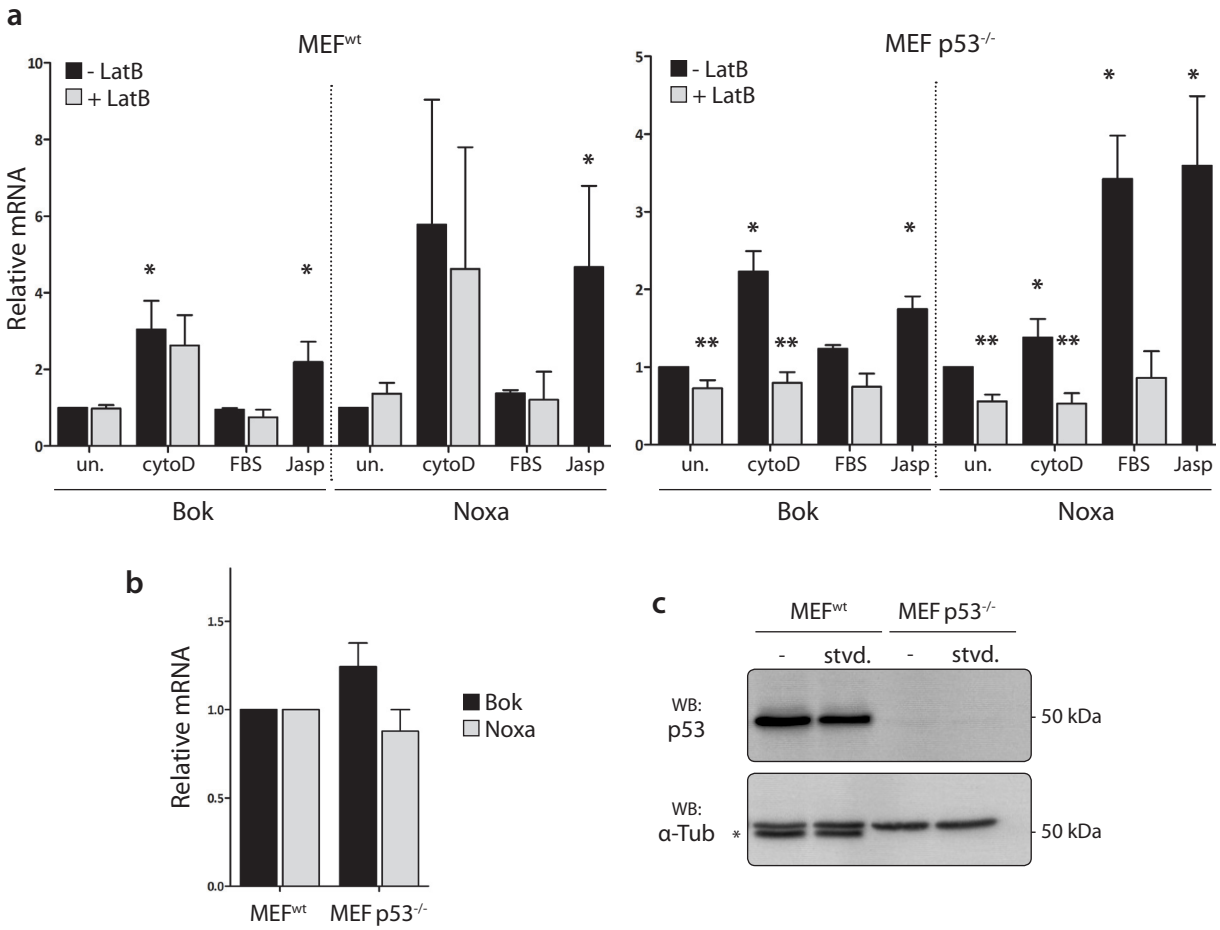

Figure IV-18: *Stimulus-dependent induction of Bok and Noxa mRNA in p53-null MEFs.* **a.** Either wild type MEFs (MEF^{wt}) or p53-*null* MEFs ($p53^{-/-}$) were starved for 24 hours and pre-incubated with 5 μM latrunculin B (LatB) for 15 minutes, then were either left untreated or stimulated with 2 μM cytochalasin D (cytoD), 15% FBS and 0.5 μM jasplakinolide (Jasp) for 90 minutes. mRNA was quantified using real-time PCR and normalized to Hprt housekeeping control. *n=3, bars - SEM, * $p < 0.05$, ** $p < 0.01$.* **b.** Alterations of basal Bok and Noxa mRNA levels in wild type versus $p53^{-/-}$ MEFs, *n=3*. **c.** Western blot showing the absence of p53 protein in p53-*null* MEFs. Asterix indicates residual p53 signal after membrane stripping. (-) cells grown in 10% FBS, stvd. - serum starvation for 24 hours (0.5% FBS).

mediated apoptosis induced by etoposide (Villunger *et al.*, 2003). Bok expression was strongly suggested to be p53-dependent (Yakovlev *et al.*, 2004), although there is still no direct evidence of direct binding of p53 to the promoter. In order to dissect the influence of the p53 on SRF-MRTF-mediated Bok and Noxa regulation, I first tested the induction of both genes in immortalized wild-type mouse embryonic fibroblasts (MEF^{wt}). Employing stimulations with serum, cytochalasin D and jasplakinolide, I established that both genes were induces, although serum-induced up-regulation was generally weak (Figure IV-17). Noteworthy, time-course analysis revealed two distinct patterns of mRNA induction - while Bok mRNA was still accumulating at 180 minutes of stimulation, similarly to the *Acta2* positive control gene, Noxa mRNA levels were stabilized at 90 minutes of stimulation and were not up-regulated further, reminiscent of another positive control gene – Srf. With this knowledge in hand, I compared Bok and Noxa mRNA induction between wild-type MEFs and p53-deficient MEFs, derived from p53 knockout mouse. Despite the fact that p53 protein was effectively absent from $p53^{-/-}$ MEFs, the basal levels of Bok and Noxa mRNA remained essentially unchanged, although Bok might have been slight up-regulated (Figure IV-18B-C). SRF-MRTF pathway-activating stimuli cytochalasin D, FCS and jasplakinolide were able to up-regulate both genes in the absence of p53, while pre-treatment with latrunculin B blocked the induction (Figure IV-18A). Of note, in $p53^{-/-}$ MEFs, latrunculin B alone had significantly impaired not only induced expression, but also basal levels of Bok and Noxa mRNA. On the other hand, while latrunculin B did not significantly influence basal expression of the genes in wild-type settings, its effect on the mRNA induction was also minimal. In summary, this data provided evidence for p53-independent regulation of Bok and Noxa by actin cytoskeleton-

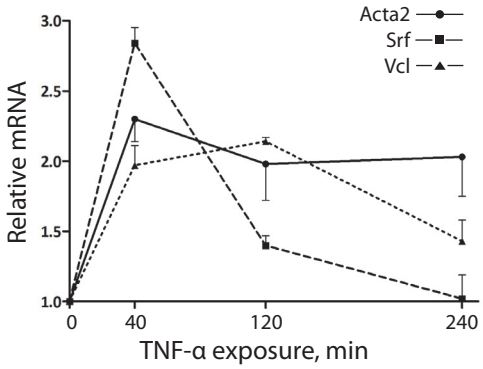

Figure IV-19: Induction of known SRF-MRTF target mRNA upon TNF-α treatment. NIH 3T3 cells were treated with 10 ng/mL TNF-α for indicated periods of time. mRNA quantified using real-time PCR and normalized to Hprt. n=3, bars - SEM

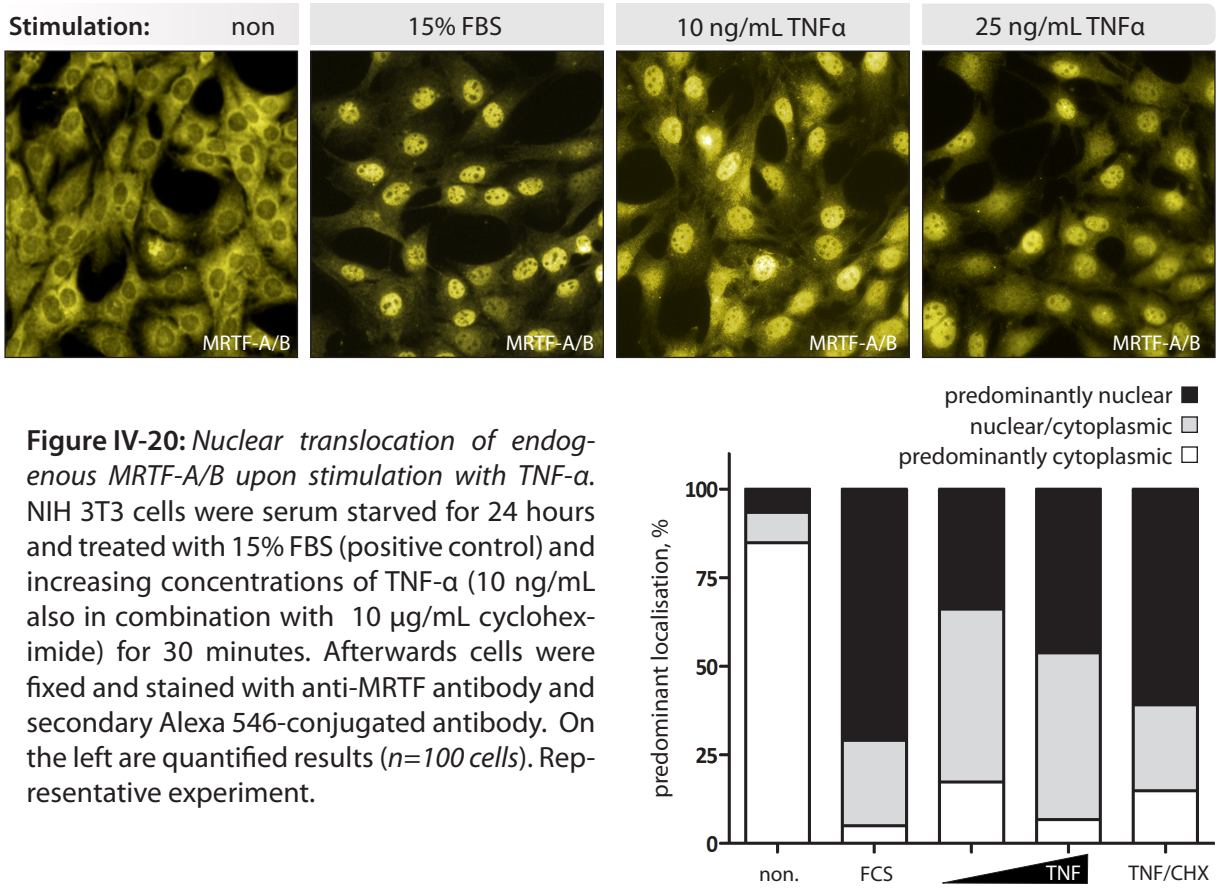

Figure IV-20: *Nuclear translocation of endogenous MRTF-A/B upon stimulation with TNF-α.* NIH 3T3 cells were serum starved for 24 hours and treated with 15% FBS (positive control) and increasing concentrations of TNF-α (10 ng/mL also in combination with 10 µg/mL cycloheximide) for 30 minutes. Afterwards cells were fixed and stained with anti-MRTF antibody and secondary Alexa 546-conjugated antibody. On the left are quantified results (*n=100 cells*). Representative experiment.

targeting agents and SRF-MRTF pathway.

IV.3.3. Are SRF-MRTFs required for apoptosis induction?

Having identified two pro-apoptotic targets of SRF-MRTF pathway we were interested to see whether MRTF activity is involved in induction of treatment-induced apoptosis. Previously, Arnaud Descot looked at the activity of SRF-MRTF pathway in TNFα- and staurosporine-induced apoptosis using luciferase reporter assays. Using NIH 3T3 fibroblasts, he found that the activity of the pathway is, indeed, induced by these agents in as dose-dependent manner and efficiently blocked by pre-treatment with latrunculin B (Shaposhnikov *et al.,* 2012). Using TNFα as an activator of extrinsic apoptotic event, I analyzed whether it is able to induce some of the classical SRF-MRTF target genes. Upon stimulation, *Acta2*, *Srf* and *Vcl* genes were quickly up-regulated in NIH 3T3 cells (Figure IV-19). mRNA levels of *Srf* and *Vcl* have dropped to the resting levels after 120 minutes, while *Acta2* expression remained elevated. This induction kinetics is similar to the one observed in cytochalasin D or serum-stimulated cells, although on a smaller absolute scale. The fact that elevated mRNA levels are detected at 40 minutes of TNFα stimulation points to the fact that MRTF activation is a direct TNF-mediated event, rather than a results of secondary indirect signaling.

Supporting the mRNA induction data, TNFα treatment efficiently induced dose-dependent nuclear accumulation of MRTFs (Figure IV-20). Moreover, this accumulation was not affected by protein synthesis inhibitor cycloheximide, confirming the notion that MRTF activation is an early event, rather than a consequence of late TNFα signaling. MRTFs accumulate in the nucleus as a result of dissociation from inhibitory complex with G-actin in cytoplasm, but their localization in the nucleus does not strictly correlate with activation of transcription since they can be repressed via binding to the nuclear G-actin (Vartiainen *et al.*, 2007). However, translocation data combined with the target gene induction allows suggesting that TNFα induces SRF-MRTF pathway. Unexpectedly, TNFα stimulation of NIH 3T3 and MEF cells failed to up-regulate either Bok or Noxa genes, while cytochalasin D led to a robust induction of the transcripts (data not shown). This strongly points to the stimulus-specific regulation of Bok and Noxa and puts their importance in extrinsic pathway of apoptosis under question mark.

Additionally, DNA-damaging agents, etoposide and doxorubicin were not active in the luciferase reporter assays for SRF-MRTF activity and failed to up-regulate Bok expression at up to 180 minutes of stimulation (data not shown). On the contrary, Noxa mRNA was strongly induced by these agents in both NIH 3T3 and wild-type MEF cells. However, this induction was completely abrogated in p53-null MEF line, arguing that DNA damage-induced apoptotic signaling uses exclusively p53 for regulation of Noxa, but not Bok. In summary, these experiments present evidence for SRF-MRTF involvement in the transcriptional regulation of pro-apoptotic genes Bok and Noxa. Although SRF-MRTF pathway appears to be activated upon certain apoptotic stimuli, e.g. TNFα and staurosporine, it does not activate the transcription of either Bok or Noxa and its role in the apoptotic signaling is not yet clear. DNA damage-induced apoptosis (after etoposide and doxorubicin treatments) does not seem to activate SRF-MRTF pathway or up-regulate Bok transcript. It is, however, accompanied by Noxa up-regulation, which appears to be strictly p53-dependent.

MRTFs and their role in the cell cycle regulation

IV.4.1. MRTF-A/B knockdown leads to increase in S and G2/M populations in the absence of growth factors.

Marked anti-proliferative effect observed upon the overexpression of the active forms of MRTF-A has also been described for a founding member of the family, myocardin. In one study, myocardin overexpression was found to positively correlate with the up-regulation of a cyclin-CDK inhibitor $p21^{Waf1}$ and a consequent G1-S arrest (Kimura *et al.*, 2010). Contradicting this data, another study has found no effect on $p21^{Waf1}$, but found down-regulation of a number of cell cycle regulatory proteins (CDK2, CDK1, S6K) and *c-myc* to be responsible for G2-M arrest and accumulation of polyploid cells (Tang *et al.*, 2008). Our analysis of anti-proliferative effects of MRTF-A overexpression did not involve any cell cycle regulators, however, during transient, siRNA-mediated, MRTF-A/B knockdown we observed an interesting phenomenon: when MRTF-A/B depleted NIH 3T3 cells were deprived from growth factors by serum starvation, they still displayed a significant amount of cells in the S and G2 phases of cell cycle. Such an effect would be consistent with the idea that if active MRTF-A conveys anti-proliferative response, depleting cells from MRTFs would give them proliferative advantage.

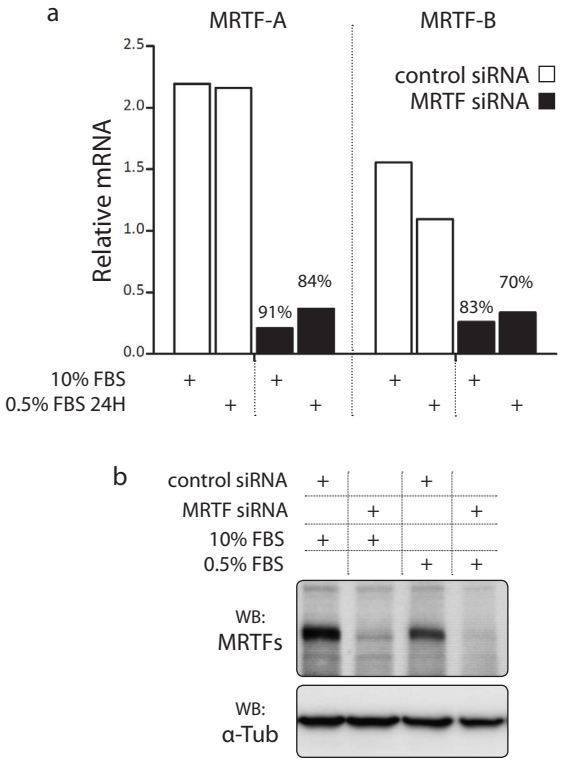

Figure IV-21: *Efficiency of a transient siRNA-mediated knockdown of MRTF-A/B.* **a.** Real-time PCR showing MRTF-A and -B mRNA levels 36 hours post-transfection in full medium or including 24 hours of serum starvation. Normalized to Hprt, *n=1*. **b.** Western blot showing MRTF-A/B protein levels on the same time scale as in **a.** Representative experiments.

In order to investigate the role of MRTF depletion in proliferation and cell cycle regulation of NIH 3T3 fibroblasts, I used siRNA sequence targeting both MRTF isoforms: A and B (Medjikane *et al.*, 2009). Quantitative PCR has shown more than 84% decrease in MRTF-A mRNA and more than 70% decrease in MRTF-B mRNA 24 hours post-transfection (Figure IV-21B). Western blotting has confirmed almost

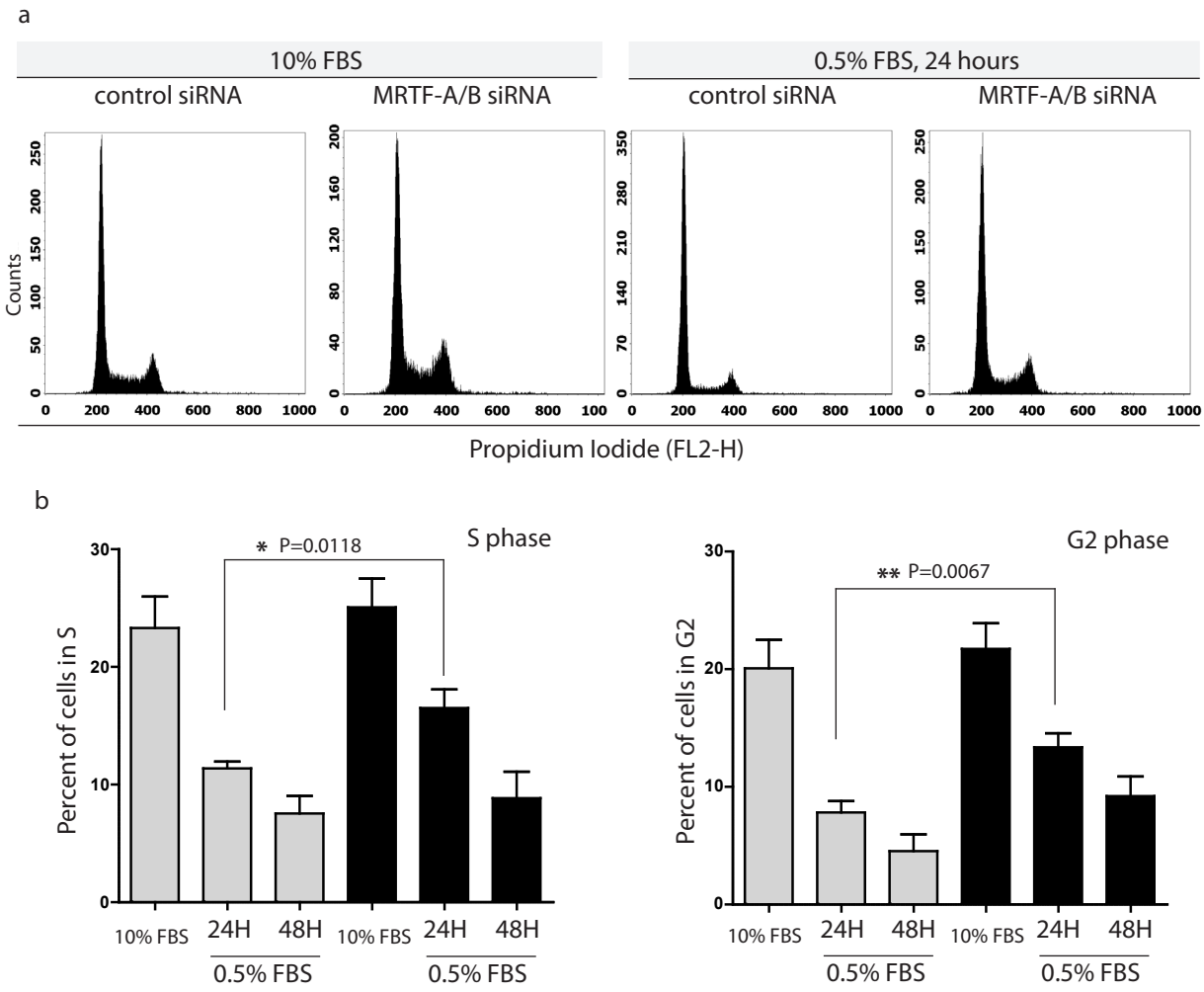

Figure IV-22: *Increased S-G2 populations following transient knockdown of MRTFs.* NIH 3T3 cells were transfected with either control siRNA or siRNA against MRTFs and grown in 10% FBS- or 0.5% FBS-containing medium for 24 hours. Cell cycle phase distribution was assesed by propidium iodide stianing and FACS analysis. 10000 cell were collected per sample. **a.** representative histograms of cell cycle distribution after gating on single cell population. **b.** quantification of S and G2 phase populations using Dean-Jet-Fox algorithm. *n ≥ 3, bars - SEM, statistical significance indicated on graphs*

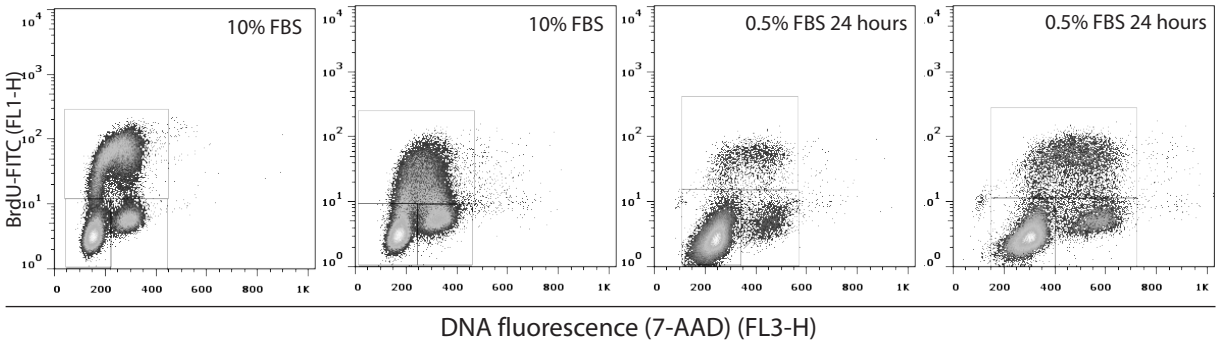

Figure IV-23: *Increased S population following MRTF knockdown is BrdU-positive.* NIH 3T3 cells were grown as in Fig. II-22, pulse-labeled with BrdU for 20 minutes and stained with FITC-conjugated anti-BrdU antibody and 7-AAD. Analysed by FACS. 50000 cells collected per sample. Representative scatter plots after gating out debris and cell clumps. Gates on G1, S and G2/M populations are shown. *n=3*

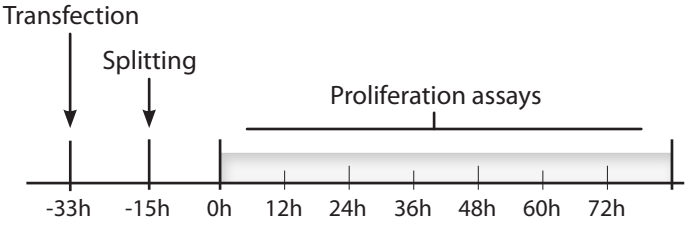

Figure IV-24: Outline of proliferation assay setup. MTT assay and cell counting were perfermed in parallel.

complete depletion of MRTF proteins at the same time point (Figure IV-21A). Propidium iodide staining of cell cycle distribution has shown that NIH 3T3 cells asynchronously growing in the full medium (10% fetal bovine serum (FBS)) did not display any significant differences between control siRNA and MRTF knockdown. However, when serum starved using 0.5% FBS in the culture medium, cells depleted from MRTFs had considerably more cells in S and G2 phases of the cell cycle (Figure IV-22). To clarify whether the increased S phase came from the slippage through G1-S checkpoint or is a result of an arrest during S phase, I pulse-labeled transfected cells with BrdU to detect newly synthesized DNA. Consistent with the experiments above, serum-starved, MRTF-depleted cells had significantly increased S and G2 populations (Figure IV-23). Cells in the S phase were clearly BrdU-positive, indicating that

Figure IV-25: *Growthcurves in serum-starved conditions following MRTF knockdown.* NIH 3T3 cells were grown in medium containing 0.5% FBS. Growth curves generated according to Figure II-24. *n=3, bars - SEM*

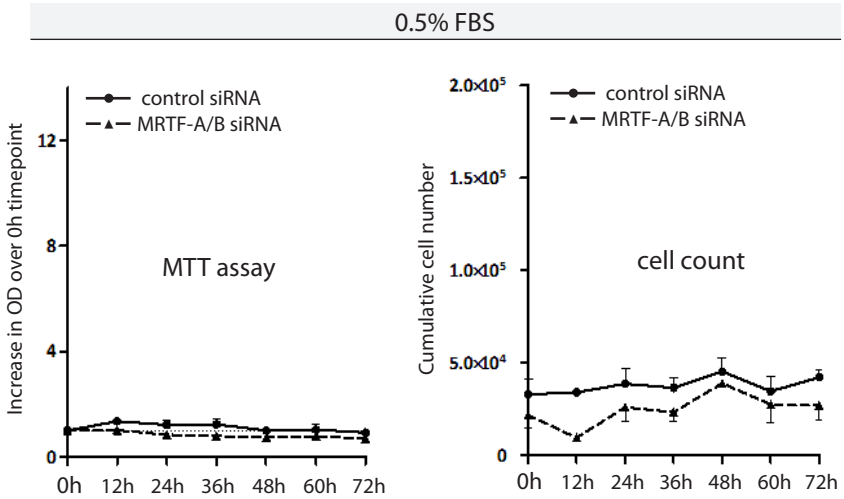

in the absence of growth factors, MRTF knockdown confers the ability of cells to escape G1-S arrest. On the other hand, cells grown in presence of 10% serum had very similar cell cycle distributions.

IV.4.2. MRTF-A/B knockdown impairs proliferation of NIH 3T3 fibroblasts.

To inspect whether this G1-S slippage allows MRTF-depleted cells to proliferate in the absence of growth factors, I constructed the growth curves of the cells with and with-

out knockdown using 2 different proliferation assays (Figure IV-24), which showed similar results. In MTT assay as well as in direct cell counting, MRTF-depleted cells failed to proliferate in 0.5% FCS (Figure IV-25), demonstrating that the increase in S and G2 populations is not followed by cell division and increase in cell numbers. Thus, the cells that abberantly entered S phase in the absence of serum are likely to be arrested and destined for apoptosis. Interestingly, in cells grown in 10% serum, MRTF knockdown led to reproducible delay in proliferation rate (Figure IV-26), which could not be accounted for by increase in apoptosis as determined by annexin V staining (not shown). This data prompts to suggest that MRTF knockdown, instead of giving cells proliferative advantage, also confers anti-proliferative effect, although on a far lesser scale than active MRTF-A over-expression.

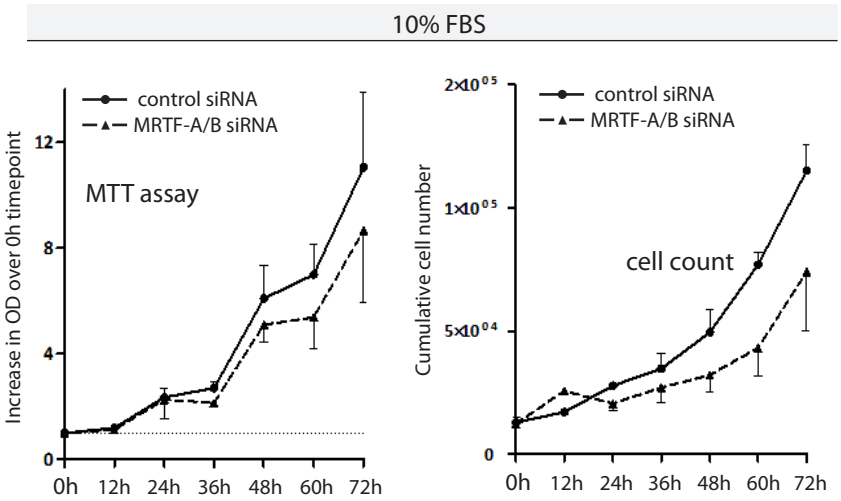

Figure IV-26: *Growth curves in 10% FBS following MRTF knockdown.* NIH 3T3 cells were grown in full medium containing 10% FBS. Growth curves generated according to Figure II-24. *n=3, bars - SEM*

IV.4.3. MRTF-A/B knockdown changes the lengths of cell cycle phases.

In order to gain a deeper understanding of MRTF depletion effects on the cell cycle, I created two stable, NIH 3T3-based, cell lines that allowed for monitoring cell cycle progression in real time. First cell line expressed histone H2B-GFP fusion protein, conferring green nuclear fluorescence to the cells throughout cell cycle. Second cell line contained so-called FUCCI markers (Sakaue-Savano *et al.*, 2008). Both marker proteins were expressed from a single vector with the help of IRES2 sequence (Figure IV-27), which represents a slight modification of the original system where markers are encoded on separate plasmids. FUCCI-expressing cells display orange nuclear fluorescence during G1 phase due to accumulation of the first marker protein – Cdt1(30-120)-mKO2 (amino acids 30-120 of a DNA

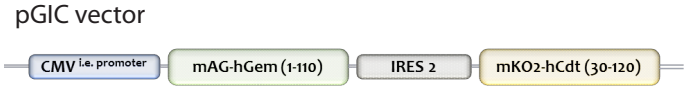

Figure IV-27: Scheme of pGIC vector, encoding FUCCI markers.

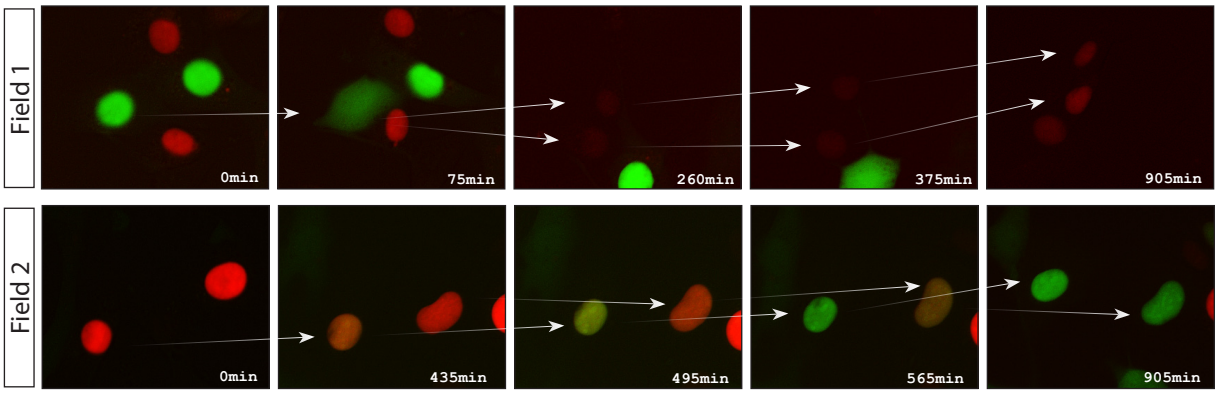

Figure IV-28: *Live cell imaging of NIH 3T3 cells stably expressing FUCCI markers.* Field 1 follows two cells in G2 phase (t=0, t=260) undergo nuclear envelope breakdown (t=75, t=375) followed by mitosis. Daugther cells develop red fluorescence. In field 2 two cells in G1 (t=0) undergo progression to S phase accompanied by the change in fluorescent color from red to green

replication factor Cdt1 fused to monomeric Kusabira Orange 2 protein). At the onset of S phase it is degraded by the SCF^{Skp2} E3 ligase complex, resulting in the disappearance of red fluorescence. At the same time, very early in the S phase, second marker – Geminin (1-110)-mAG (amino acids 1-110 of DNA replicator inhibitor Geminin fused to monomeric Azami Green protein) becomes de-repressed. Its accumulation gives cells green nuclear fluores-

Figure IV-29: *Comparison of knockdown efficiency between non-labeled MRTF siRNA and MRTF siRNA labeled with Cy5 on 3' end of the sense strand.* NIH 3T3 cells transfected with indicated siRNAs were assayed 36 hours post-transfection. Cy5 label does not affect siRNA's potency.

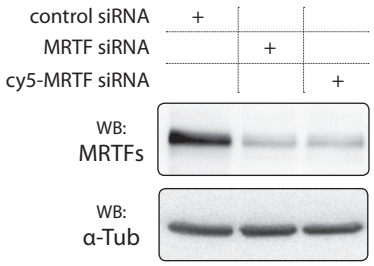

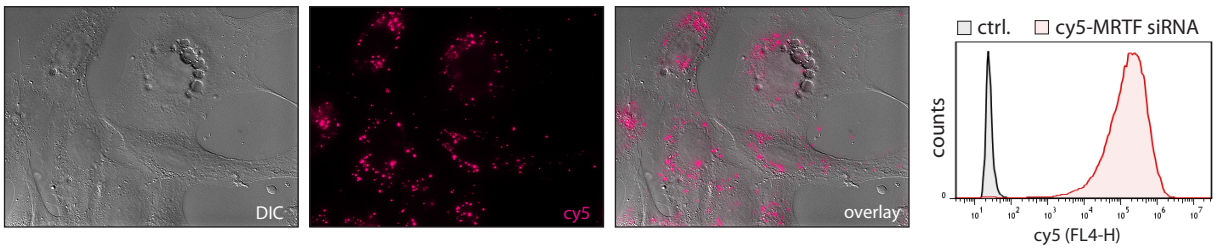

Figure IV-30: *siRNA transfection efficiency.* NIH 3T3 cells were transfected with cy5-labeled anti-MRTF siRNA and 24 hours later efficiency of transfection was estimated using microscopy and FACS analysis. Micrographs showing fixed cells exposed in DIC and Cy5 channels at 20x magnification On the right, FACS analysis showing histograms of non-labeled siRNA (ctrl.) and cy5-labeled anti-MRTF siRNA. Transfection efficiency is >98%.

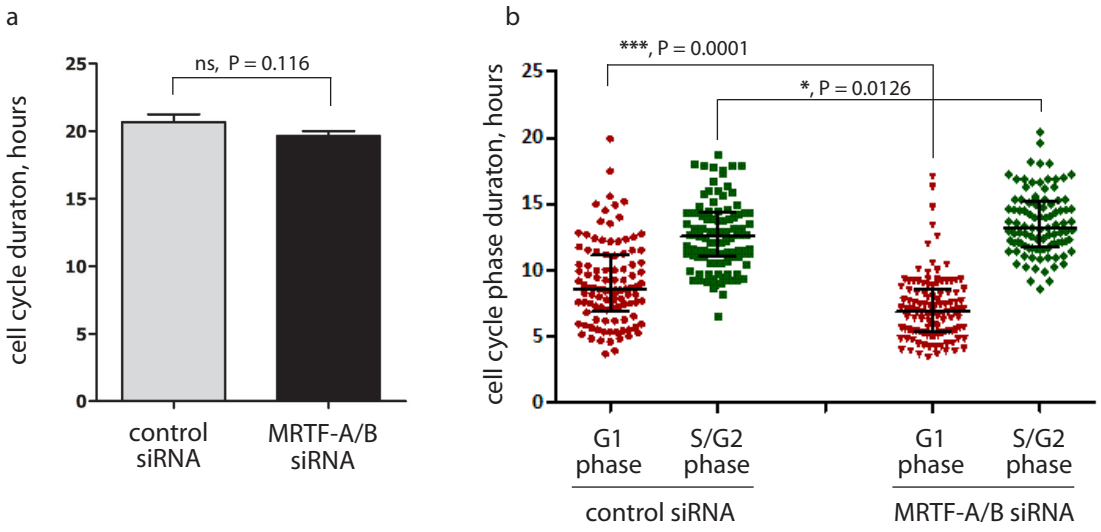

Figure IV-31: *Quantification of live cell imaging of FUCCI-expressing NIH 3T3 cells.* **a.** Total time between two cell division is not significantly changed upon MRTF knockdown. *n=54* for control siRNA, *n=62* for MRTF siRNA. bars -SEM. **b.** Duration of individual cell cycle phases is changed following MRTF knockdown. *n > 100 cells* for each sample. Median and interquartile distance are indicated.

cence which persists through S, G2 and most of the M phase. During late mitosis, Geminin(1-110)-mAG is degraded by the APC^{Cdh1} E3 ligase complex, which remains active until the end of G1 phase. An example of cell cycle-dependent shifts in fluorescent color of the cells is presented in Figure IV-28 for stably transfected NIH 3T3 cells. I used these cells to monitor the duration of the cell cycle changes upon transient MRTF knockdown. In order to monitor the siRNA transfection efficiency and to focus only on siRNA-positive cells, all live imaging experiments have been performed using cy5-labeled siRNA against MRTFs. Prior to undertaking imaging experiments I have shown that the addition of fluorescent dye to the 5'-end of siRNA did not influence its ability to knock down MRTFs (Figure IV-29). Moreover, fluorescent imaging of transfected cells have clearly shown that the efficiency of siRNA delivery is close to 100% (Figure IV-30), giving me confidence to count every analyzed cell as siRNA-positive. As revealed by three independent live imaging experiments, the total duration of cell cycle between control siRNA and MRTF-targeting siRNA remained essentially unchanged (Figure IV-31A). Quantification of the duration of individual cell cycle phases has unveiled that

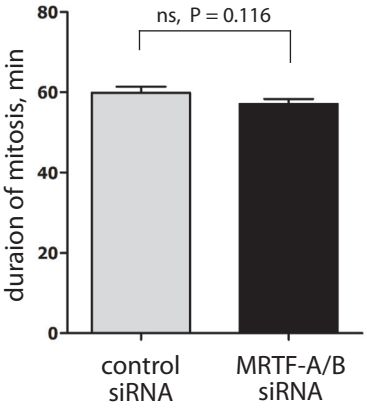

Figure IV-32: *Duration of mitosis upon MRTF knockdown.* NIH3T3-H2B-GFP cells transfected with the indicated siRNAs. *n ≥ 35* cells for each sample, *bars - SEM*

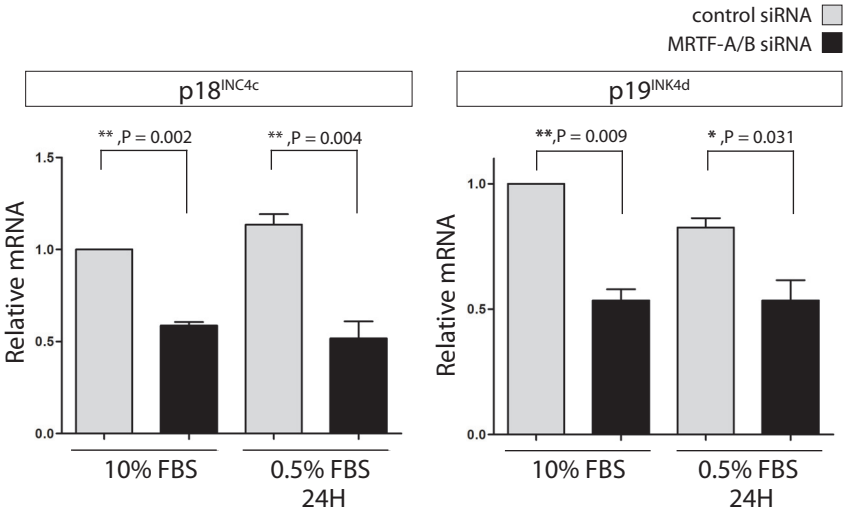

Figure IV-33: *Downregulation of p18INK4c and p19INK4d upon MRTF knockdown.* RNA was prepared 36 hours post-transfection (36h in 10% FBS or 12h + 24h in 0.5% FBS). mRNA was quantified using real-time PCR and normalized to Hprt. *n=3, bars - SEM.* Statistical significance indicated on graphs.

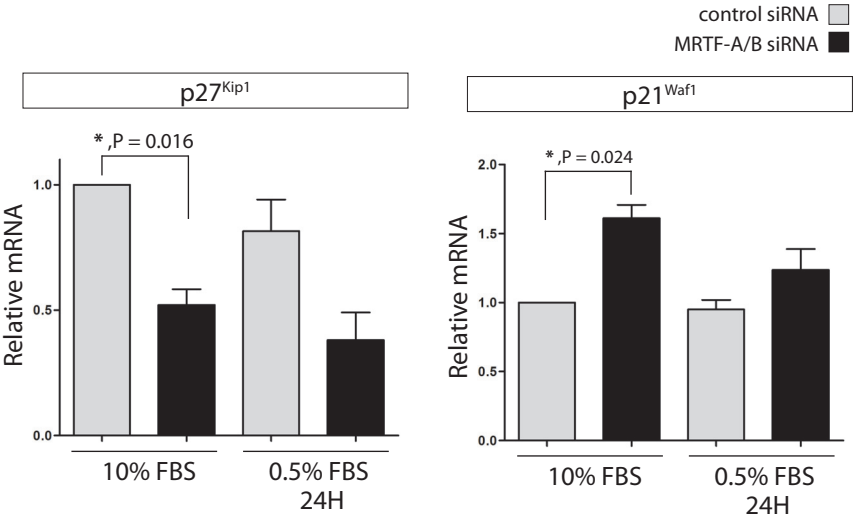

Figure IV-34: *Changes in mRNA of CIP/KIP family members upon MRTF knockdown.* RNA was prepared 36 hours post-transfection (36h in 10% FBS or 12h + 24h in 0.5% FBS). mRNA was quantified using real-time PCR and normalized to Hprt. *n=3, bars - SEM.* Statistical significance indicated on graphs.

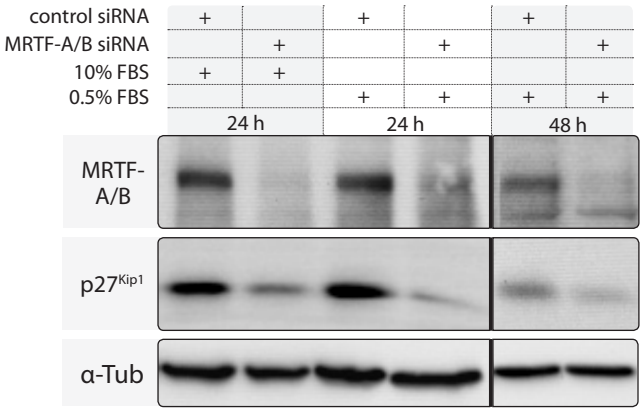

Figure IV-35: *Downregulation of p27Kip1 following MRTF knockdown.* 12 hours post-transfection NIH 3T3 cells were either incubated in full medium (10% FBS) for 24 hours or in serum-depleted medium (0.5% FBS) for 24 and 48 hours. Knockdown efficiency assessed by blotting against MRTF-A/B protein. Representative western blot pictures from 3 independent experiments.

MRTF knockdown leads to significant shortening of the G1 phase, from 9.028 ± 0.3 (SEM, n=104) hours in control siRNA to 7.154 ± 0.24 (SEM, n=112) hours in targeting siRNA. S-G2 phase, on the other hand, was slightly, but significantly longer (12.65 ± 0.26 hours for control versus 13.54 ± 0.24 for MRTF knockdown) (Figure IV-31B). Duration of the mitosis was com-

pared between two conditions with the help of H2B-GFP expressing NIH 3T3 cells. I calculated the time cells required from the nuclear envelope breakdown to complete cytokinesis and found no significant differences between control transfection and MRTF knockdown (Figure IV-32).

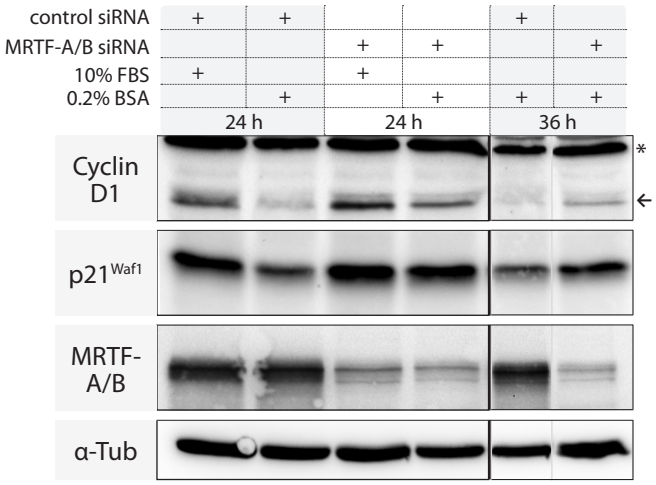

Figure IV-36: *Changes in p21^{Waf1} and cyclin D1 levels following MRTF knockdown.* NIH 3T3 cells were transfected with siRNAs (control or anti-MRTF) for 12 hours and incubated in either full medium (10% FBS) for 24 hours or in medium lacking FBS (0.2% BSA) for 24 and 36 hours. Asterix indicates non-specific signal. Representative western blot pictures from three independent experiments.

IV.4.4. MRTF-A/B knockdown influences cel cycle protein levels.

To link the observed changes in cell cycle phase durations to the molecular events I examined the effects of MRTF depletion on some key cell cycle regulators. Members of the cyclin-CDK inhibitor family INK4 play an important role in progression through G1-S checkpoint (Besson et al., 2008). Three out of five existing family members – p15^{INK4b}, p16^{INK4a}, p19^{ARF} – could not be detected in NIH 3T3 cells (data not shown), while other two – p18^{INK4c} and p19^{INK4d} – were significantly down-regulated on mRNA level following MRTF knockdown (Figure IV-33). Members of the second family of cyclin-CDK inhibitors, CIP/KIP proteins p21^{Waf1} and p27^{Kip1} were differentially affected by the knockdown. While p27^{Kip1} was down-regulated, p21^{Waf1}

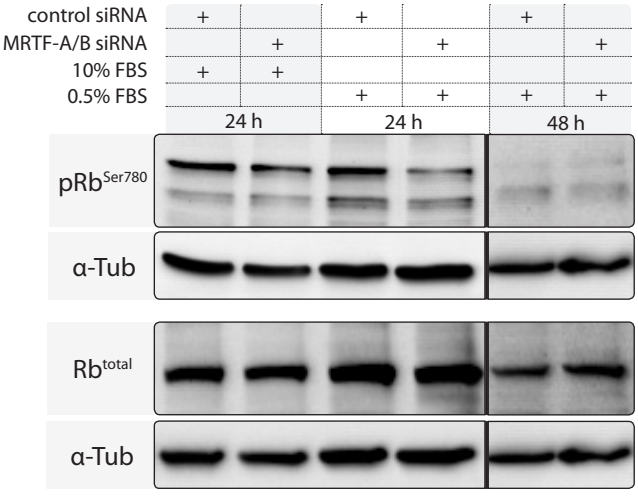

Figure IV-37: *Changes in Rb protein upon MRTF knockdown.* NIH 3T3 cells were transfected with the indicated siRNAs (control and anti-MRTF) for 12 hours and then incubated either in full medium (10% FBS) for 24 hours or in serum-depleted medium (0.5% FBS) for 24 and 48 hours. For MRTF knockdown efficiency see Figure II-35. Representative western blot pictures from three independent experiments.

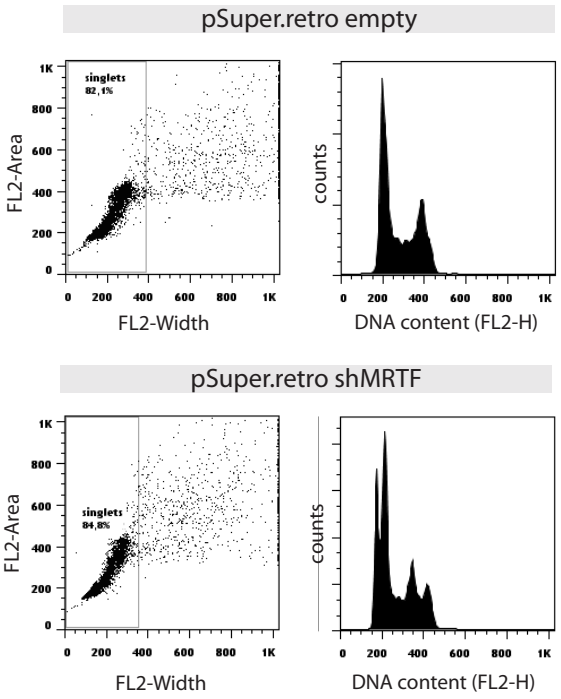

Figure IV-38: *Aneuploidy in stable MRTF knock-down.* NIH 3T3 cells stransfected with either empty pSuper.retro.puro plasmid or pSuper.retro.puro-shMRTF and selected with puromycin for 3 weeks. FACS analysis of propidium iodide stained cells. 10000 cells collected per sample. On the right - scatter plot used to gate out cell clumps, singlet population is indicated.

displayed elevated mRNA levels following siRNA treatment (Figure IV-34). Of note, these effects were similar in both growth conditions (10% serum versus 0.5% serum). Consistent with mRNA data, protein levels of $p27^{Kip1}$ were reduced upon MRTF depletion (Figure IV-35). This reduction was even more pronounced after serum starvation, because unlike control cells, MRTF-depleted fibroblasts failed to accumulate the protein. $p21^{Waf1}$ protein levels were slightly up-regulated in the cells growing in presence of 10% FBS (Figure IV-36). Under serum-starved conditions (0.2% BSA), MRTF depleted fibroblasts, unlike control cells, failed to down-regulate $p21^{Waf1}$ protein levels. Another important regulator of G1-S transitions –

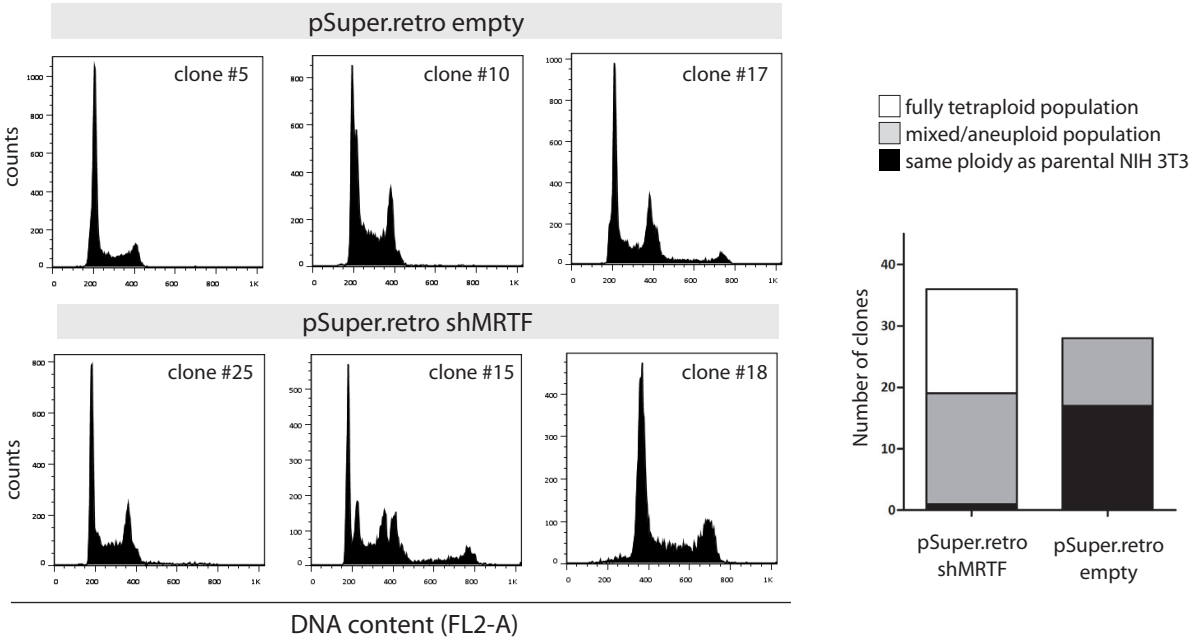

Figure IV-39: *Aneuploidy in clonal lines stably expressing shRNA against MRTFs.* Stable cell pools shown in Figure II-38 were sub-cloned for further 3 weeks. Monoclonal cell lines were isolated and analysed for DNA content. On the left - DNA histograms of representative clones, generated after gating out cell clumps. On the right - chart showing distribution of clones according to their DNA profile. 37 clones for shMRTF and 28 clones for pSR empty were analyzed.

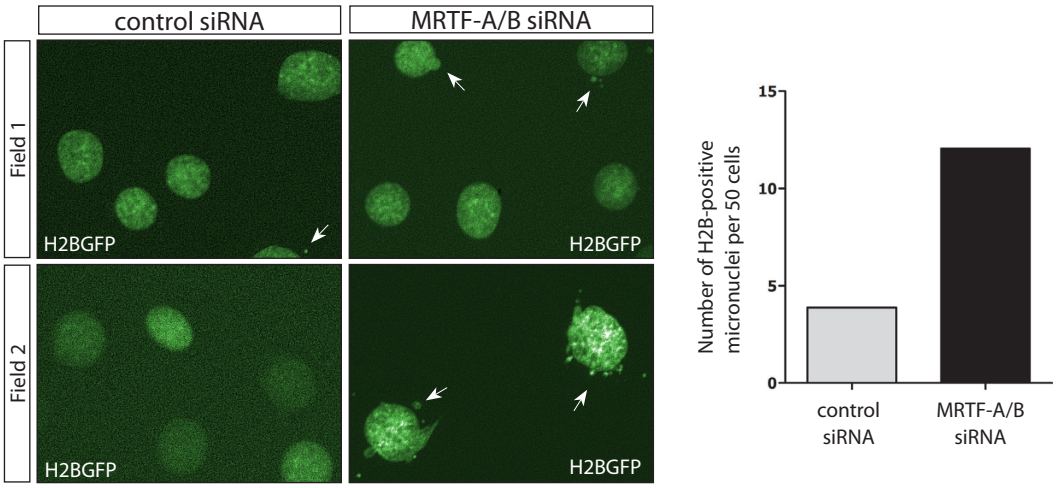

Figure IV-40: *Micronuclei formation: live cell imaging of H2B-GFP.* NIH 3T3 cell stably expressing H2B-GFP were transfected with the indicated siRNAs and live cell imaging was performed for 48 hours. Number of micronuclei and nuclear buds was counted at the last time point, normalised to 50 cells (graph on the right). Representative micrographs are shown on the left. Micronuclei are inducated with arrows.

Figure IV-41: *Micronulei formation: DAPI satining of fixed cells.* NIH 3T3 cells were transfected either with the control siRNA or siRNA against MRTFs for 72 hours on coverslips, followed by fixation and staining with DAPI. Mironuclei/nuclear buds as well as bi-nucleated cells were counted. ≥200 cells analysed per sample per experiment. Results are shown in bar charts. *n=3, bars - SEM.* statistical significance is indicated on the graphs. Representative micrographs from two fields of view are shown above. Nuclear defects are indicated with arrows.

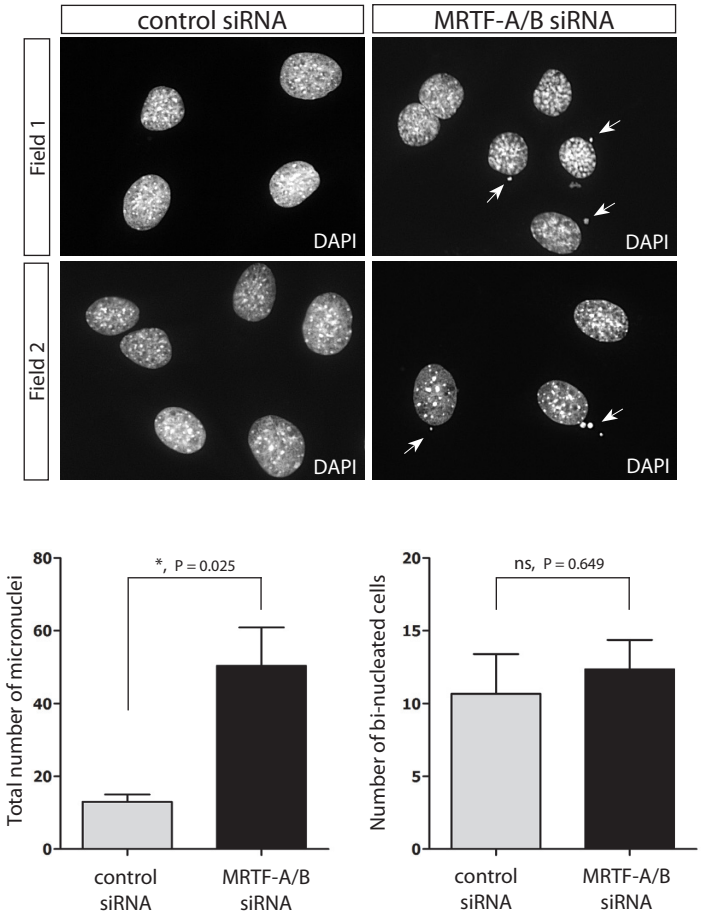

Rb protein – was not affected by the knockdown on the total protein level (Figure IV-37); however, de-activating phosphorylation on Ser^{780} was slightly decreased in comparison to the control at 24 hours of serum starvation, while remained comparable under full serum conditions and 48 hours of serum starvation. Levels of cyclin D1 protein changed similarly to the p21^{Waf1}, showing weak up-regulation by the knockdown in 10% FBS medium and impaired degradation in the absence of growth factors (0.2% BSA) (Figure IV-36).

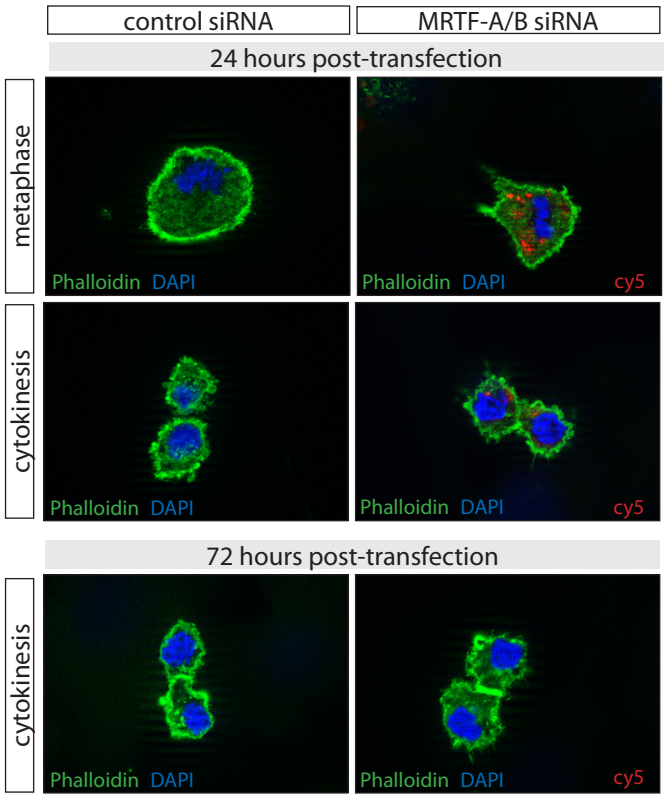

Figure IV-42: *Actin cytockeleton in dividing cells upon MRTF knockdown.* NIH 3T3 cells were transfected with either control of anti-MRTF-cy5 siRNAs and incubated for 24 and 72 hours followed by staining with phalloidin and DAPI. Dividing cells were photographed at 63x magnification.

In summary, observed patterns of changes in cell cycle regulatory proteins allows speculating that the shortening of G1 phase in the MRTF knockdown is potentially caused by general down-regulation of cyclin-CDK inhibitors from CIP/KIP and INK4 families as well as slight up-regulation of cyclin D1. On the other hand, the same factors plus defective degradation of p21^{Waf1} could contribute to increase S-G2 populations in the absence of growth factors.

IV.4.5. MRTF-A/B knockdown leads to defects in chromosomal stability.

Faster progression through G1 phase, coupled with the ability to forgo G1-S arrest in serum starved conditions does not explain the anti-proliferative effect of the knockdown and the lengthening of the G2 phase. A hint for solving this phenomenon comes from analysis of the cell cycle distribution in NIH 3T3 fibroblasts stably transfected with shRNA against MRTFs. Following retroviral delivery of shRNA and selection of stable polyclonal line with puromycin for 3 weeks, the cells became aneuploid (Figure IV-38). I sub-cloned this line, together with control cells transfected with empty vector, and analyzed DNA content of individual clones. In cells, transfected with empty vector 11 out of 28 clones displayed various degrees of aneuploidisation, which points to inherent genomic instability of NIH 3T3 cell line. Interestingly,

all clones expressing shRNA against MRTFs, except for one, were aneuploid with 17 out of 37 clones fully doubling their DNA content (Figure IV-39). Of note, proliferation rates of this monoclonal lines was not negatively affected by the knockdown and some of the clones apparently grew even faster than the parental NIH 3T3 cells (data not shown). Somewhat unexpectedly, I did not observe any signs of aneuploidisation in transient MRTF knockdown (data not shown), suggesting that it might be an effect requiring long-term MRTF depletion. However while performing live imaging experiments with H2B-GFP expressing cells, I noticed that MRTF-depleted cells exhibited a significant increase in mitotic defects, manifesting themselves as micronuclei and nuclear buds. This increase became apparent after more than 48 hours post-transfection; at 60 hours there was approximately 3-fold increase in cells harbouring nuclear defects (Figure IV-40). To quantify these defects, I transfected NIH 3T3 cells with either control or MRTF siRNA for 72 hours and counted cells carrying nuclear defects in fixed, DAPI-stained samples. Figure IV-41 demonstrates a significant increase in micronuclei/nuclear buds formation upon MRTF depletion, essentially confirming data from live imaging experiments. Noteworthy, at the chosen time point (72 hours), knockdown did not result in increased numbers of bi-nucleated cells. Whether these effects contribute to the impaired proliferation rate and what are the exact molecular mechanisms involved here, are still open questions. Actin cytoskeleton organization, which plays an important role in mitosis, however, did not seem to be affected during cell division of MRTF-depleted cells (Figure IV-42).

Identification of proteins competing with MRTFs for binding to G-actin. (Performed in collaboration with dept. of Mathias Mann, MPI, Martinsried. Collaborating partners – **Marco Hein-Yannic** and **Christian Eberl**)

Nucleocytoplasmic shuttling of MRTFs is thought to be regulated via binding of their RPEL motifs to G-actin, which is believed to mask the nuclear localization signal located between RPEL motifs (Miralles *et al.*, 2003, Posern *et al.*, 2004, Vartiainen *et al.*, 2007, Guettler *et al.*, 2008, Hirano *et al.*, 2011). Rho-mediated drop in cellular G-actin availability leads to exposure of NLS motif and subsequent nuclear accumulation of MRTFs with the help of importin α/β (Pawlowski *et al.*, 2010, Nakamura *et al.,* 2010). In addition, Crm1-dependent nuclear export of MRTF-A has been shown to be important for re-distribution of MRTF-A back to cytoplasm (Vartiainen *et al.*, 2007). However, molecular details of MRTF-G actin complex dissociation are still poorly understood. One hypothesis originating from our group suggests that G-actin is actively displaced from MRTFs by a competing G-actin-binding protein which becomes active following Rho-mediated signaling events. To identify potential candidates that could compete with MRTFs for G-actin binding, I performed SILAC-based mass-spectrometry analysis of G-actin bound proteins before and after stimulation with serum. An indispensable tool for this experiment was the NIH 3T3 cell line which inducibly expresses FLAG-tagged G-actin upon treatment with doxycyclin (Figure IV-43). This

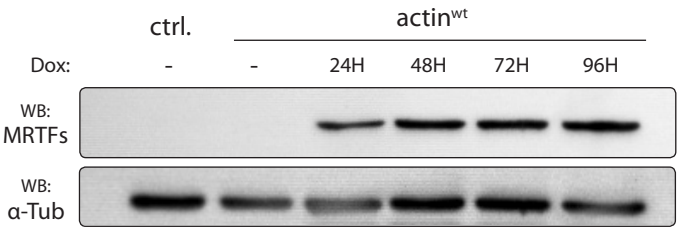

Figure IV-43: *Tet-regulated expression of FLAG-tagged actin^{wt}.* NIH 3T3 TR-TO empty vector (crtl.) and NIH 3T3 TR-TO actinwt cells were treated with 1 µg/mL doxycycline for indicated periods of time. Actin was detected with anti-FLAG antibody.

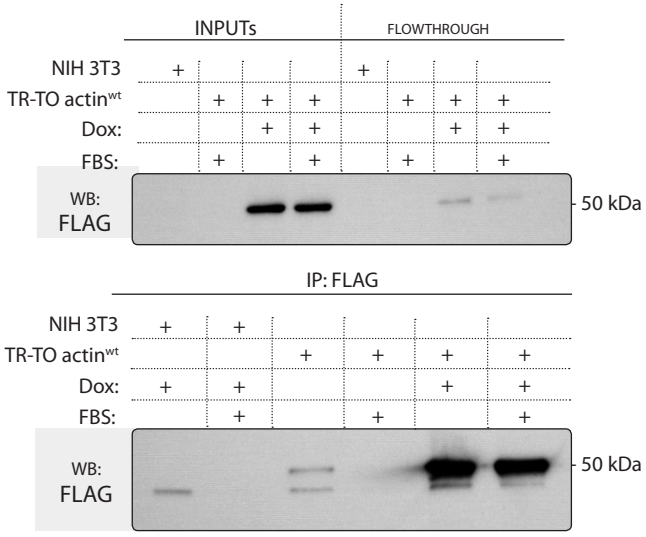

Figure IV-44: *co-Immunoprecipitation of FLAG-tagged actin.* Either parental NIH 3T3 cells or TR-TO actin^{wt} cells were subjected to co-IP with anti-FLAG antibody as detailed in Materials and Methods section. IP efficiency is close to 90%. TR-TO actin^{wt} cell line has very little leakage in the absence of Dox (see lane 3, lower western blot). Not all samples are included in the upper picture (inputs and flowthrough).

cell line was created previously by Arnaud Descot. Experimental set-up included co-immunoprecipitation of doxycycline-induced FLAG-actin in cells either stimulated with 15% serum for 30 minutes or left untreated. Both conditions were serum-starved for 24 hours using 0.5% FBS (Figure IV-44). To identify and remove contaminating proteins, which do not come from FLAG-actin interactions, we considered using either parental NIH 3T3 cells or pcDNA4-TO empty vector monoclonal clonal cell line (both of them do not express FLAG-actin and therefore are suitable for establishing non-specific binding events). Coomassie-staining of co-IP samples (Figure IV-45) revealed little differences between the two and it was decided to use pcDNA4-TO empty vector-expressing cells as a background control. Prior to doxycycline induction and immunoprecipitation, both cell lines were labeled with either light or heavy amino acids, according to SILAC method (Ong, 2007). Light label consisted of unlabeled arginine and lysine (*R0K0*) in the growth medium, while heavy label contained $^{13}C_6$, $^{15}N_4$ -L-arginine (*R10*) and $^{13}C_6$,$^{15}N_2$-L-lysine (*K8*). Cells were grown in the labeling medium for 6 passages which was enough to achieve more than 99% incorporation rate for heavy aminoacids (Figure IV-46). Design of the experiment is shown in Figure IV-47. We used three principal conditions to compare: 1) non-stimulated empty vector and FLAG-actin expressing cells. This sample was used to define true interacting partners of actin before serum stimulation; 2) serum-stimulated empty vector and FLAG-actin expressing cells. Here we could identify true actin-interacting partners after serum stimulation; 3) non-stimulated and serum-stimulated FLAG-actin express-

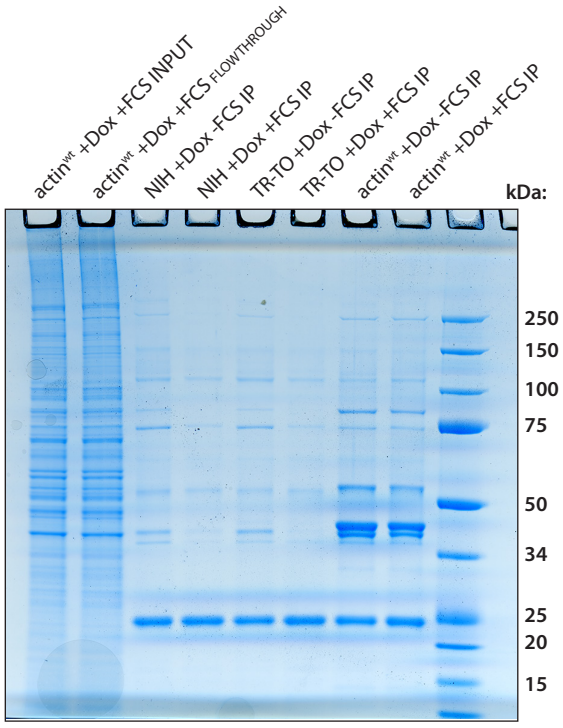

Figure IV-45: *Comparison of control co-IP samples.* Parental NIH 3T3, TR-TO empty vector cell line and TR-TO actin^{wt} cells were subjected to co-IP using indicated conditions and the samples were run on a gradient 4-12% polyacrylamide gel No apparent differences between parental cells and TR-TO empty vector line are visible.

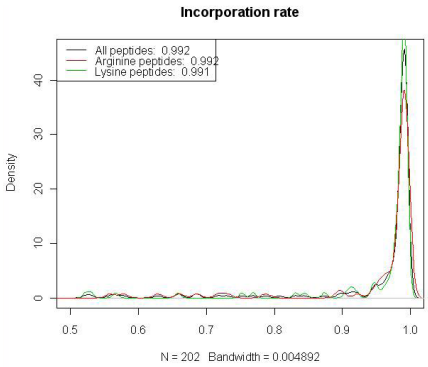

Figure IV-46: *SILAC label incorporation efficiency.* Graph showing the efficiency of heavy label incorporation, which is >99%.

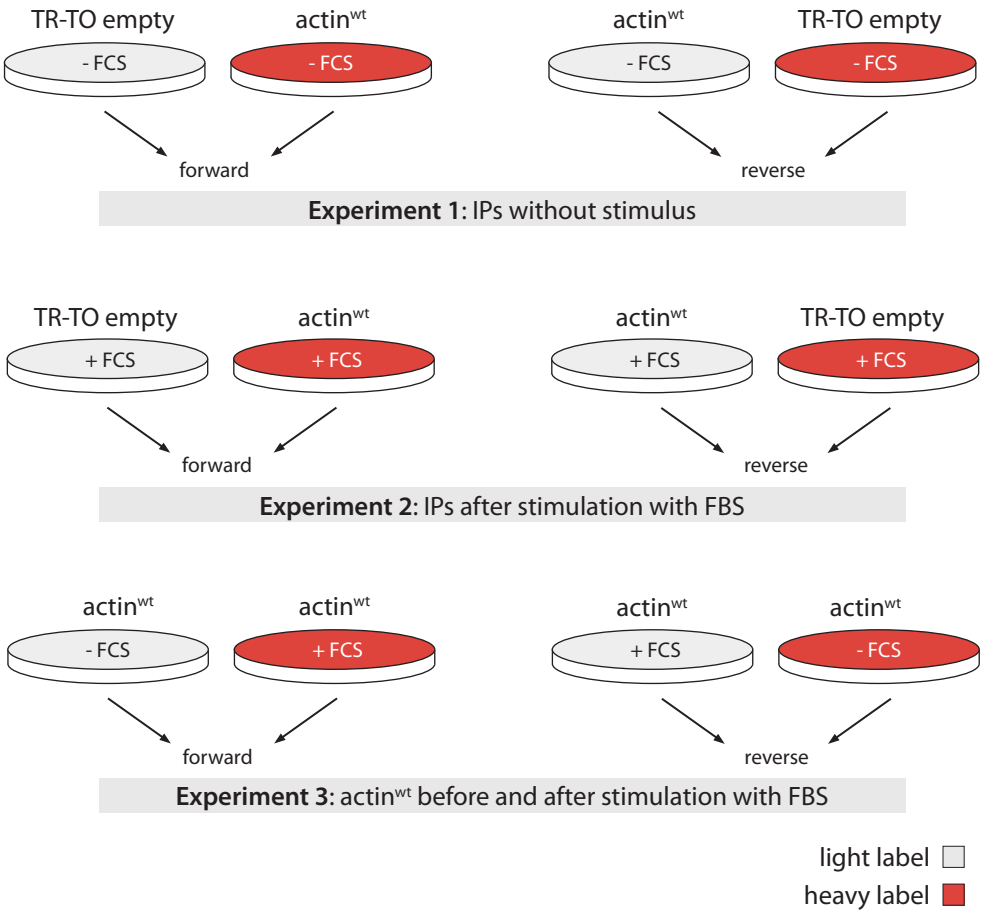

Figure IV-47: *Sample and labeling setup.* Arrows indicate pooling of samples.

ing cells. With this sample we were able to detect the changes in G-actin interactome after the serum stimulation. As an additional internal control, each principal sample consisted of two sub-samples mixed together – one with light label and the other one with heavy label. Immunoprecipitation samples were run on gradient polyacrylamide gels and processed for mass-spectrometry using in-gel digest protocol (Figure IV-48). Mass spectrometer handling and the analysis of the results were performed by Marco Hein-Yannic and Christian Eberl. Proteins that were identified as interactors in both empty vector and FLAG-actin expressing cells were defined as contaminants and removed from analysis. All true G-actin-interacting proteins (identified only in FLAG-actin expressing cells) were defined as 'outliers' with the calculated significance $B < 0.01$ and were taken into further analysis (Figure IV-49, marked in blue). After hierarchical clustering and sorting, proteins that were differentially bound to the FLAG-actin before and after serum stimulation were defined (Figure IV-50). In the forward ratio column green color represents proteins that display decreased binding to G-actin after serum stimulation, while red color designates increased binding to actin. Grey/black color represents no change in binding. Reverse ratio serves as internal control and should have

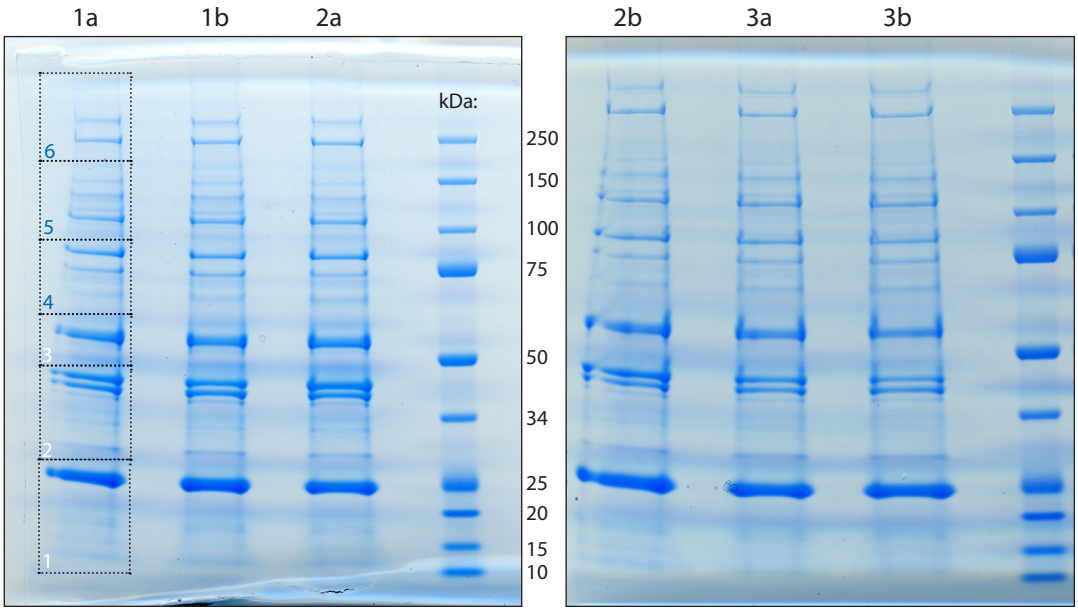

Figure IV-48: *co-IP samples used in mass-spectrometry.* Coomassie-stained gradient (4-12%) polyacrylamide gels with co-IP samples mixed as indicated below the pictures. First lane shows slices (numbered 1 to 6) for in-gel digestion. Actual gels used for mass-spectrometry.

the colors reversed with respect to the forward ratio. Somewhat surprisingly, only a relatively small number of proteins were found to be differentially bound to G-actin before and after the stimulation. Preliminary analysis of the data identified MRTF-A and MRTF-B as proteins

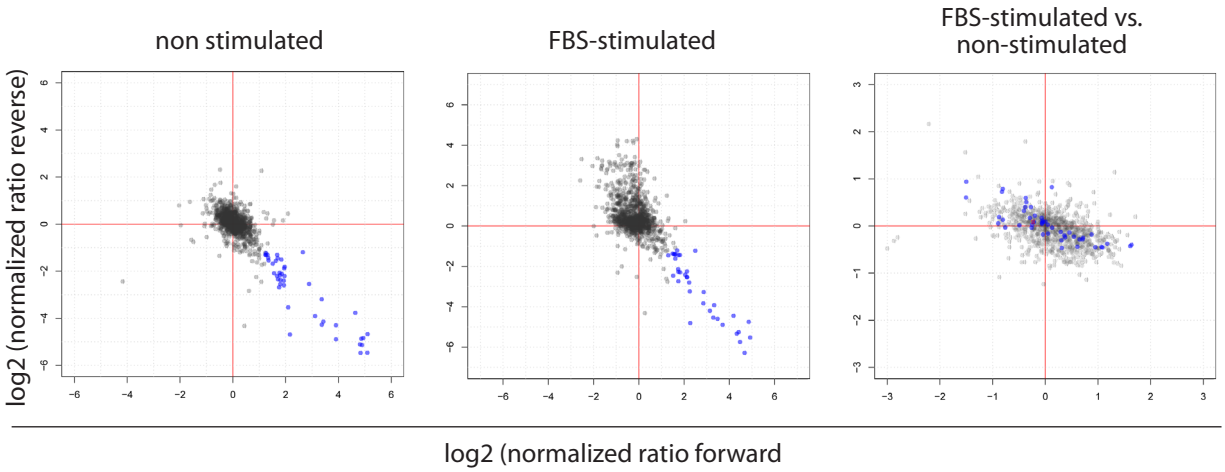

Figure IV-49: *G-actin-interacting proteins: definition.* Plot of *log2* forward (heavy/light) ratios versus *log2* reverse (light/heavy) ratios in non-stimulated and FBS-stimulated sampes allows for identification of true G-actin interacting partners (they have inverted ratios). Graph on the right highlights proteins identified as true interactors; actin itself is indicated in red.

which binding to G-actin is strongly reduced upon serum stimulation - finding that gives a good indication that the results of this screen are robust. Among proteins whose binding to actin increases upon stimulation, we found all seven sub-units of the Arp 2/3 complex, which is an indispensable component of actin polymerization machinery and might be a good candidate for MRTF competitor for G-actin binding. Unexpectedly, non of the classical WH2-containing actin nucleator proteins (formins, WASP, WAVE) were identified as differentially bound to actin, possibly due to the transient nature of interaction, which could not be captured by the immunoprecipitation protocol used for this experiment. Intriguingly, one actin nucleator, Spir1, was found to be significantly less bound to G-actin after the stimulation and therefore presents an interesting observation to follow up. Several other targets in this group, for example, histones (H1a, H2b, H3), appear to be of interest not only in the context of MRTF-G-actin interaction, but also for the G-actin involvement in the regulation of transcription in general. Follow-up studies will be necessary for in-depth analysis of the results of this screen, and I provide more detailed theoretical analysis of the screen in the chapter Discussion.

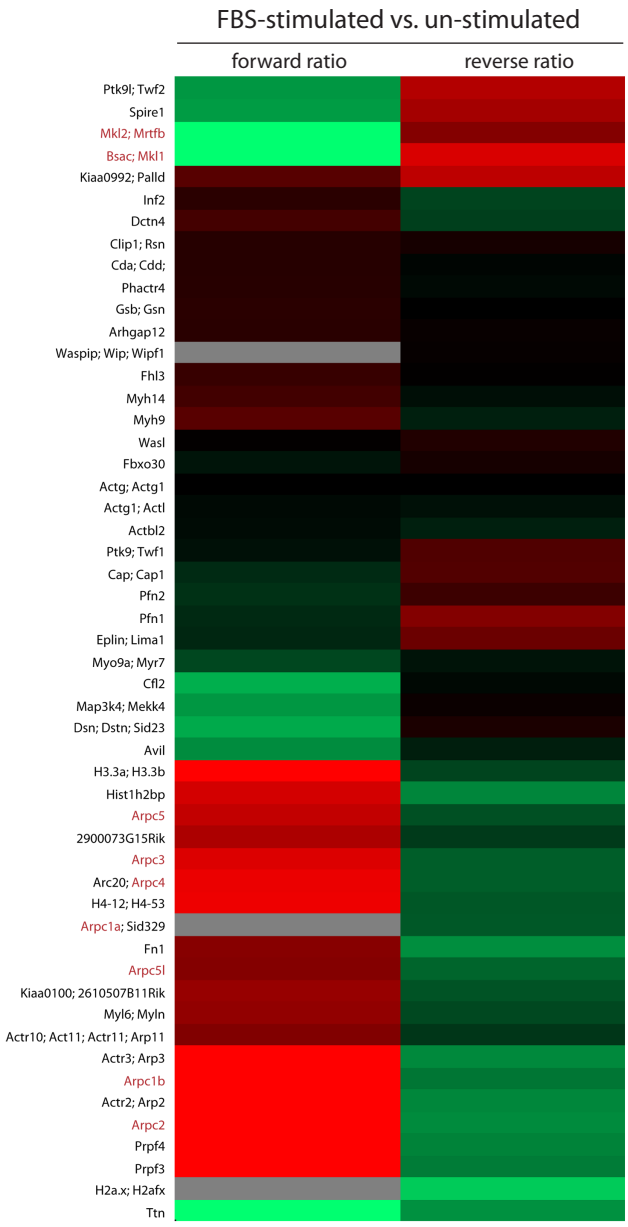

Figure IV-50: *Heatmap of targets differentially bound to G-actin before and after FBS stimulation.* MRTFs and 7 subunits of Arp-2/3 complex are highlighted in red.

Fluorescently tagged MRTF-A: characterization of the fusion proteins.

MRTF-A C-terminally fused to GFP (in pEGFP-N3 vector), as well as tetracyclin-inducible MRTF-A-GFP cell line based on NIH 3T3 have been described (Vartiainen *et al.*, 2007). In a separate project during my studies I attempted to create and characterize GFP-tagged MRTF-A isoforms in order be able to monitor anti-proliferative effects of MRTF-A in live cell imaging. This project was accomplished with a very helpful input from a practical student Lissa Princz (LMU, Munich).

First, MRTF-A protein has been found to be translated from a non-canonical codon coding for leucine, at amino acid position -92 (from ATG start codon in the reference sequence, GeneBank accession number NM_001082536.1). It has been shown that replacement of Leu -92 with methionine codon (ATG) reduces expression of MRTF-A dramatically (Miralles *et al.*, 2003). To address this, I cloned full length MRTF-A cDNA into pEGFP-N1 vector with the following modifications: a) total absence of ATG start codon in front of Leu -92; b) with ATG start codon in front of Leu-92; c) ATG codon and Kozak sequence instead of Leu-92. Western blotting results have shown that MRTF-A-GFP fusion was expressed even without ATG codon in place, although to a much lesser extent than constructs having methionine as start codon (Figure IV-51). Moreover, addition of Kozak sequence did not influence expression levels. Next, I transiently over-expressed these fusion proteins in NIH 3T3 cells and monitored their localization. Unexpectedly, MRTF-A-GFP fusions in vast majority of the cells showed signs of severe protein aggregation, potentially localizing to Golgi apparatus in the form of dense, amorphous clusters of green fluorescence (Figure IV-52). However, cells that contained properly folded proteins, with previously described localization to cytoplasm, could also be observed. Apart from the aggregation problem, I have noticed that GFP fluorescence was significantly dimmer in MRTF-A-GFP fusions

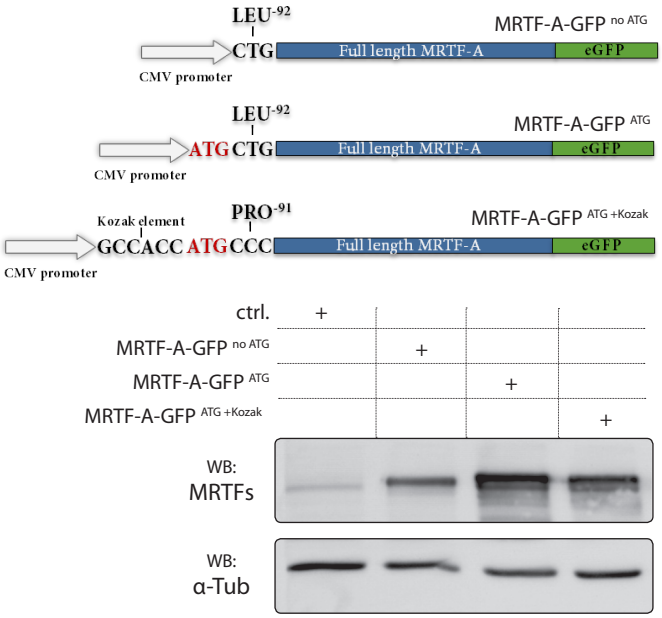

Figure IV-51: *Schemes and expression test of full length MRTF-A GFP fusion proteins.* Start codons and Kozak sequence are highlighted. Western blot is showing expression levels relative to the endogenous MRTFs (ctrl., empty pEGFP-N1 vector).

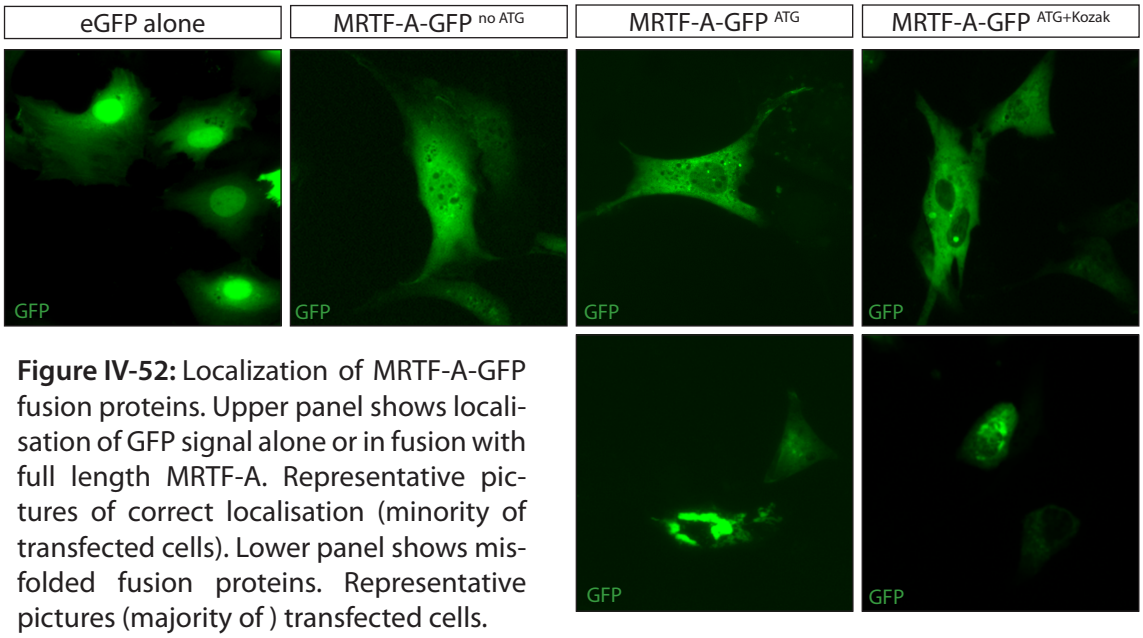

Figure IV-52: Localization of MRTF-A-GFP fusion proteins. Upper panel shows localisation of GFP signal alone or in fusion with full length MRTF-A. Representative pictures of correct localisation (minority of transfected cells). Lower panel shows misfolded fusion proteins. Representative pictures (majority of) transfected cells.

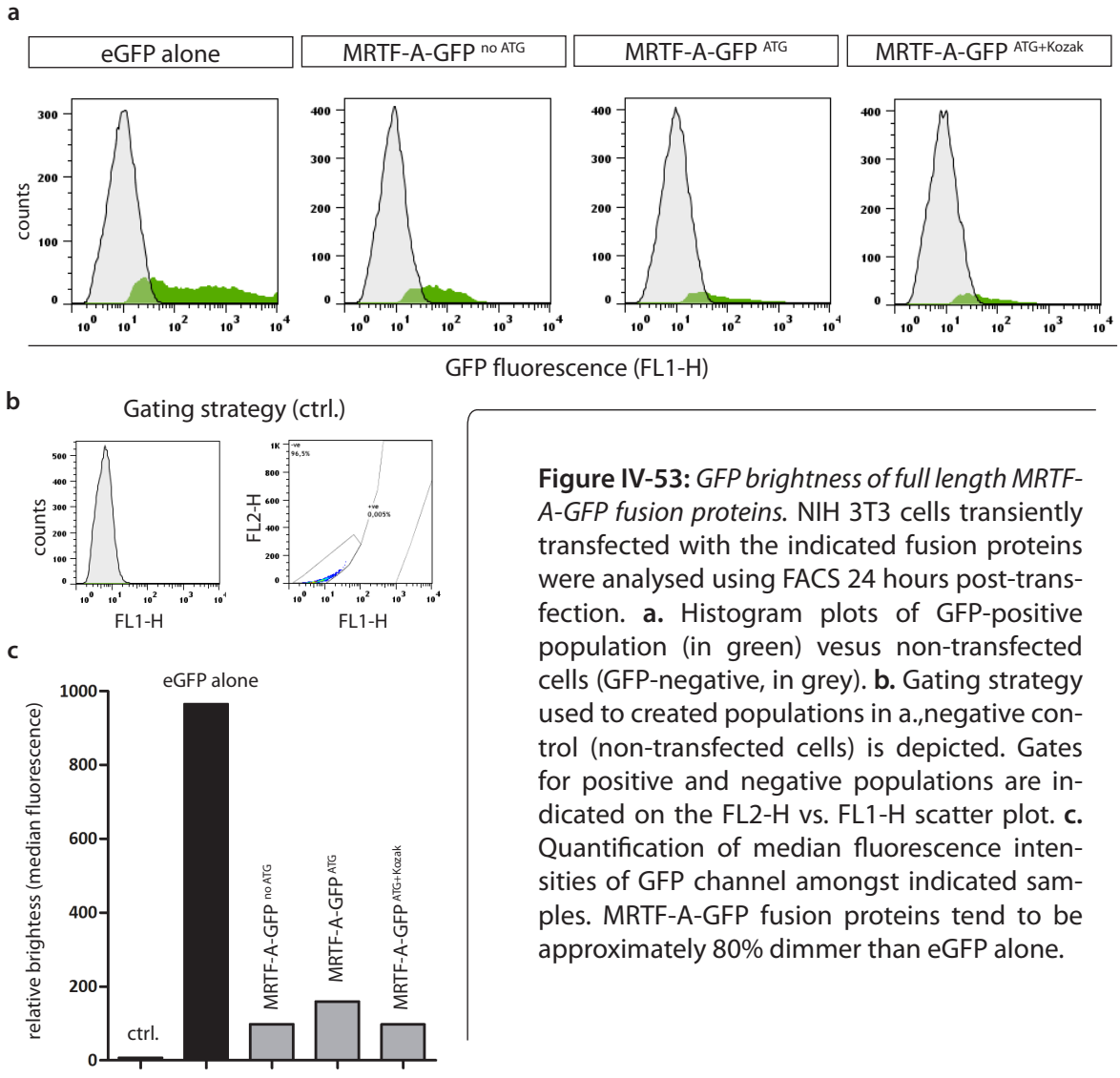

Figure IV-53: *GFP brightness of full length MRTF-A-GFP fusion proteins.* NIH 3T3 cells transiently transfected with the indicated fusion proteins were analysed using FACS 24 hours post-transfection. **a.** Histogram plots of GFP-positive population (in green) vesus non-transfected cells (GFP-negative, in grey). **b.** Gating strategy used to created populations in a.,negative control (non-transfected cells) is depicted. Gates for positive and negative populations are indicated on the FL2-H vs. FL1-H scatter plot. **c.** Quantification of median fluorescence intensities of GFP channel amongst indicated samples. MRTF-A-GFP fusion proteins tend to be approximately 80% dimmer than eGFP alone.

when compared to GFP alone. To determine the extent of the fluorescence loss, I subjected transiently transfected NIH 3T3 cells to FACS analysis, which revealed that all fusion proteins were more than 80% dimmer than GFP alone (Figure IV-53). Finally, measuring SRF-MRTF transcriptional activity using luciferase assays, I have shown that all three fusion proteins caused slight basal up-regulation of SRF reporter, but failed to produce any effect upon serum stimulation (Figure IV-54). Taken together, this data suggests that, while C-terminal MRTF-A-GFP fusions could show proper localization in some of the transfected cells, most of them turned out to be aggregated and mis-localized. Moreover, their use in functional studies does not appear to be possible, since MRTF-A transcriptional activity is severely affected by the presence of GFP next to the C-terminal transactivation domain. In addition to full length MRTF-A, I generated GFP fusions of constitutively active ΔN MAL with eGFP either on C- or N-terminus. Both of the fusions were properly expressed (Figure IV-55). Localization of C-terminal ΔN MAL –eGFP protein was similar to its full length counterpart with majority of cells displaying amorphous perinuclear staining, while some cells contained either exclusively nuclear or both nuclear and cytoplasmic protein. On the other hand, localization of N-terminally tagged eGFP -ΔN MAL in majority of cells was according

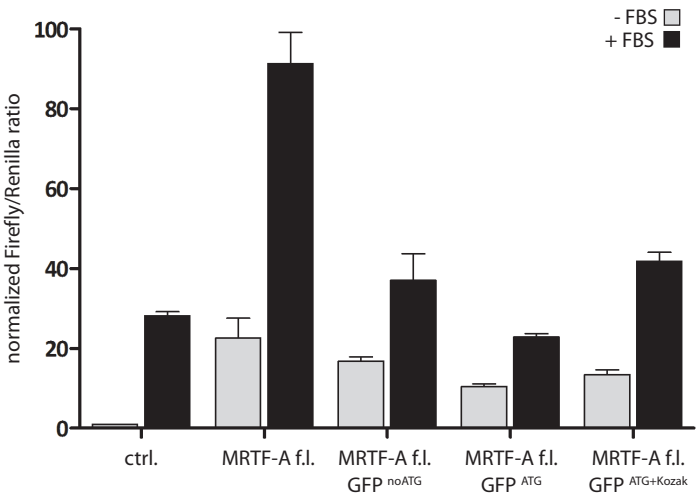

Figure IV-54: *Transcriptional activity of full length MRTF-A-GFP fusion proteins.* NIH 3T3 cells were co-transfected with the indicated proteins, SRF-MRTF reporter plasmid (p3D.A, expresses Firefly luciferase) and Renilla luciferase plasmid (ptkRL). Transfected cells were serum starved for 24 hours and stimulated with 15% FBS for 7 hours. Luciferase assay shows the transcriptional activity of endogenous MRTFs (ctrl, empty vector), activity of ectopic MRTF-A (MRTF-A f.l.without GFP tag) and the activities of the fusion proteins. *n=3, bars - SEM*

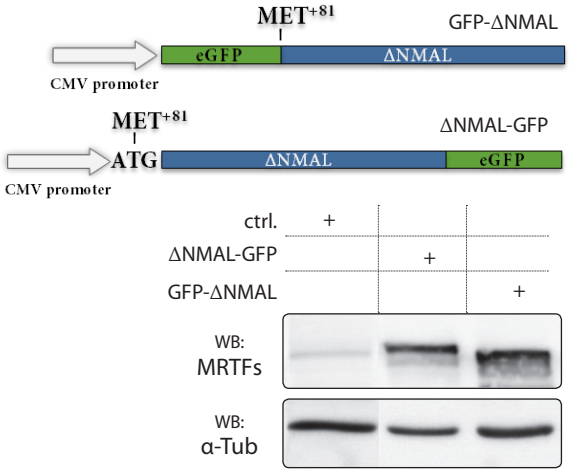

Figure IV-55: *Schemes and expression test of ΔN MAL -GFP fusion proteins.* Western blot showing expression levels in comparison to endogenous MRTFs (ctrl.)

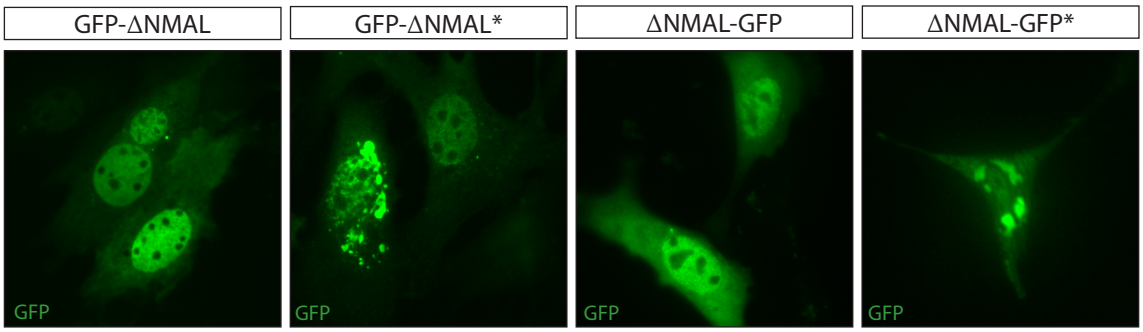

Figure IV-56: Localization of ΔN MAL-GFP fusion proteins.Representative pictures of correct localisation (minority of transfected cells) and mis-folded fusion proteins (majority of cells, indicated with asterix).

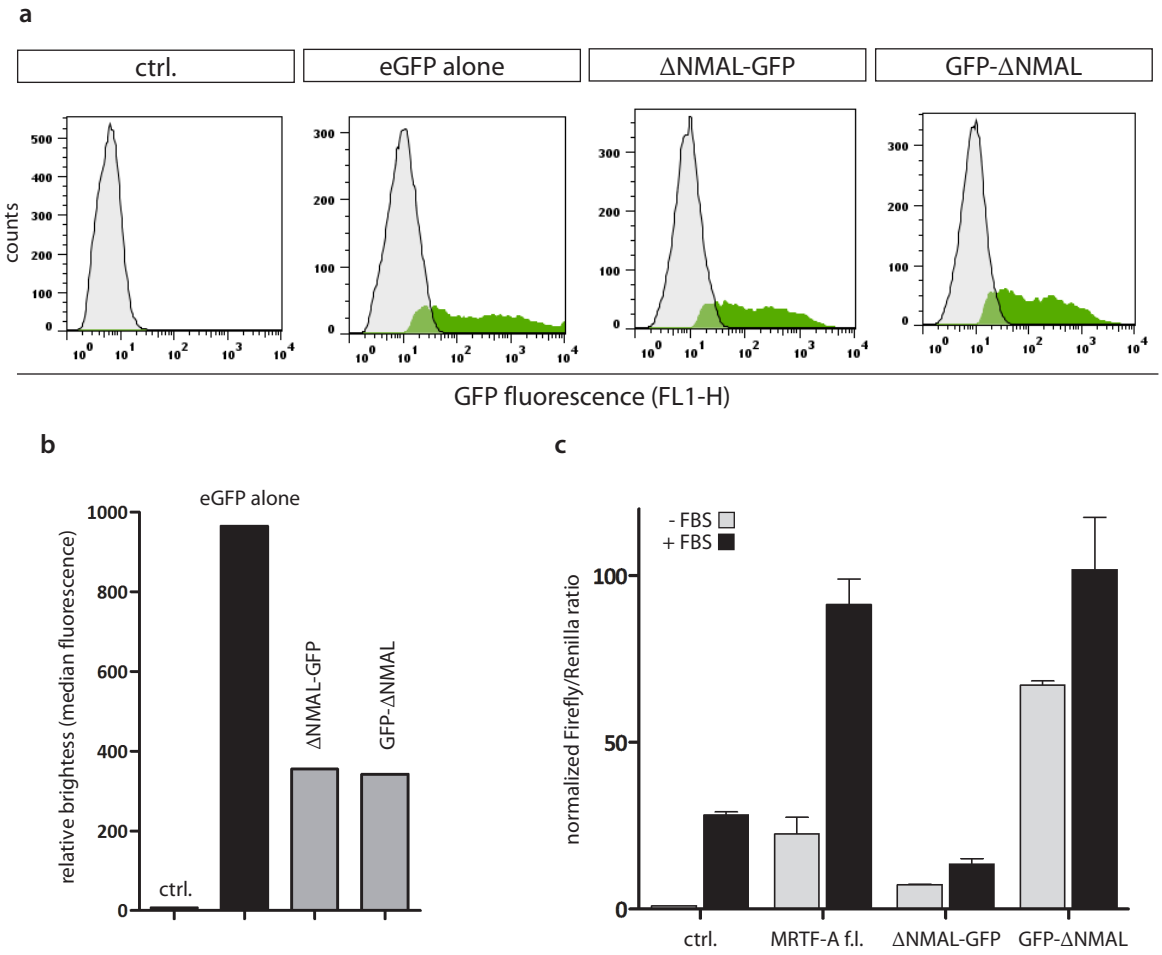

Figure IV-57: *GFP brightness of ΔN MAL-GFP fusion proteins.* NIH 3T3 cells transiently transfected with the indicated fusion proteins were analysed using FACS 24 hours post-transfection. **a.** Histogram plots of GFP-positive population (in green) vesus non-transfected cells (GFP-negative, in grey). **b.** Quantification of median fluorescence intensities of GFP channel amongst indicated samples. ΔN MAL-GFP fusion proteins tend to be approximately 60% dimmer than eGFP alone. **c.** Transcriptional activity of ΔN MAL-GFP fusions. Samples were processed identically to Figure II-54. *n=3, bars - SEM*

to previously described – exclusively nuclear (Figure IV-56), although misfolding has also been observed. GFP brightness was also negatively affected (Figure IV-57A-B). Both N- and C-terminally tagged fusion proteins were approximately 40% as bright as eGFP alone. Transcriptional activity analysis using luciferase assays has revealed that unlike C-terminally tagged version, whose functional activity was severely impaired, N-terminally tagged eGFP -ΔN MAL displayed high transcriptional activity characteristic of constitutively active MRTF-A (Figure IV-57C). In summary, this data has indicated that eGFP orientation in MRTF-A fusions has a profound effect on transcriptional activity with N-terminally located eGFP being permissive for MRTF-A function.

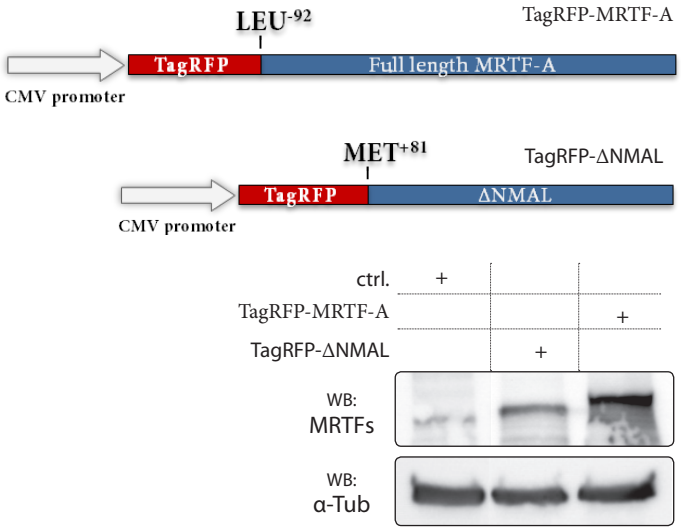

Figure IV-58: *Schemes and expression test of TagRFP-MRTF fusion proteins.* Western blot showing expression levels in comparison to endogenous MRTFs (ctrl.)

In an attempt to solve the problem with brightness of the fusion proteins I created N-terminal fusions of both full length MRTF-A and ΔN MAL with another fluorescent protein – TagRFP, which is the brightest monomeric red fluorescent protein (Figure IV-58). Both TagRFP-full length MRTF-A and TagRFP-ΔN MAL fusion proteins were still mislocalized and aggregated in majority of cells (Figure IV-59). Luciferase assays have shown that the activity of the full length MRTF-A was not restored by placing fluorescent protein on the N-terminus, while ΔN MAL transcriptional activity was comparable to the N-terminally tagged eGFP counterpart (data not shown).

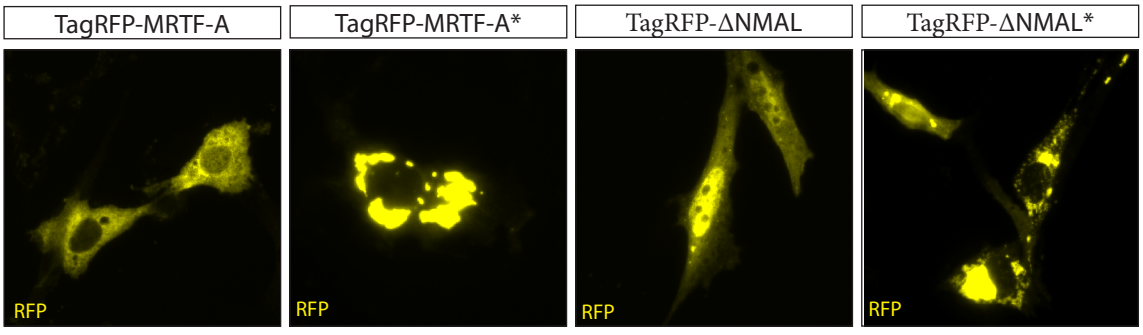

Figure IV-59: *Localization of full length TagRFP-MRTF-A and TagRFP-ΔN MAL fusion proteins.* Representative pictures of correct localisation (minority of transfected cells) and mis-folded fusion proteins (majority of cells, indicated with asterix).

I. DISCUSSION

Binding of SRF and MRTFs to the promoters of target genes.

Analysis of the recruitment of serum response factor and MRTFs to the promoter regions of their putative target genes have revealed several interesting observations. The majority of the consensus CArG boxes in SRF target genes have been previously identified to reside in a proximal promoter, relatively close to the transcription start site (Sun *et al.*, 2006). *In silico* analysis confirmed that the 500 base pairs upstream of TSS is indeed the area with the highest frequency of CArG boxes (Benson *et al.*, 2011). However, as a consequence of the high degree of degeneracy (1216-fold), CArG boxes can be found in other parts of the gene. In human genome, consensus CArG boxes identified within -4000 bp..+4000 bp window around transcription start site, had the following distribution: 40% in 5'-promoter region, 25% in exons, 30% in intronic regions and 6% in 5' exon UTR (Benson *et al.*, 2011). However, high occurrence of SRF-binding sites in a genome does not automatically suggest that every CArG box is a functional one. Moreover, a number of non-consensus CArG-like elements differing from the canonical sequence by 1 or more nucleotide substitutions, have been identified as true SRF-binding sites (Zhang *et al.*, 2005); some were located in the intronic regions (Chen *et al.*, 2010, Mack and Owens, 1999). In this study we have identified several patterns of SRF-MRTF binding to the target genes (Table 1). Eplin-α promoter resembles classical SRF target promoters, such as in Cyr61, Vcl and Srf genes with a single consensus CArG box in the immediate promoter at position -124. Mig-6 and Bok genes contain a single, non-consensus CArG box in the proximal promoter (at positions -260 and -99, respectively), which is responsible for SRF-mediated transcription. Pkp2 gene has non-canonical CArG-like element

in the immediate promoter, which does not bind SRF, however, consensus CArG box in the first intron of the gene, at position +2894, does and it is required for the SRF-mediated transcription. Genes encoding Fhl1, Pai-1 and Noxa, despite having CArG-like elements in their proximal promoters (and in the case of Noxa – consensus CArG box in the first intron), did not bind SRF or MRTFs on these elements. They were, however, regulated by the pathway similarly to the known MRTF targets (Leitner *et al.*, 2011). Probably, the most typical example of the latter phenomenon is the myocardin gene – founding member of the myocardin family. No SRF responsive element has been identified in the *myocd* gene (Sun *et al.*, 2006a), despite the presence of a single consensus CArG box at the position +6714 (Miano, 2003). Nevertheless, there is extensive evidence from SRF knockout studies pointing to the facts that myocardin is indeed a direct SRF target (Parlakian *et al.*, 2004, Miano *et al.*, 2004, Niu *et al.*, 2005).

The most challenging question arising from this data is how the position and exact sequence of SRF-binding element defines if this element will be functionally regulated by SRF. It seems there is no simple answer to this question. Nucleotide sequence surrounding CArG box is obviously important, as exemplified by the CArG-associated Ets-motif, necessary for binding of ternary complex factors (TCFs) to SRF (McMahon and Monroe, 1995). However, no such CArG-surrounding sequences have been identified for MRTF family of co-activators. One *in silico* study has proposed the existence of conserved nucleotides in the flanking regions of functional CArG boxes (at positions -15, -8, +8) that contribute to selective recognition by SRF (Wu *et al.*, 2010). Whole-genome ChiP-seq of SRF binding sites (Valouev *et al.*, 2008) has established that a large fraction of SRF peaks (29%) occurred within close proximity (100 bp) of the peaks for another transcription factor – GABP – which might indicate that on certain promoters SRF physically interacts with additional factors to form functional transcription initiation complexes. This hypothesis is further supported by the importance of TGF-β control element (TCE) in the SRF-mediated transcription of SM22α gene (Adam *et al.*, 2000) and Sp1-binding negative element in the regulation of smooth muscle myosin heavy chain (SM-MHC) gene (Madsen *et al.*, 1997). Yet another mechanism has been described that could potentially explain SRF-MRTF dependent regulation of genes whose promoters do not contain SRF-responsive elements. Using genome-wide SRF binding profiles, Sullivan *et al.*, 2011 and He *et al.*, 2011 discovered that SRF often bind distantly located intra- or inter-genic regions; this, however, is not sufficient to activate transcription of target gene. Transcription is evidently activated by simultaneous co-occupation of the same genomic location by additional cell type-specific transcription factors. This discovery makes

SRF binding to the proximal promoters of certain genes unnecessary and therefore, impossible to detect by low throughput methods, like chromatin immunoprecipitation. In addition, higher level chromatin organization and gene modifications might have a profound effect on SRF-mediated transcription, but this area remains extremely poorly studied. We have shown that genes encoding Mig-6, Eplin-α, Pkp2 and Bok are all regulated via and physically bound by SRF and MRTFs. However, in light of the presented research, their regulation might be much more complex and cell type specific, with involvement of additional regulatory elements beside SRF-MRTFs. Genes encoding Fhl1, Pai-1 and Noxa represent good candidates for investigating regulatory mechanisms that involve binding of SRF to the distant enhancer elements.

Table I-1: Summary of serum response elements tested in this study.

Gene name	SREs tested	SRF/MRTF binding (ChiP)
Mig6	non-consensus, immediate promoter	+
Eplin-α	consensus, immediate promoter	+
Pkp2	consensus, intronic	+ (inducible SRF)
	non-consensus, immediate promoter	-
Bok	non-consensus, immediate promoter	+ (inducibe SRF)
Noxa	non-consensus, immediate promoter	-
	consensus, intronic	-
Fhl1 and Pai1	non-consensus, immediate promoter	-

Additionally, I have noticed an unusual behavior of SRF on the promoters of Pkp2 and Bok. In classical cases, SRF is bound to the CArG boxes in target promoters constitutively, even in the absence of growth factors in the medium (Miralles *et al.*, 2003, Vartiainen *et al.*, 2007, Descot *et al.*, 2009). Additional, stimulus-dependent SRF recruitment is relatively weak. However, Bok and Pkp2 promoters displayed different picture, where SRF was essentially absent from the promoter in serum-starved conditions, but became recruited to it in a stimulus-dependent manner. Evidently, this effect does not depend on the consensus/non-consensus state of the SRF-binding site, because Pkp2 contains CArG box and Bok – CArG-like element. The basis of this phenomenon is currently being investigated (http://www.london-research-institute.org.uk/research /richard-treisman/projects).

MRTF activity and apoptosis.

Retrovirus-mediated over-expression of active, or partially active, forms of MRTF-A confers strong cytotoxicity, accompanied by extensive cell death. It was observed on NIH 3T3 fibroblast cells and rat bladder carcinoma cell line NBT-II. Importantly, full length protein, containing all three G-actin binding RPEL domains, as well as mutants, lacking transactivation domain and RPEL domains (ΔNΔC), or transactivation domain and SRF-binding interface (ΔNΔB) do not affect the wellbeing of fibroblasts. These observations make obvious two facts: 1) SRF-mediated transcriptional activity is required; and 2) there is extremely tight control of MRTF-A regulation via binding to G-actin, because the degree of cytotoxicity always correlates with the number of RPEL domains present in the over-expressed protein. Literature on the effects of MRTF overexpression on cellular proliferation remains scarce. Full length MRTF-A over-expression in cardiac fibroblasts did not have any effect on their proliferation (Small *et al.*, 2010). Studies on the Drosophila homolog of MRTF-A (DMRTF) shown that the over-expression of wild-type DMRTF did not evoke any phenotype when expressed in mesoderm or tracheal system, while the effects of constitutively active DMRTF were not associated with extensive cell death, but rather with the defects in cell migration during development (Han *et al.*, 2004). Study that initially identified mouse MRTF-A (Sasazuki *et al.*, 2002) implicated its over-expression in the protection against TNF-induced apoptosis. This highly cited paper, however, contains plethora of contradictory data, which deserves mentioning here. First, all experiments were done in Traf2/Traf5 double knockout MEF cells which are extremely sensitive to TNF-induced apoptosis due to defects in NFκB module activation (Tada *et al.*, 2001). Wild type MEFs are not susceptible for TNF-induced cell death. Since NFκB pathway was shown to directly interact with SRF-myocardin pathway (Tang *et al.*, 2008), deleting NFκB axis does not make interpretation of these results straightforward. Moreover, authors show that the protein they overexpress is constitutively nuclear, but translocates to cytoplasm when 500 N-terminal amino acids are deleted. This is exactly opposite from what is generally known about murine MRTF-A – it is localized to cytoplasm, but upon deletion of N-terminus, which contains RPEL motifs, re-localizes to the nucleus (e.g. Miralles *et al.*, 2003). This, together with the fact the paper could not detect interaction between SRF and the protein in question, prompts us to raise a question whether it actually was MRTF-A, that could protect the cells from TNF-induced apoptosis.

Because MRTF activity depends on the binding to SRF, it is logical to suggest that the over-expression of SRF will also lead to the same effects. However, little data on this subject does not support this hypothesis. Over-expression of constitutively active SRF was not associated with increased cells death but on the contrary, stimulated DNA synthesis and entry into cell cycle of PC12 cells (Poser *et al.*, 2000). In another study, SRF-VP16 prevented activation of caspase-3, reduced camptothecin-induced apoptosis in vitro as well as had neuroprotective effects in vivo (Stern *et al.*, 2012). In fact, the only study which has reported strong anti-proliferative effects of SRF over-expression linked this effect to non-specific consequences of high expression levels (Lin *et al.*, 2007). Phenomenon in which artificially introduced high levels of a potent transcriptional activator cause non-specific repression of transcription was termed squelching (Natesan *et al.*, 1997, Lee *et al.,* 1998). In Lin *et al.*, 2007, the authors show that SRF-mediated transcriptional squelching led to severe cytotoxicity in range of cell types, including primary MSCs (porcine bone marrow-derived mesenchymal stem cells), cardiomyocytes, Sol8 myoblasts, P19 embryonal carcinoma cells and HIIEC3 hepatoma cells. This cell death, similarly to MRTF-A induced cell death, required intact transactivation domain and was not sensitive to caspase inhibitor z-VAD-FMK. Obvious parallels between SRF-driven transcriptional squelching and constitutively active MRTF-A over-expression raise question if the latter could also be explained by the non-specific effects of high expression levels. The same paper contains evidence arguing against such a hypothesis. High levels of SRF protein in the cell repressed promoter activities not only of SRE-containing genes, but also SRE-lacking promoter targets. On the other hand, MRTF-A overexpression up-regulated transcription of target genes, pointing towards more specific mechanisms of anti-proliferative effect. Nevertheless, linking MRTF-A activity to the induction of classical apoptosis proved to be difficult. Caspase-3 was apparently activated, but to a very modest degree, which did not correlate with the extent of cell death. Moreover, pan-caspase nhibitor zVAD-FMK could not inhibit cytotoxicity. Together, the data indicates limited role of caspases in the MRTF-A mediated cell death. It is still plausible that apoptosis under these conditions takes place either without or with minimal caspase involvement at early stages – a phenomenon that have been described for staurosporine-induced cell death (Belmokhtar *et al.*, 2001). Another apoptotic marker – phosphatidylserine switch - was clearly present, although a significant portion of cells in annexin V assays also displayed damaged plasma membrane (double propidium iodide and annexin V positive cells). In apoptosis, membrane has been found to be intact throughout most part of the process and its integrity was compromised only during the final necrotic blister (Andrade *et al.*, 2010). This final stage of apoptosis has been termed

secondary necrosis (Savill *et al.*, 2002). This could serve as one explanation of the relatively big double PI-annexin V positive population of cells. Primary necrosis, on the other hand, is characterized by the compromised plasma membrane integrity at early stages. Data generated in this study does not exclude the possibility of primary necrosis occurring in parallel with true apoptosis upon active MRTF-A over-expression.

Second question that we intended to address with this study is whether MRTFs are involved in the apoptosis signaling induced by various stimuli. We show that stimulation with TNF-α, which triggers extrinsic apoptotic pathway (Budihardjo *et al.*, 1999) and a broad spectrum protein kinase inhibitor staurosporine (Chae *et al.*, 2000) increase MRTF-mediated transcriptional activity. Moreover, TNF-α does positively affect expression of MRTF-target genes in a transient manner and correlate with nuclear translocation of MRTFs. While exact consequences of staurosporine-induced MRTF activity remain obscure, TNF-α pathway has an interesting connection to SRF-mediated transcription. Upon stimulation with lypopolysacharide (LPS), extracellular signal-regulated kinase (ERK) activates the transcription of TNF-α gene by the concerted action of several transcription factors, which include second family of SRF co-activators – Ets-1 and Elk1 (Tsai *et al.*, 2000), implicating SRF in the production of TNF-α. It is easy to suggest that secreted TNF-α acting in autocrine-paracrine manner, again induces SRF-mediated transcription, but on promoters responsive to actin-SRF-MRTF axis, instead of (or in addition to) ERK-responsive targets. Whether this activation directly relates to apoptosis induction remains to be investigated in different cell type, because neither NIH 3T3 cells nor MEFs undergo apoptosis upon TNF-α treatment due to parallel activation of pro-survival NFκB module (Javelaud *et al.*, 2001, Tang *et al.*, 2001). Somewhat unexpectedly, another member of TNF family of ligands – TRAIL (TNF-related apoptosis-inducing ligand) – has been shown to induce caspase-dependent cleavage of SRF accompanied by loss of c-fos expression (Bertolotto *et al.*, 2000). Similar findings were reported for Burkitt's lymphoma BJAB cell line upon Fas ligation (Drewett *et al.*, 2001). This discrepancy might reflect the differences in fine-tuning of apoptotic pathways induced by similar ligands in different cellular types. Finally, it remains plausible that MRTF activity contributes to TNF-α effects other than cell death, e.g. modulation of fibroblast migration during wound healing (Schirren *et al.*, 1990).

Pro-apoptotic genes Bok and Noxa are MRTF-A targets.

In this study pro-apoptotic genes Bok and Noxa were shown to be regulated by SRF-MRTF pathway. However, physiologically relevant regulation of both genes appears to be more complex than that. Members of E2F transcription factor family have been implicated in the regulation of Bok expression upon serum-stimulated cell cycle re-entry (Rodriguez *et al.*, 2006). In comparison, our work relied on a much longer stimulation times compared to our relatively short time-scale analysis, implying different modes of Bok regulation by two serum-inducible transcription factors. In neuroblastoma cell line SH-SY5Y, but not in breast carcinoma MCF7 cells, up-regulation of Bok expression during DNA damage-induced apoptosis was found to be p53-dependent (Yakovlev *et al.*, 2004). In NIH 3T3 cells used in this study, no significant up-regulation of Bok was detected following treatment with etoposide or doxorubicin, indicating cell type and stimulus-specific regulation of Bok expression. Similarly, transcription of Noxa probably involves more than a single factor. Initially, Noxa was thought as a primary p53 target, regulated vie a bona fide p53 response element in the proximal promoter, at position -195 (Oda *et al.*, 2000). However, p53-independent regulation has also been demonstrated, involving transcription factors c-myc, HIFα and members of E2F family (Elgendy *et al.*, 2011, Fei *et al.,* 2002, Lau *et al.*, 2008, Hershko and Ginsberg, 2004). Present study shows that direct activation of SRF-MRTF pathway using characterized stimuli leads to p53-independent up-regulation of Noxa gene. Moreover, depletion of p53 somewhat enhanced the regulatory pattern seen for SRF-MRTF targets and sensitized cells for latrunculin B-mediated block of induction. Consistent with this, we observed that in wild-type cells, basal levels of Noxa were slightly up-regulated by latrunculin B, which depolymerizes F-actin and this turns into slight repression in p53-depleted cells. This suggests that p53 and MRTFs could cooperate in regulating Noxa in a manner where p53 is involved in sensing F-actin status, while MRTFs respond to changes in G-actin. Unexpectedly, apoptosis-triggering etoposide and doxorubicine both induced Noxa expression, but this induction was completely abolished in p53-depleted cells. This adds a big question mark to the involvement of SRF-MRTF-mediated regulation of Noxa during DNA damage-induced apoptosis, at least in fibroblast cells. In addition, neither Bok nor Noxa could be induced by TNF-α treatment, even in the MEFs lacking NEMO protein and therefore, sensitive to TNF-induced cell death. This suggests that both genes are most likely not required for the extrinsic apoptotic signaling in the tested cells. Also, over-expression of either Bok or Noxa failed to induce cell death in NIH 3T3 filbroblasts (Shaposhnikov *et al.*, 2012 and Shibue *et al.*, 2006), pointing to the fact that both proteins do not play deciding roles in the apopto-

sis induction. The physiologically relevant link between SRF-MRTF-mediated Bok and Noxa expression and apoptosis signaling remains therefore elusive. We do not exclude the possibility that some other direct MRTF targets might play significant role in inducing cell death. For example, it has been shown that extracellular matrix protein Cyr61, which is one of the classical SRF-MRTF targets, induces apoptosis in fibroblasts (Todorovic *et al.*, 2005). It does so when used as an adhesion matrix, and does not require new transcription for apoptosis induction, implying that in our system MRTF-A-induced Cyr61 production could trigger death of the adjacent cells in a paracrine fashion.

Effects of MRTF depletion on cell cycle.

Serum response factor is without doubt a very important element in the cell cycle progression and proliferation of many cell types. It appears to be a part of the immediate early gene response (Herschman, 1991), where, upon exposure to mitogens, cells in quiescent state (G0) activate transcription factors which subsequently regulate genes necessary for G1 entry and progression through cell cycle (Almendral *et al.*, 1988, Lau and Nathans, 1985). According to this model, immediate early SRF target genes c-fos and egr-1 are activated via MAP kinase pathway, involving cooperation of ternary complex factors (TCFs) and SRF (Gille *et al.*, 1992, Treisman, 1996). In addition to cell cycle entry, SRF homologue MCM1 was found to be required for G2-M transition in yeast (Althoefer *et al.*, 1995, Maher *et al.*, 1995). SRF involvement in the regulation of proliferation does not however appear to be absolutely universal: SRF-deficient mouse embryonic stem cells despite having severe defects in both immediate early gene activation and actin expression were able to proliferate normally (Schratt *et al.*, 2001). Nevertheless, presence of SRF seems to be critical for many cell types. Unlike the well-established role of ternary complex factors (Vickers *et al.*, 2004: Schratt *et al.*, 2004), the contribution of actin-regulated MRTF co-activators of SRF in this process is still not clear. During the course of this study I aimed at characterization of the effects of MRTF depletion on cell proliferation and cell cycle progression. Using siRNA, targeting both MRTF-A and MRTF-B, I essentially depleted NIH 3T3 cells from all members of MRTF family, essentially alleviating redundancy problem. Myocardin, the founding member of the family has been reported to be expressed in primary fibroblasts under certain conditions (serum starvation, contact inhibition), however, immortalized cells, like hTERT-immortalised Wi38 cell line are not able to induce its expression (Shats *et al.*, 2007; Milyavsky *et al.*, 2003). Similarly, I was not able to detect myocardin expression in cycling or serum-starved NIH 3T3 cells (unpub-

lished observations). Given the observed anti-proliferative effects of active MRTF-A over-expression together with established cytotoxic effect of myoradin expression (see above), it is logical to suggest that depletion of MRTFs will confer growth advantage to the cells. Previously, knockdown of MRTF-A and MRTF-B was shown not to affect cell cycle phase distribution when breast carcinoma MDA-MB-231 or melanoma B16F2 cells were grown in 10% FBS (Medjkane *et al.*, 2009). In the same study, knockdown also did not induce apoptosis as measured by annexin V assay. Another study has shown that MRTF-A/B-deficient neuronal precursor cells proliferate normally, but have slightly elevated levels of apoptosis (Mokalled *et al.*, 2010). In my experiments with NIH 3T3 cells, apoptosis could not be detected by Annexin V assay, while cell cycle distribution of asynchronously cycling cells remained seemingly normal. However, in growth factor-deprived conditions (0.5%) FCS, MRTF-depleted cells consistently displayed elevated S and G2 phases, which, however, did not lead to subsequent cell division and proliferation as judged by direct cell counting. Such picture can theoretically be observed under two scenarios: a) MRTF-depleted cells forgo G1-S checkpoint in the absence of mitogens present in serum; b) MRTF-depleted cells are arrested during S and G2 phases and cannot complete cell cycle upon withdrawal of growth factors. BrdU staining experiments, showing newly-synthesized DNA in serum-starved cells, fully support the first scenario. However, it is likely that there might be a second G2-M arrest, which might be a consequence of strong accumulation of $p21^{Waf1}$ in MRTF-depleted cells, which is known to induce G2-M arrest by targeting cdc2 kinase for degradation (Dash and El-deiry, 2005). When we look at asynchronously growing cells in 10% FBS, differences in cell cycle phase distributions can only be detected by tracing single cells. And while the total time of the cell cycle progression remained unchanged, MTRF knockdown led to a significant shortening of G1 phase and slight lengthening of S-G2 phase. Exactly the same effect has been observed upon over-expression of various cyclins, for example cyclin E in primary fibroblasts (Ohtsubo and Roberts, 1993), cyclin E in HeLa cells (Wimmel *et al.*, 1994), cyclin D1 in human breast cancer T-47D cells (Musgrove *et al.*, 1994), cyclin D1 in Rat6 embryo fibroblasts (Jiang *et al.*, 1993), either cyclin E or cyclin D using tetracyclin-inducible system in Rat-1 cells (Resnitzky *et al.*, 1994). Results of this study indicate that there is only a marginal (if at all) increase in total cyclin D1 levels upon MRTF depletion, while cyclin E was not analysed. I propose, however, that identified down-regulation of the majority of cyclin-CDK inhibitor members – $p18^{Ink4c}$, $p19^{Ink4d}$ and $p27^{Kip1}$ – along with the absence of detectable $p15^{Ink4b}$, $p16^{Ink4a}$ and p19ARF, increases activity of G1 cyclins, which confers effects, similar to overexpression. Concerning lengthening of S-G2 phase, potential reasons and implications have been analyzed in great

detail in Cooper, 1998 and boil down to additional effects of cyclins on S phase or unknown compensatory mechanisms. Interestingly, pharmacological inhibition of the upstream effector of MRTFs, Rho, with C. botulinum C3 exoenzyme, led to a very similar one hour delay in G2-M progression (Ando *et al.*, 2007), indicating that the observed effect on S-G2 phase might be MRTF-specific. Up-regulation of another member of cyclin-CDK inhibitor, $p21^{Waf1}$ might be explained by several lines of evidence. First, $p21^{Waf1}$ has been reported to be transcriptionally regulated by a ternary complex factor Elk1-SRF complex in a ERK-dependent manner. Given that the competition between MRTFs and TCFs exists (Wang *et al.*, 2004, Murai and Treisman, 2002), it is plausible that the absence of MRTFs could enhance the transcription of targets where such competition takes place. Alternatively, Lee *et al.*, 2007 reported that $p21^{Waf1}$ expression is impaired in cells over-expressing SRF. They discovered that high levels of SRF led to displacement of Smad3 complex from $p21^{Waf1}$ promoter, leading to down-regulation of protein expression. Moreover, siRNA-mediated knockdown of SRF led to increased $p21^{Waf1}$ levels. It is not clear whether $p21^{Waf1}$ can be expressed via MRTF activation, but its promoter does contain consensus CArG box and can be regulated via myocardin (Kimura *et al.*, 2010). Taken together, these studies allow suggesting that MRTF depletion could lead to $p21^{Waf1}$ up-regulation via lack of repressive SRF binding to its promoter. Yet another possibility stems from the discovery that up-regulated cyclin D1 levels were found to be correlating with the increased protein stability (and consequently, accumulation) of $p21^{Waf1}$ (Coleman *et al.*, 2003). Given that there is potential excess of free active cyclin D1 upon MRTF knockdown, as discussed earlier, it might be employed for $p21^{Waf1}$ binding and stabilization. Finally, it has been shown that inhibition of Rho signaling lead to induction of $p21^{Waf1}$ protein levels by Ras, while over-expression of active form of V12 H-Ras leads to $p21^{Waf1}$ up-regulation and $p27^{Kip1}$ repression (Olson *et al.*, 1998). These findings might serve as a potential link between upstream signaling from small GTPases and downstream SRF-MRTF axis. The effects of elevated $p21^{Waf1}$ in MRTF-depleted cells are not clear, but apparently it does not hinder the faster progression through G1 phase.

Another prominent feature of MRTF knockdown was the accumulation of cells harbouring such nuclear defects as micronuclei and nuclear buds. Micronuclei originate from displaced chromosomes that failed to attach properly to the spindle during segregation process (reviewed in Fenech *et al.*, 2011). Interestingly, over-expression of H-Ras and subsequent activation of MAP kinase pathway also have been shown to cause increase in mucronuclei count in NIH 3T3 cells (Saavedra *et al.*, 1999), along with chromosomal aberrations, such as dicentric chromosomes, acentric chromosomes, double minute chromosomes

(Denko *et al.*, 1994), improper segregation of chromosomes and exclusion of chromosomes form daughter nuclei (Hagag *et al.*, 1990). I was not able to detect increase in aneuploidy or binucleated cells on a 72 hour time scale of transient experiments, however, clonal selection of stable MRTF-depleted NIH 3T3 clones have revealed that all of them, except one, became either aneuploidy or completely doubled their DNA content. Together, these results point to the fact that MRTF depletion might severely affect a delicate balance between two signaling pathways – Ras-MAP kinase (which signal to TCFs-SRF axis) and Rho-actin pathway (which signals to MRTFs-SRF), which is necessary to maintain normal growth and proliferation of fibroblast cells.

Potential competition candidates for dissociation of G-actin-MRTF complex.

Genes whose binding to G-actin increases upon stimulation of actin-MRTF pathway are potential candidates for releasing MRTFs from inhibitory complex with G-actin. Comparing partial proteomes of NIH 3T3 cells before and after serum stimulation we were able to identify proteins that display required behaviour. For example, all seven members of actin nucleator Arp2/3 complex were detected as proteins whose binding to actin increases upon FBS stimulation. Interestingly, although it is known that Arp 2/3 complex requires nucleation promoting factors such as N-WASP or WAVE for its activity (Marchand *et al.*, 2001 Goley and Welch, 2006), none of the known NPFs were consistently found as differentially bound to actin. Counterintuitively, second type of actin nucleator, Spir1 (Quinlan *et al.*, 2005, Bosch *et al.*, 2007), was less bound to actin upon stimulation. The third known class of actin nucleators, formins (Kovar, 2006, Goode and Eck 2007), were not found as differentially bound, probably because they are mostly associated with F-actin structures and not detected in the screen. Another G-actin-sequestering protein Twinfilin-2 (but not Twinfilin-1) was found to be dissociating from G-actin following stimulation, in line with its function of limiting actin polymerization (Palmgren *et al.*, 2002). Intriguingly, increased binding of actin was detected for several histones (H2B, H4), signifying the role of nuclear actin in chromatin remodeling complexes and gene regulation (reviewed in Olave *et al.*, 2002 and Bettinger *et al.*, 2004). In conclusion, several potentially interesting G-actin-interacting proteins were found, however, more thorough experimental follow-up is required for identification of MRTF competitor for G-actin binding.

VI. BIBLIOGRAPHY

1. **Adam, P. J., Regan, C. P., Hautmann, M. B., and Owens, G. K.** (*2000*). Positive- and negative-acting Kruppel-like transcription factors bind a transforming growth factor beta control element required for expression of the smooth muscle cell differentiation marker SM*22*alpha in vivo. The Journal of Biological Chemistry *275*, *37798–37806*.

2. **Alberti, S., Krause S.M., Kretz O., Philippar, U., Lemberger, T., Casanova, E., Wiebel, F.F., Schwarz, H., Frotscher M., Schütz G. and Nordheim, A.** (*2005*). Neuronal migration in the murine rostral migratory stream requires serum response factor. Proceedings of the National Academy of Sciences of the United States of America *102*, *6148–6153*.

3. **Allingham, J. S., Klenchin, V. a, and Rayment, I.** (*2006*). Actin-targeting natural products: structures, properties and mechanisms of action. Cellular and Molecular Life Sciences : CMLS *63*, *2119–2134*.

4. **Almendral, J. M., Sommer, D., Macdonald-Bravo, H., Burckhardt, J., Perera, J., and Bravo, R.** (*1988*). Complexity of the Early Genetic Response to Growth Factors in Mouse Fibroblasts. Molecular and Cellular Biology *8*, *2140–2148*.

5. **Althoefer, H., Schleiffer, a, Wassmann, K., Nordheim, a, and Ammerer, G.** (*1995*). Mcm*1* is required to coordinate G*2*-specific transcription in Saccharomyces cerevisiae. Molecular and Cellular Biology *15*, *5917–5928*.

6. **Anderson, J. P., Dodou, E., Heidt, A. B., Val, S. J. De, Jaehnig, E. J., Greene, S. B., Olson, E. N., and Black, B. L.** (*2004*). HRC Is a Direct Transcriptional Target of MEF*2* during Cardiac , Skeletal , and Arterial Smooth Muscle Development In Vivo. Molecular and Cellular Biology *24*, *3757–3768*.

7. **Ando, Y., Yasuda, S., Oceguera-yanez, F., and Narumiya, S.** (*2007*). Inactivation of Rho GTPases with Clostridium difficile Toxin B Impairs Centrosomal Activation of Aurora-A in G*2* / M Transition of HeLa Cells. Molecular Biology of the Cell *18*, *3752–3763*.

8. **Andrade, R., Crisol, L., Prado, R., Boyano, M. D., Arluzea, J., and Aréchaga, J.** (*2010*). Plasma membrane and nuclear envelope integrity during the blebbing stage of apoptosis: a time-lapse study. Biology of the Cell *102*, *25–35*.

9. **Aravind, L., and Koonin, E. V** (*2000*). SAP - a putative DNA-binding motif involved in chromosomal organization. Trends in Biochemical Sciences *25*, *112–114*.

10. **Arsenian, S., Weinhold, B., Oelgeschläger, M., Rüther, U., and Nordheim, A.** (*1998*). Serum response factor is essential for mesoderm formation during mouse embryogenesis. The EMBO Journal *17*, *6289–6299*.

11. **Asparuhova, M. B., Ferralli, J., Chiquet, M., and Chiquet-Ehrismann, R.** (*2011*). The transcriptional regulator megakaryoblastic leukemia-*1* mediates serum response factor-independent activation of tenascin-C transcription by mechanical stress. The FASEB Journal : Official Publication of the Federation of American Societies for Experimental Biology, *1–12*.

12. **Ayadi, A., Zheng, H., Sobieszczuk, P., Buchwalter, G., Moerman, P., Alitalo, K., and Wasylyk, B.** (*2001*). Net-targeted mutant mice develop a vascular phenotype and up-regulate egr-*1*. The EMBO Journal *20*, *5139–5152*.

13. **Bass-Zubek, A. E., Godsel, L. M., Delmar, M., and Green, K. J.** (*2009*). Plakophilins: multifunctional scaffolds for adhesion and signaling. Current Opinion in Cell Biology *21*, *708–716*.

14. **Beck, H., Flynn, K., Lindenberg, K. S., Schwarz, H., Bradke, F., Di Giovanni, S., and Knöll, B.** (*2012*). Serum Response Factor (SRF)-cofilin-actin signaling axis modulates mitochondrial dynamics. Proceedings of the National Academy of Sciences of the United States of America *109*, E*2523–32*.

15. **Belaguli, N. S., Sepulveda, J. L., Nigam, V., Charron, F., Nemer, M., and Schwartz, R. J.** (*2000*). Cardiac Tissue Enriched Factors Serum Response Factor and GATA-*4* Are Mutual Coregulators. Molecular and Cellular Biology *20*, *7550–7558*.

16. **Belmokhtar, C. A., Hillion, J., and Ségal-Bendirdjian, E.** (*2001*). Staurosporine induces apoptosis through both caspase-dependent and caspase-independent mechanisms. Oncogene *20*, *3354–3362*.

17. **Benson, C. C., Zhou, Q., Long, X., and Miano, J. M.** (*2011*). Identifying functional single nucleotide polymorphisms in the human CArGome. Physiological Genomics *43*, *1038–1048*.

18. **Bertolotto, C., Ricci, J. E., Luciano, F., Mari, B., Chambard, J. C., and Auberger, P.** (*2000*). Cleavage of the serum response factor during death receptor-induced apoptosis results in an inhibition of the c-FOS promoter transcriptional activity. The Journal of Biological Chemistry *275*, *12941–12947*.

19. **Bettinger, B. T., Gilbert, D. M., and Amberg, D. C.** (*2004*). Actin up in the nucleus. Nature Reviews. Molecular Cell Biology *5*, *410–415*.

20. **Bosch, M., Le, K. H. D., Bugyi, B., Correia, J. J., Renault, L., and Carlier, M.-F.** (*2007*). Analysis of the function of Spire in actin assembly and its synergy with formin and profilin. Molecular Cell *28*, *555–568*.

21. **Boxer, L. M., Prywes, R., Roeder, R. G., and Kedeslt, L.** (*1989*). The Sarcomeric Actin CArG-Binding Factor Is Indistinguishable from the c-fos Serum Response Factor. Molecular and Cellular Biology *9*, *515–522*.

22. **Brandt, D. T., Xu, J., Steinbeisser, H., and Grosse, R.** (*2009*). Regulation of myocardin-related transcriptional coactivators through cofactor interactions in differentiation and cancer. Cell Cycle (Georgetown, Tex.) *8*, *2523–2527*.

23. **Buchwalter, G., Gross, C., and Wasylyk, B.** (*2004*). Ets ternary complex transcription factors. Gene *324*, *1–14*.

24. **Budihardjo, I., Oliver, H., Lutter, M., Luo, X., and Wang, X.** (*1999*). Biochemical pathways of caspase activation during apoptosis. Annual Review of Cell and Developmental Biology *15*, *269–290*.

25. **Busche, S., Descot, A., Julien, S., Genth, H., and Posern, G.** (*2008*). Epithelial cell-cell contacts regulate SRF-mediated transcription via Rac-actin-MAL signalling. Journal of Cell Science *121*, *1025–1035*.

26. **Busche, S., Kremmer, E., and Posern, G.** (*2010*). E-cadherin regulates MAL-SRF-mediated transcription in epithelial cells. Journal of Cell Science *123*, *2803–2809*.

27. **Cao, D., Wang, C., Tang, R., Chen, H., Zhang, Z., Tatsuguchi, M., and Wang, D.-Z.** (*2012*). Acetylation of myocardin is required for the activation of cardiac and smooth muscle genes. The Journal of Biological Chemistry *287*, *38495–38504*.

28. **Chae, H. J., Kang, J. S., Byun, J. O., Han, K. S., Kim, D. U., Oh, S. M., Kim, H. M., Chae, S. W., and Kim, H. R.** (*2000*). Molecular mechanism of staurosporine-induced apoptosis in osteoblasts. Pharmacological Research *42*, *373–381*.

29. **Chang, D.F., Belaguli N.S., Iyer, D., Roberts, W.B., Wu, S-P., Dong, X-R., Marx, J.G., Moore, M.S., Beckerle, M.C., Majesky M.W., Schwarz, R.J.** (*2003*). Cysteine-rich LIM-only proteins CRP*1* and CRP*2* are potent smooth muscle differentiation cofactors. Developmental Cell *4*, *107–118*.

30. **Charvet, C., Houbron, C., Parlakian, A., Giordani, J., Lahoute C., Bertrand, A., Sotiropoulos, A., Renou, L., Schmitt, A., Melki, J., Li, Z., Daegelen, D. and Tuil, D.** (*2006*). New role for serum response factor in postnatal skeletal muscle growth and regeneration via the interleukin *4* and insulin-like growth factor *1* pathways. Molecular and Cellular Biology *26*, *6664–6674*.

31. **Chen, C. Y. I., and Schwartz, R. J.** (*1996*). Recruitment of the tinman homolog Nkx-*2.5* by serum response factor activates Cardiac alpha-Actin Gene Transcription. Molecular and Cellular Biology *16*, *6372–6384*.

32. **Chen, C.-H., Wu, M.-L., Lee, Y.-C., Layne, M. D., and Yet, S.-F.** (*2010*). Intronic CArG box regulates cysteine-rich protein *2* expression in the adult but not in developing vasculature. Arteriosclerosis, Thrombosis, and Vascular Biology *30*, *835–842*.

33. **Chen, J., Kitchen, C.M., Streb, J.W. and Miano, J.M.** (*2002*). Myocardin: A Component of a Molecular Switch for Smooth Muscle Differentiation. Journal of Molecular and Cellular Cardiology *34*, *1345–1356*.

34. **Chen, J., Yin, H., Jiang, Y., Radhakrrishnan, S.K., Huang, Z-P., Li, J., Shi, Z., Kilsdonk, E.P., Gui, Y., Wang, D-Z. and Zheng, X-L.** (*2011*). Induction of microRNA-*1* by myocardin in smooth muscle cells inhibits cell proliferation. Arteriosclerosis, Thrombosis, and Vascular Biology *31*, *368–375*.

35. **Chervin-Pétinot, A., Courçon, M., Almagro, S., Nicolas, A., Grichine, A., Grunwald, D., Prandini, M.-H., Huber, P., and Gulino-Debrac, D.** (*2012*). Epithelial protein lost in neoplasm (EPLIN) interacts with α-catenin and actin filaments in endothelial cells and stabilizes vascular capillary network in vitro. The Journal of Biological Chemistry *287*, *7556–7572*.

36. **Chung, K., Gomes, I., Wang, D., Lester, F., and Rosner, M. R.** (*1998*). Raf and Fibroblast Growth Factor Phosphorylate Elk*1* and Activate the Serum Response Element of the Immediate Early Gene pip*92* by Mitogen-Activated Protein Kinase-Independent as Well as -Dependent Signaling Pathways. Molecular and Cellular Biology *18*, *2272–2281*.

37. **Coleman, M. L., Marshall, C. J., and Olson, M. F.** (*2003*). Ras promotes p*21*(Waf*1*/Cip*1*) protein stability via a cyclin D*1*-imposed block in proteasome-mediated degradation. The EMBO Journal *22*, *2036–2046*.

38. **Cooper, S.** (*1998*). On the Interpretation of the Shortening of the G*1*-Phase by Overexpression of Cyclins in Mammalian Cells. Experimental Cell Research *115*, *110–115*.

39. **Copeland, J. W., and Treisman, R.** (*2002*). The Diaphanous-related Formin mDia*1* Controls Actin Polymerization. Molecular Biology of the Cell *13*, *4088–4099*.

40. **Creemers, E. E., Sutherland, L. B., McAnally, J., Richardson, J. A., and Olson, E. N.** (*2006*a). Myocardin is a direct transcriptional target of Mef*2*, Tead and Foxo proteins during cardiovascular development. Development *133*, *4245–4256*.

41. **Creemers, E. E., Sutherland, L. B., Oh, J., Barbosa, A. C., and Olson, E. N.** (*2006*b). Coactivation of MEF*2* by the SAP domain proteins myocardin and MASTR. Molecular Cell *23*, *83–96*.

42. **Dalton, S., and Treisman, R.** (*1992*). Characterization of SAP-*1*, a protein recruited by serum response factor to the c-fos serum response element. Cell *68*, *597–612*.

43. **Dash, B. C., and El-deiry, W. S.** (*2005*). Phosphorylation of p*21* in G *2* / M Promotes Cyclin B-Cdc*2* Kinase Activity. Molecular Biology of the Cell *25*, *3364–3387*.

44. **Denko, N. C., Giaccia, A. J., Stringer, J. R., and Stambrook, P. J.** (*1994*). The human Ha-ras oncogene induces genomic instability in murine fibroblasts within one cell cycle. Proceedings of the National Academy of Sciences of the United States of America *91*, *5124–5128*.

45. **Deschamps, J., Meijlink, F., and Verma, I. M.** (*1985*). Identification of a transcriptional enhancer element upstream from the proto-oncogene fos. Science *230*, *1174–1177*.

46. **Descot, A., Hoffmann, R., Shaposhnikov, D., Reschke, M., Ullrich, A., and Posern, G.** (*2009*). Negative regulation of the EGFR-MAPK cascade by actin-MAL-mediated Mig*6*/Errfi-*1* induction. Molecular Cell *35*, *291–304*.

47. **Drewett, V., Devitt, a, Saxton, J., Portman, N., Greaney, P., Cheong, N. E., Alnemri, T. F., Alnemri, E., and Shaw, P. E.** (*2001*). Serum response factor cleavage by caspases *3* and *7* linked to apoptosis in human BJAB cells. The Journal of Biological Chemistry *276*, *33444–33451*.

48. **Du, K. L., Ip, H. S., Li, J., Chen, M., Dandre, F., Yu, W., Lu, M. M., Owens, G. K., and Parmacek, M. S.** (*2003*). Myocardin Is a Critical Serum Response Factor Cofactor in the Transcriptional Program Regulating Smooth Muscle Cell Differentiation. Molecular and Cellular Biology *23*, *2425–2437*.

49. **Ducret, C., Maira, S., Dierich, A., and Wasylyk, B.** (*1999*). The Net Repressor Is Regulated by Nuclear Export in Response to Anisomycin , UV , and Heat Shock. Molecular and Cellular Biology *19*, *7076–7087*.

50. **Ducret, C., Maira, S.-M., Lutz, Y., and Wasylyk, B.** (*2000*). The ternary complex factor Net contains two distinct elements that mediate different responses to MAP kinase signalling cascades. Oncogene *19*, *5063–5072*.

51. **Elgendy, M., Sheridan, C., Brumatti, G., and Martin, S. J.** (*2011*). Oncogenic Ras-induced expression of Noxa and Beclin-*1* promotes autophagic cell death and limits clonogenic survival. Molecular Cell *42*, *23–35*.

52. **Fadok, V. a, Voelker, D. R., Campbell, P. a, Cohen, J. J., Bratton, D. L., and Henson, P. M.** (*1992*). Exposure of phosphatidylserine on the surface of apoptotic lymphocytes triggers specific recognition and removal by macrophages. Journal of Immunology (Baltimore, Md. : *1950*) *148*, *2207–2216*.

53. **Fei, P., Bernhard, E. J., and El-deiry, W. S.** (*2002*). Tissue-specific Induction of p*53* Targets in Vivo Tissue-specific Induction of p*53* Targets in Vivo *1*. Cancer Research *62*, *7316–7327*.

54. **Fenech, M., Kirsch-Volders, M., Natarajan, a T., Surralles, J., Crott, J. W., Parry, J., Norppa, H., Eastmond, D. a, Tucker, J. D., and Thomas, P.** (*2011*). Molecular mechanisms of micronucleus, nucleoplasmic bridge and nuclear bud formation in mammalian and human cells. Mutagenesis *26*, *125–132*.

55. **Franke, W. W., Borrmann, C. M., Grund, C., and Pieperhoff, S.** (*2006*). The area composita of adhering junctions connecting heart muscle cells of vertebrates. I. Molecular definition in intercalated disks of cardiomyocytes by immunoelectron microscopy of desmosomal proteins. European Journal of Cell Biology *85*, *69–82*.

56. **Geneste, O., Copeland, J. W., and Treisman, R.** (*2002*). LIM kinase and Diaphanous cooperate to regulate serum response factor and actin dynamics. The Journal of Cell Biology *157*, *831–838*.

57. **Gille, H., Kortenjann, M., Strahl, T., and Shaw, P. E.** (*1996*). Phosphorylation-dependent formation of a quaternary complex at the c-fos SRE. Molecular and Cellular Biology *16*, *1094–1102*.

58. **Gille, H., Sharrocks, A. D., and Shaw, P. E.** (*1992*). Phosphorylation of transcription factor p*62*TCF by MAP kinase stimulates ternary complex formation at c-fos promoter. Nature *358*, *414–417*.

59. **Gineitis, D., and Treisman, R.** (*2001*). Differential usage of signal transduction pathways defines two types of serum response factor target gene. The Journal of Biological Chemistry *276*, *24531–24539*.

60. **Giovane, A., Pintzas, A., Maira, S.-M., Sobieszczuk, P., and Wasylyk, B.** (*1994*). Net, a new ets transcription factor that is activated by Ras. Genes & Development *8*, *1502–1513*.

61. **Goley, E. D., and Welch, M. D.** (*2006*). The ARP*2/3* complex: an actin nucleator comes of age. Nature Reviews. Molecular Cell Biology *7*, *713–726*.

62. **Goode, B. L., and Eck, M. J.** (*2007*). Mechanism and function of formins in the control of actin assembly. Annual Review of Biochemistry *76*, *593–627*.

63. **Greenberg, M. E., and Ziff, E. B.** (*1984*). Stimulation of *3*T*3* cells induces tarnscription of the c-fos proto-oncogene. Nature *311*, *433–438*.

64. **Gross, C., Buchwalter, G., Dubois-Pot, H., Cler, E., Zheng, H., and Wasylyk, B.** (*2007*). The ternary complex factor net is downregulated by hypoxia and regulates hypoxia-responsive genes. Molecular and Cellular Biology *27*, *4133–4141*.

65. **Gross, C., Dubois-Pot, H., and Wasylyk, B.** (*2008*). The ternary complex factor Net/Elk-*3* participates in the transcriptional response to hypoxia and regulates HIF-*1* alpha. Oncogene *27*, *1333–1341*.

66. **Grossmann, K. S., Grund, C., Huelsken, J., Behrend, M., Erdmann, B., Franke, W. W., and Birchmeier, W.** (*2004*). Requirement of plakophilin *2* for heart morphogenesis and cardiac junction formation. The Journal of Cell Biology *167*, *149–160*.

67. **Grueneberg, D. A., Natesan, S., Alexandre, C., and Gilman, M. Z.** (*1992*). Human and Drosophila Homeodomain Proteins That Enhance the DNA-Binding Activity of Serum Response Factor. Science *257*.

68. **Guettler, S., Vartiainen, M. K., Miralles, F., Larijani, B., and Treisman, R.** (*2008*). RPEL motifs link the serum response factor cofactor MAL but not myocardin to Rho signaling via actin binding. Molecular and Cellular Biology *28*, *732–742*.

69. **Hagag, N., Diamond, L., Palermo, R., and Lyubsky, S.** (*1990*). High expression of ras p*21* correlates with increased rate of abnormal mitosis in NIH*3*T*3* cells. Oncogene *5*, *1481–1489*.

70. **Han, Z., Li, X., Wu, J., and Olson, E. N.** (*2004*). A myocardin-related transcription factor regulates activity of serum response factor in Drosophila. Proceedings of the National Academy of Sciences of the United States of America *101*, *12567–12572*.

71. **Hassler, M., and Richmond, T. J.** (*2001*). The B-box dominates SAP-*1* - SRF interactions in the structure of the ternary complex. The EMBO Journal *20*, *3018–3028*.

72. **Hautmann, M. B., Thompson, M. M., Swartz, E. A., Olson, E. N., and Owens, G. K.** (*1997*). Angiotensin II–Induced Stimulation of Smooth Muscle α-Actin Expression by Serum Response Factor and the Homeodomain Transcription Factor MHox. Circulation Research *81* , *600–610*.

73. **He, A., Kong, S. W., Ma, Q., and Pu, W. T.** (*2011*). Co-occupancy by multiple cardiac transcription factors identifies transcriptional enhancers active in heart. Proceedings of the National Academy of Sciences of the United States of America, *2–7*.

74. **Hellemans, J., Mortier, G., De Paepe, A., Speleman, F., and Vandesompele, J.** (*2007*). qBase relative quantification framework and software for management and automated analysis of real-time quantitative PCR data. Genome Biology *8*, R*19*.

75. **Herschman, H. R.** (*1991*). Primary response genes induced by growth factors and tumor promoters. Annual Review of Biochemistry *60*, *281–319*.

76. **Hershko, T., and Ginsberg, D.** (*2004*). Up-regulation of Bcl-*2* homology *3* (BH*3*)-only proteins by E*2*F*1* mediates apoptosis. The Journal of Biological Chemistry *279*, *8627–8634*.

77. **Hill, C. S., and Treisman, R.** (*1995*). Differential activation of c-fos promoter elements by serum, lysophosphatidic acid, G proteins and polypeptide growth factors. The EMBO Journal *14*, *5037–5047*.

78. **Hill, C. S., Wynne, J., and Treisman, R.** (*1994*). Serum-regulated transcription by serum response factor (SRF): a novel role for the DNA binding domain. The EMBO Journal *13*, *5421–5432*.

79. **Hill, C. S., Wynne, J., and Treisman, R.** (*1995*). The Rho family GTPases RhoA, Rac*1*, and CDC*42*Hs regulate transcriptional activation by SRF. Cell *81*, *1159–1170*.

80. **Hipskind, R. A, Buscher, D., Nordheim, A., and Baccarini, M.** (*1994*). Ras/MAP kinase-dependent and -independent signaling pathways target distinct ternary complex factors. Genes & Development *8*, *1803–1816*.

81. **Hipskind, R. A., Rao, V. N., Meuller, C. G. F., Reddy, E. S. P., and Nordheim, A.** (*1991*). Ets-related protein Elk-*1* is homologous to the c-fos regulatory factor p*62*TCF. Nature *354*, *531–534*.

82. **Hirano, H., and Matsuura, Y.** (*2011*). Sensing actin dynamics: structural basis for G-actin-sensitive nuclear import of MAL. Biochemical and Biophysical Research Communications *414*, *373–378*.

83. **Iwasaki, K., Hayashi, K., Fujioka, T., and Sobue, K.** (*2008*). Rho/Rho-associated kinase signal regulates myogenic differentiation via myocardin-related transcription factor-A/Smad-dependent transcription of the Id*3* gene. The Journal of Biological Chemistry *283*, *21230–21241*.

84. **Iyer, D., Belaguli, N., Flu, M., Rowan, B. G., Wei, L., Weigel, N. L., Booth, F. W., Epstein, H. F., Schwartz, R. J., and Balasubramanyam, A.** (*2003*). Novel Phosphorylation Target in the Serum Response Factor MADS Box Regulates alpha-Actin Transcription. Biochemistry *42*, *7477–7486*.

85. **Iyer, D., Chang, D., Marx, J. G., Wei, L., Olson, E. N., Parmacek, M. S., Balasubramanyam, A., and Schwartz, R. J.** (*2006*). Serum response factor MADS box serine-*162* phosphorylation switches proliferation and myogenic gene programs. Proceedings of the National Academy of Sciences of the United States of America *103*, *4516–4521*.

86. **Janknecht, R., Ernst, W. H., Pingoud, V., and Nordheim, A.** (*1993*). Activation of ternary complex factor Elk-*1* by MAP kinases. The EMBO Journal *12*, *5097–5104*.

87. **Javelaud, D. and Besançon, F.** (*2001*). NF-kB activation results in rapid inactivation of JNK in TNFa-treated Ewing sarcoma cells : a mechanism for the anti-apoptotic effect of NF-kB. Oncogene *20*, *4365–4372*.

88. **Jiang, W., Kahn, S. M., Zhou, P., Zhang, Y., Cacace, A. M., Infante, A. S., Doi, S., Santell, R. M., and Weinstein, I. B.** (*1993*). Overexpression of cyclin D*1* in rat fibroblasts causes abnormalities in growth control, cell cycle progression and gene expression. Oncogene *8*, *3447–3457*.

89. **Johansen, F. E., and Prywes, R.** (*1994*). Two pathways for serum regulation of the c-fos serum response element require specific sequence elements and a minimal domain of serum response factor. Molecular and Cellular Biology *14*, *5920–5928*.

90. **Johansen, F., and Prywes, R.** (*1993*). Identification of transcriptional activation and inhibitory domains in serum response factor (SRF) by Using GAL*4*-SRF Constructs. Molecular and Cellular Biology *13*, *4640–4647*.

91. **Kalita, K., Kharebava, G., Zheng, J.-J., and Hetman, M.** (*2006*). Role of megakaryoblastic acute leukemia-*1* in ERK*1/2*-dependent stimulation of serum response factor-driven transcription by BDNF or increased synaptic activity. The Journal of Neuroscience *26*, *10020–10032*.

92. **Kemp, P. R., and Metcalfe, J. C.** (*2000*). Four isoforms of serum response factor that increase or inhibit smooth- muscle-specific promoter activity. Biochemical Journal *345*, *445–451*.

93. **Kimura, Y., Morita, T., Hayashi, K., Miki, T., and Sobue, K.** (*2010*). Myocardin functions as an effective inducer of growth arrest and differentiation in human uterine leiomyosarcoma cells. Cancer Research *70*, *501–511*.

94. **Knöll, B., Kretz, O., Fiedler, C., Alberti, S., Schütz, G., Frotscher, M., and Nordheim, A.** (*2006*). Serum response factor controls neuronal circuit assembly in the hippocampus. Nature Neuroscience *9*, *195–204*.

95. **Kovar, D. R.** (*2006*). Molecular details of formin-mediated actin assembly. Current Opinion in Cell Biology *18*, *11–17*.

96. **Kuwahara, K., Kinoshita, H., Kuwabara, Y., Nakagawa, Y., Usami, S., Minami, T., Yamada, Y., Fujiwara, M., and Nakao, K.** (*2010*). Myocardin-related transcription factor A is a common mediator of mechanical stress- and neurohumoral stimulation-induced cardiac hypertrophic signaling leading to activation of brain natriuretic peptide gene expression. Molecular and Cellular Biology *30*, *4134–4148*.

97. **Laemmli, U. K.** (*1970*). Cleavage of Structural Proteins during the Assembly of the Head of Bacteriophage T*4*. Nature *227*, *680–685*.

98. **Latasa, M. U., Couton, D., Charvet, C., Lafanechère, A., Guidotti, J.-E., Li, Z., Tuil, D., Daegelen, D., Mitchell, C., and Gilgenkrantz, H.** (*2007*). Delayed liver regeneration in mice lacking liver serum response factor. American Journal of Physiology. Gastrointestinal and Liver Physiology *292*, G*996–*G*1001*.

99. **Lau, L. F., and Nathans, D.** (*1985*). Identification of a set of genes expressed during the GO / G*1* transition of cultured mouse cells. The EMBO Journal *4*, *3145–3151*.

100. **Lau, L. M. S., Nugent, J. K., Zhao, X., and Irwin, M. S.** (*2008*). HDM*2* antagonist Nutlin-*3* disrupts p*73*-HDM*2* binding and enhances p*73* function. Oncogene *27*, *997–1003*.

101. **Lee, H.-J., Yun, C.-H., Lim, S. H., Kim, B.-C., Baik, K. G., Kim, J.-M., Kim, W.-H., and Kim, S.-J.** (*2007*). SRF is a nuclear repressor of Smad*3*-mediated TGF-beta signaling. Oncogene *26*, *173–185*.

102. **Lee, T., Bradley, M. E., and Walowitz, J. L.** (*1998*). Influence of promoter potency on the transcriptional effects of YY*1*, SRF and Msx-*1* in transient transfection analysis. Nucleic Acids Research *26*, *3215–3220*.

103. **Leitner, L., Shaposhnikov, D., Descot, A., Hoffmann, R., and Posern, G.** (*2010*). Epithelial Protein Lost in Neoplasm alpha (Eplin-alpha) is transcriptionally regulated by G-actin and MAL/MRTF coactivators. Molecular Cancer *9*, *60*.

104. **Leitner, L., Shaposhnikov, D., Mengel, A., Descot, A., Julien, S., Hoffmann, R., and Posern, G.** (*2011*). MAL/MRTF-A controls migration of non-invasive cells by upregulation of cytoskeleton-associated proteins. Journal of Cell Science *124*, *4318-31*

105. **Li, J., Zhu, X., Chen, M., Cheng, L., Zhou, D., Lu, M. M., Du, K., Epstein, J. a, and Parmacek, M. S.** (*2005*a). Myocardin-related transcription factor B is required in cardiac neural crest for smooth muscle differentiation and cardiovascular development. Proceedings of the National Academy of Sciences of the United States of America *102*, *8916–8921*.

106. **Li, S., Chang, S., Qi, X., Richardson, J. A., and Olson, E. N.** (*2006*). Requirement of a myocardin-related transcription factor for development of mammary myoepithelial cells. Molecular and Cellular Biology *26*, *5797–5808*.

107. **Li, S., Czubryt, M. P., McAnally, J., Bassel-Duby, R., Richardson, J. A., Wiebel, F. F., Nordheim, A., and Olson, E. N.** (*2005*b). Requirement for serum response factor for skeletal muscle growth and maturation revealed by tissue-specific gene deletion in mice. Proceedings of the National Academy of Sciences of the United States of America *102*, *1082–1087*.

108. **Li, S., Wang, D.-Z., Wang, Z., Richardson, J. A., and Olson, E. N.** (*2003*). The serum response factor coactivator myocardin is required for vascular smooth muscle development. Proceedings of the National Academy of Sciences of the United States of America *100*, *9366–9370*.

109. **Lin, H., McGrath, J., Wang, P., and Lee, T.** (*2007*). Cellular toxicity induced by SRF-mediated transcriptional squelching. Toxicological Sciences : an Official Journal of the Society of Toxicology *96*, *83–91*.

110. **Long, X., Creemers, E. E., Wang, D.-Z., Olson, E. N., and Miano, J. M.** (*2007*). Myocardin is a bifunctional switch for smooth versus skeletal muscle differentiation. Proceedings of the National Academy of Sciences of the United States of America *104*, *16570–16575*.

111. **Ma, Z. et al.** (*2001*). Fusion of two novel genes, RBM*15* and MKL*1*, in the t(*1*;*22*)(p*13*;q*13*) of acute megakaryoblastic leukemia. Nature Genetics *28*, *220–221*.

112. **Mack, C. P., and Owens, G. K.** (*1999*). Regulation of Smooth Muscle -Actin Expression In Vivo Is Dependent on CArG Elements Within the *5'* and First Intron Promoter Regions. Circulation Research *84*, *852–861*.

113. **Mack, C. P., Somlyo, A V, Hautmann, M., Somlyo, A P., and Owens, G. K.** (*2001*). Smooth muscle differentiation marker gene expression is regulated by RhoA-mediated actin polymerization. The Journal of Biological Chemistry *276*, *341–347*.

114. **Madsen, C. S., Regan, C. P., and Owens, G. K.** (*1997*). Interaction of CArG elements and a GC-rich repressor element in transcriptional regulation of the smooth muscle myosin heavy chain gene in vascular smooth muscle cells. The Journal of Biological Chemistry *272*, *29842–29851*.

115. **Maher, M., Cong, F., Kindelberger, D., Nasmyth, K., Dalton, S., Maher, M., Cong, F., Kindelberger, D., Nasmyth, K. I. M., and Dalton, S.** (*1995*). Cell cycle-regulated transcription of the CLB*2* gene is dependent on Mcm*1* and a ternary complex factor. Molecular and Cellular Biology *15*, *3129–3137*.

116. **Maira, S.-M., Wurtz, J.-M., and Wasylyk, B.** (*1996*). Net (ERP/SAP*2*), one of the Ras-inducible TCFs, has a novel inhibitory domain with resemblance to the helix-loop-helix motif. The EMBO Journal *15*, *5849–5865*.

117. **Marchand, J. B., Kaiser, D. a, Pollard, T. D., and Higgs, H. N.** (*2001*). Interaction of WASP/Scar proteins with actin and vertebrate Arp*2/3* complex. Nature Cell Biology *3*, *76–82*.

118. **McMahon, S. B., and Monroe, J. G.** (*1995*). A ternary complex factor-dependent mechanism mediates induction of egr-*1* through selective serum response elements following antigen receptor cross-linking in B lymphocytes. Molecular and Cellular Biology *15*, *1086–1093*.

119. **Medjkane, S., Perez-Sanchez, C., Gaggioli, C., Sahai, E., and Treisman, R.** (*2009*). Myocardin-related transcription factors and SRF are required for cytoskeletal dynamics and experimental metastasis. Nature Cell Biology *11*, *257–268*.

120. **Mercher, T. et al.** (*2001*). Involvement of a human gene related to the Drosophila spen gene in the recurrent t(*1*;*22*) translocation of acute megakaryocytic leukemia. Proceedings of the National Academy of Sciences of the United States of America *98*, *5776–5779*.

121. **Miano, J. M.** (*2003*). Serum response factor: toggling between disparate programs of gene expression. Journal of Molecular and Cellular Cardiology *35*, *577–593*.

122. **Miano, J. M.** (*2010*). Role of serum response factor in the pathogenesis of disease. Laboratory Investigation; a Journal of Technical Methods and Pathology *90*, *1274–1284*.

123. **Miano, J. M., Ramanan, N., Georger, M. a, De Mesy Bentley, K. L., Emerson, R. L., Balza, R. O., Xiao, Q., Weiler, H., Ginty, D. D., and Misra, R. P.** (*2004*). Restricted inactivation of serum response factor to the cardiovascular system. Proceedings of the National Academy of Sciences of the United States of America *101*, *17132–17137*.

124. **Milyavsky, M., Shats I., Cholostoy A., Brosh R., Buganim Y., Weisz L. et al.** (*2007*). Inactivation of myocardin and p*16* during malignant transformation contributes to a differentiation defect. Cancer Cell *11*, *133–146*.

125. **Milyavsky, M., Shats, I., Erez, N., and Tang, X.** (*2003*). Prolonged culture of telomerase-immortalized human fibroblasts leads to a premalignant phenotype. Cancer Research, *7147–7157*.

126. **Minty, A., and Kedes, L.** (*1986*). Upstream regions of the human cardiac actin gene that modulate its transcription in muscle cells: presence of an evolutionarily conserved repeated motif. Molecular and Cellular Biology *6*, *2125–2136*.

127. **Miralles, F., Posern, G., Zaromytidou, A., and Treisman, R.** (*2003*). Actin Dynamics Control SRF Activity by Regulation of Its Coactivator MAL. Cell *113*, *329–342*.

128. **Misra, R. P., Rivera, V. M., Wang, J. M., Fan, P., and Greenberg, M. E.** (*1991*). The Serum Response Factor Is Extensively Modified by Phosphorylation Following Its Synthesis in Serum-Stimulated Fibroblasts. Molecular and Cellular Biology *11*, *4545–4554*.

129. **Mo, Y., Vaessen, B., Johnston, K., and Marmorstein, R.** (*2000*). Structure of the Elk-*1* – DNA complex reveals how DNA- distal residues affect ETS domain recognition of DNA. Nature Structural Biology *7*, *3–8*.

130. **Mokalled, M. H.** (*2009*) Roles of myocardin related transcription factors in muscle and brain. Doctoral dissertation

131. **Mokalled, M. H., Johnson, A., Kim, Y., Oh, J., and Olson, E. N.** (*2010*). Myocardin-related transcription factors regulate the Cdk*5*/Pctaire*1* kinase cascade to control neurite outgrowth, neuronal migration and brain development. Development *137*, *2365–2374*.

132. **Moriarty, M., Ryan, R., Lalor, P., Dockery, P., Byrnes, L., and Grealy, M.** (*2012*). Loss of plakophilin *2* disrupts heart development in zebrafish. The International Journal of Developmental Biology *56*, *711–718*.

133. **Morin, S., Paradis, P., Aries, A., and Nemer, M.** (*2001*). Serum Response Factor-GATA Ternary Complex Required for Nuclear Signaling by a G-Protein-Coupled Receptor. Molecular and Cellular Biology *21*.

134. **Morita, T., Mayanagi, T., and Sobue, K.** (*2007*). Dual roles of myocardin-related transcription factors in epithelial mesenchymal transition via slug induction and actin remodeling. The Journal of Cell Biology *179*, *1027–1042*.

135. **Mouilleron, S., Langer, C. a, Guettler, S., McDonald, N. Q., and Treisman, R.** (*2011*). Structure of a pentavalent G-actin*MRTF-A complex reveals how G-actin controls nucleocytoplasmic shuttling of a transcriptional coactivator. Science Signaling *4*, ra*40*.

136. **Muehlich, S., Wang, R., Lee, S.-M., Lewis, T. C., Dai, C., and Prywes, R.** (*2008*). Serum-induced phosphorylation of the serum response factor coactivator MKL*1* by the extracellular signal-regulated kinase *1/2* pathway inhibits its nuclear localization. Molecular and Cellular Biology *28*, *6302–6313*.

137. **Murai, K., and Treisman, R.** (*2002*). Interaction of Serum Response Factor (SRF) with the Elk-*1* B Box Inhibits RhoA-Actin Signaling to SRF and Potentiates Transcriptional Activation by Elk-*1*. Molecular and Cellular Biology *22*, *7083–7092*.

138. **Musgrove, E. A., Lee, C. S., Buckley, M. F., and Sutherland, R. L.** (*1994*). Cyclin D*1* induction in breast cancer cells shortens G*1* and is sufficient for cells arrested in G*1* to complete the cell cycle. Proceedings of the National Academy of Sciences of the United States of America *91*, *8022–8026*.

139. **Nakade, K., Zheng, H., Ganguli, G., Buchwalter, G., Gross, C., and Wasylyk, B.** (*2004*). The Tumor Suppressor p*53* Inhibits Net , an Effector of Ras/Extracellular Signal-Regulated Kinase Signaling. Molecular and Cellular Biology *24*, *1132–1142*.

140. **Nakagawa, K., and Kuzumaki, N.** (*2005*). Transcriptional activity of megakaryoblastic leukemia *1* (MKL*1*) is repressed by SUMO modification. Genes to Cells *10*, *835–850*.

141. **Nakamura, S., Hayashi, K., Iwasaki, K., Fujioka, T., Egusa, H., Yatani, H., and Sobue, K.** (*2010*). Nuclear import mechanism for myocardin family members and their correlation with vascular smooth muscle cell phenotype. The Journal of Biological Chemistry *285*, *37314–37323*.

142. **Natesan, S., Rivera, V. M., Molinari, E., and Gilman, M.** (*1997*). Transcriptional squelching reexamined. Nature *390*, *349–350*.

143. **Niu, Z., Yu, W., Zhang, S. X., Barron, M., Belaguli, N. S., Schneider, M. D., Parmacek, M., Nordheim, A., and Schwartz, R. J.** (*2005*). Conditional mutagenesis of the murine serum response factor gene blocks cardiogenesis and the transcription of downstream gene targets. The Journal of Biological Chemistry *280*, *32531–32538*.

144. **Norman, C., Runswick, M., Pollock, R., and Treisman, R.** (*1988*). Isolation and properties of cDNA clones encoding SRF, a transcription factor that binds to the c-fos serum response element. Cell *55*, *989–1003*.

145. **Oda, E.** (*2000*). Noxa, a BH*3*-Only Member of the Bcl-*2* Family and Candidate Mediator of p*53*-Induced Apoptosis. Science *288*, *1053–1058*.

146. **Odelberg, S. J., Kollhoff, A., and Keating, M. T.** (*2000*). Dedifferentiation of Mammalian Myotubes Induced by msx*1*. Cell *103*, *1099–1109*.

147. **Oh, J., Richardson, J. A., and Olson, E. N.** (*2005*). Requirement of myocardin-related transcription factor-B for remodeling of branchial arch arteries and smooth muscle differentiation. Proceedings of the National Academy of Sciences of the United States of America *102*, *15122–15127*.

148. **Oh, J., Wang, Z., Wang, D., Lien, C., Xing, W., and Olson, E. N.** (*2004*). Target Gene-Specific Modulation of Myocardin Activity by GATA Transcription Factors. Molecular and Cellular Biology *24*, *8519–8528*.

149. **Ohtsubo, M., and Roberts, J. M.** (*1993*). Cyclin-Dependent Regulation of G*1* in Mammalian Fibroblasts. Science *259*, *1908–1912*.

150. **Olave, I. A, Reck-Peterson, S. L., and Crabtree, G. R.** (*2002*). Nuclear actin and actin-related proteins in chromatin remodeling. Annual Review of Biochemistry *71*, *755–781*.

151. **Olsen, J. V, Blagoev, B., Gnad, F., Macek, B., Kumar, C., Mortensen, P., and Mann, M.** (*2006*). Global, in vivo, and site-specific phosphorylation dynamics in signaling networks. Cell *127*, *635–648*.

152. **Olson, E. N., and Nordheim, A.** (*2010*). Linking actin dynamics and gene transcription to drive cellular motile functions. Nature Reviews. Molecular Cell Biology *11*, *353–365*.

153. **Olson, M. F., Paterson, H. F., and Marshall, C. J.** (*1998*). Signals from Ras and Rho GTPases interact to regulate expression of p*21*Waf*1*/Cip*1*. Nature *394*, *19–23*.

154. **Ong, S.-E., and Mann, M.** (*2006*). A practical recipe for stable isotope labeling by amino acids in cell culture (SILAC). Nature Protocols *1*, *2650–2660*.

155. **Owens, G. K., Kumar, M. S., and Wamhoff, B. R.** (*2004*). Molecular Regulation of Vascular Smooth Muscle Cell Differentiation in Development and Disease. Physiological Reviews *84*, *767–801*.

156. **Palmgren, S., Vartiainen, M., and Lappalainen, P.** (*2002*). Twinfilin, a molecular mailman for actin monomers. Journal of Cell Science *115*, *881–886*.

157. **Parlakian, A., Tuil, D., Hamard, G., Hentzen, D., Concordet, J., Li, Z., and Daegelen, D.** (*2004*). Targeted Inactivation of Serum Response Factor in the Developing Heart Results in Myocardial Defects and Embryonic Lethality. Molecular and Cellular Biology *24*, *5281–5289*.

158. **Pawłowski, R., Rajakylä, E. K., Vartiainen, M. K., and Treisman, R.** (*2010*). An actin-regulated importin α/β-dependent extended bipartite NLS directs nuclear import of MRTF-A. The EMBO Journal *29*, *3448–3458*.

159. **Pellegrini, L., Tan, S., and Richmond, T. J.** (*1995*). Strucure of serum response factor core bound to DNA. Nature *376*, *490–498*.

160. **Phan-Dihn-Tuy, F., Tuil, D., Schweighoffer, F., Pinset, C., Kahn, A., and Minty, A.** (*1988*). The "CC.Ar.GG" box A protein-binding site common to transcription-regulatory regions of the cardiac actin, c-fos and interleukin-*2* receptor genes. European Journal of Biochemistry *515*, *507–515*.

161. **Philippar, U. et al.** (*2004*). The SRF target gene Fhl*2* antagonizes RhoA/MAL-dependent activation of SRF. Molecular Cell *16*, *867–880*.

162. **Poser, S., Impey, S., Trinh, K., Xia, Z., and Storm, D. R.** (*2000*). SRF-dependent gene expression is required for PI*3*-kinase-regulated cell proliferation. The EMBO Journal *19*, *4955–4966*.

163. **Posern, G., Miralles, F., Guettler, S., and Treisman, R.** (*2004*). Mutant actins that stabilise F-actin use distinct mechanisms to activate the SRF coactivator MAL. The EMBO Journal *23*, *3973–3983*.

164. **Posern, G., Sotiropoulos, A., and Treisman, R.** (*2002*). Mutant Actins Demonstrate a Role for Unpolymerized Actin in Control of Transcription by Serum Response Factor. Molecular Biology of the Cell *13*, *4167–4178*.

165. **Prywes, R., and Roeder, R. G.** (*1986*). Inducible binding of a factor to the c-fos enhancer. Cell *47*, *777–784*.

166. **Qiu, P., Ritchie, R. P., Fu, Z., Cao, D., Cumming, J., Miano, J. M., Wang, D.-Z., Li, H. J., and Li, L.** (*2005*). Myocardin enhances Smad*3*-mediated transforming growth factor-beta*1* signaling in a CArG box-independent manner: Smad-binding element is an important cis element for SM*22*alpha transcription in vivo. Circulation Research *97*, *983–991*.

167. **Quinlan, M. E., Heuser, J. E., Kerkhoff, E., and Mullins, R. D.** (*2005*). Drosophila Spire is an actin nucleation factor. Nature *433*, *382–388*.

168. **Ramanan, N., Shen, Y., Sarsfield, S., Lemberger, T., Schütz, G., Linden, D. J., and Ginty, D. D.** (*2005*). SRF mediates activity-induced gene expression and synaptic plasticity but not neuronal viability. Nature Neuroscience *8*, *759–767*.

169. **Rappsilber, J., Ishihama, Y., and Mann, M.** (*2003*). Stop and go extraction tips for matrix-assisted laser desorption/ionization, nanoelectrospray, and LC/MS sample pretreatment in proteomics. Analytical Chemistry *75*, *663–670*.

170. **Resnitzky, D., Gossen, M., and Bujard, H.** (*1994*). Expression of cyclins D*1* and E with an acceleration of the G*1* / S Phase transition byexpression of cyclins D*1* and E with an inducible system. Molecular and Cellular Biology *14*, *1669–1679*.

171. **Riccardi, C., and Nicoletti, I.** (*2006*). Analysis of apoptosis by propidium iodide staining and flow cytometry. Nature Protocols *1*, *1458–1461*.

172. **Rodriguez, J. M., Glozak, M. a, Ma, Y., and Cress, W. D.** (*2006*). Bok, Bcl-*2*-related Ovarian Killer, Is Cell Cycle-regulated and Sensitizes to Stress-induced Apoptosis. The Journal of Biological Chemistry *281*, *22729–22735*.

173. **Saavedra, H., Fukasawa, K., Conn, C. W., and Stambrook, P. J.** (*1999*). MAPK mediates RAS-induced chromosome instability. The Journal of Biological Chemistry *274*, *38083–38090*.

174. **Sahai, E., Alberts, A. S., and Treisman, R.** (*1998*). RhoA effector mutants reveal distinct effector pathways for cytoskeletal reorganization, SRF activation and transformation. The EMBO Journal *17*, *1350–1361*.

175. **Sakaue-Sawano, A. et al.** (*2008*). Visualizing spatiotemporal dynamics of multicellular cell-cycle progression. Cell *132*, *487–498*.

176. **Salinas, S., Briançon-Marjollet, A., Bossis, G., Lopez, M.-A., Piechaczyk, M., Jariel-Encontre, I., Debant, A., and Hipskind, R. a** (*2004*). SUMOylation regulates nucleo-cytoplasmic shuttling of Elk-*1*. The Journal of Cell Biology *165*, *767–773*.

177. **Salvesen, G. S., and Dixit, V. M.** (*1997*). Caspases: intracellular signaling by proteolysis. Cell *91*, *443–446*.

178. **Sambrook, J., and Russel, D.** (*2001*). Molecular Cloning: A laboratory manual, Cold Spring Habor Laboratory Press.

179. **Sasazuki, T. et al.** (*2002*). Identification of a novel transcriptional activator, BSAC, by a functional cloning to inhibit tumor necrosis factor-induced cell death. The Journal of Biological Chemistry *277*, *28853–28860*.

180. **Savill, J., Dransfield, I., Gregory, C., and Haslett, C.** (*2002*). A blast from the past: clearance of apoptotic cells regulates immune responses. Nature Reviews. Immunology *2*, *965–975*.

181. **Schirren, C. G., Scharffetter, K., Hein, R., Braun-Falco, O., and Krieg, T.** (*1990*). Tumor Necrosis Factor alpha Induces Invasiveness of Human Skin Fibroblasts In Vitro. Journal of Investigative Dermatology *94*, *706–710*.

182. **Schratt, G., Philippar, U., Hockemeyer, D., Schwarz, H., Alberti, S., and Nordheim, A.** (*2004*). SRF regulates Bcl-*2* expression and promotes cell survival during murine embryonic development. The EMBO Journal *23*, *1834–1844*.

183. **Schratt, G., Weinhold, B., Lundberg, A. S., Schuck, S., Berger, J., Schwarz, H., Weinberg, R. A., Ruether, U., and Nordheim, A.** (*2001*). Serum Response Factor Is Required for Immediate-Early Gene Activation yet Is Dispensable for Proliferation of Embryonic Stem Cells. Molecular and Cellular Biology *21*, *2933–2943*.

184. **Selvaraj, A., and Prywes, R.** (*2003*). Megakaryoblastic leukemia-*1/2*, a transcriptional co-activator of serum response factor, is required for skeletal myogenic differentiation. The Journal of Biological Chemistry *278*, *41977–41987*.

185. **Sepulveda, J. L., Vlahopoulos, S., Iyer, D., Belaguli, N., and Schwartz, R. J.** (*2002*). Combinatorial expression of GATA*4*, Nkx*2-5*, and serum response factor directs early cardiac gene activity. The Journal of Biological Chemistry *277*, *25775–25782*.

186. **Serchov, T., Dubois-Pot-Schneider, H., Charlot, C., Rösl, F., and Wasylyk, B.** (*2010*). Involvement of net and Hif*1*alpha in distinct yet intricately linked hypoxia-induced signaling pathways. The Journal of Biological Chemistry *285*, *21223–21232*.

187. **Shaposhnikov, D., Descot, A., Schilling, J. and Posern G.** (*2012*). Myocardin-related transcription factor A regulates expression of Bok and Noxa and is involved in apoptotic signaling. Cell Cycle *11*, *141–150*.

188. **Shats, I., Milyavsky, M., Cholostoy, A., Brosh, R., and Rotter, V.** (*2007*). Myocardin in Tumor Suppression and Myofibroblast Differentiation. Cell Cycle *6*, *1141–1146*.

189. **Shaw, P. E., Schröter, H., and Nordheim, A.** (*1989*). The ability of a ternary complex to form over the serum response element correlates with serum inducibility of the human c-fos promoter. Cell *56*, *563–572*.

190. **Shibue, T., Suzuki, S., Okamoto, H., Yoshida, H., Ohba, Y., Takaoka, A., and Taniguchi, T.** (*2006*). Differential contribution of Puma and Noxa in dual regulation of p*53*-mediated apoptotic pathways. The EMBO Journal *25*, *4952–4962*.

191. **Shore, P., and Sharrocks, A. D.** (*1995*). The MADS-box family of transcription factors. European Journal of Biochemistry / FEBS *229*, *1–13*.

192. **Slee, E. A., Zhu, H., Chow, S. C., MacFarlane, M., Nicholson, D. W., and Cohen, G. M.** (*1996*). Benzyloxycarbonyl-Val-Ala-Asp (OMe) fluoromethylketone (Z-VAD. FMK) inhibits apoptosis by blocking the processing of CPP*32*. Biochemical Journal *24*, *21–24*.

193. **Small, E. M., Thatcher, J. E., Sutherland, L. B., Kinoshita, H., Gerard, R. D., Richardson, J. a, Dimaio, J. M., Sadek, H., Kuwahara, K., and Olson, E. N.** (*2010*). Myocardin-Related Transcription Factor-A Controls Myofibroblast Activation and Fibrosis in Response to Myocardial Infarction. Circulation Research, *294–304*.

194. **Small, E. M., Warkman, A. S., Wang, D.-Z., Sutherland, L. B., Olson, E. N., and Krieg, P. a** (*2005*). Myocardin is sufficient and necessary for cardiac gene expression in Xenopus. Development *132*, *987–997*.

195. **Smith, E. C. et al.** (*2012*). MKL*1* and MKL*2* play redundant and crucial roles in megakaryocyte maturation and platelet formation. Blood *120*, *2317–2329*.

196. **Sotiropoulos, a, Gineitis, D., Copeland, J., and Treisman, R.** (*1999*). Signal-regulated activation of serum response factor is mediated by changes in actin dynamics. Cell *98*, *159–169*.

197. **Spencer, J. A., and Misra, R. P.** (*1996*). Expression of the serum response factor gene is regulated by serum response factor binding sites. The Journal of Biological Chemistry *271*, *16535–16543*.

198. **Stern, S., Sinske, D., and Knöll, B.** (*2012*). Serum response factor modulates neuron survival during peripheral axon injury. Journal of Neuroinflammation *9*, *78*.

199. **Strahl, T., Gille, H., and Shaw, P. E.** (*1996*). Selective response of ternary complex factor Sap*1*a to different mitogen-activated protein kinase subgroups. Proceedings of the National Academy of Sciences of the United States of America *93*, *11563–11568*.

200. **Sullivan, A. L., Benner, C., Heinz, S., Huang, W., Xie, L., Miano, J. M., and Glass, C. K.** (*2010*). SRF utilizes distinct promoter and enhancer-based mechanisms to regulate cytoskeletal gene expression in macrophages. Molecular and Cellular Biology *31*, *861–875*.

201. **Sun, K., Battle, M. a, Misra, R. P., and Duncan, S. a** (*2009*a). Hepatocyte expression of serum response factor is essential for liver function, hepatocyte proliferation and survival, and postnatal body growth in mice. Hepatology *49*, *1645–1654*.

202. **Sun, Q., Chen, G., Streb, J. W., Long, X., Yang, Y., Stoeckert, C. J., and Miano, J. M.** (*2006*a). Defining the mammalian CArGome. Genome Research *16*, *197–207*.

203. **Sun, Q., Taurin, S., Sethakorn, N., Long, X., Imamura, M., Wang, D.-Z., Zimmer, W. E., Dulin, N. O., and Miano, J. M.** (*2009*b). Myocardin-dependent Activation of the CArG Box-rich Smooth Muscle gamma-Actin Gene. The Journal of Biological Chemistry *284*, *32582–32590*.

204. **Sun, Y. et al.** (*2006*b). Acute myeloid leukemia-associated Mkl*1* (Mrtf-a) is a key regulator of mammary gland function. Molecular and Cellular Biology *26*, *5809–5826*.

205. **Tada, K. et al.** (*2001*). Critical roles of TRAF*2* and TRAF*5* in tumor necrosis factor-induced NF-kappa B activation and protection from cell death. The Journal of Biological Chemistry *276*, *36530–36534*.

206. **Tait, S. W. G., and Green, D. R.** (*2010*). Mitochondria and cell death: outer membrane permeabilization and beyond. Nature Reviews. Molecular Cell Biology *11*, *621–632*.

207. **Tang, G., Minemoto, Y., Dibling, B., Purcell, N. H., Li, Z., Karin, M., and Lin, A.** (*2001*). Inhibition of JNK activation through NF-kB target genes. Nature *414*, *313–317*.

208. **Tang, R.-H., Zheng, X.-L., Callis, T. E., Stansfield, W. E., He, J., Baldwin, A. S., Wang, D.-Z., and Selzman, C. H.** (*2008*). Myocardin inhibits cellular proliferation by inhibiting NF-kappaB(p*65*)-dependent cell cycle progression. Proceedings of the National Academy of Sciences of the United States of America *105*, *3362–3367*.

209. **Taylor, M., Treisman, R., Garrett, N., and Mohun, T.** (*1989*). Muscle-specific (CArG) and serum-responsive (SRE) promoter elements are functionally interchangeable in Xenopus embryos and mouse fibroblasts. Development *106*, *67–78*.

210. **Thornberry, N. A., and Lazebnik, Y.** (*1998*). Caspases: Enemies Within. Science *281*, *1312–1316*.

211. **Tjian, R., and Maniatis, T.** (*1994*). Transcriptional Activation : A Complex Puzzle with Few Easy Pieces. Cell *77*, *5–8*.

212. **Todaro, G. J., and Green, H.** (*1963*). Quantitative studies of the growth of mouse embryo cells in culture and their development into established lines. The Journal of Cell Biology *17*, *299–313*.

213. **Todorovic, V., Chen, C.-C., Hay, N., and Lau, L. F.** (*2005*). The matrix protein CCN*1* (CYR*61*) induces apoptosis in fibroblasts. The Journal of Cell Biology *171*, *559–568*.

214. **Tominaga, T., Sahai, E., Chardin, P., McCormick, F., Courtneidge, S. a, and Alberts, a S.** (*2000*). Diaphanous-related formins bridge Rho GTPase and Src tyrosine kinase signaling. Molecular Cell *5*, *13–25*.

215. **Treisman, R.** (*1985*). Transient accumulation of c-fos RNA following serum stimulation requires a conserved *5*' element and c-fos *3*' sequences. Cell *42*, *889–902*.

216. **Treisman, R.** (*1986*). Identification of a protein-binding site that mediates transcriptional response of the c-fos gene to serum factors. Cell *46*, *567–574*.

217. **Treisman, R.** (*1996*). Regulation of transcription by MAP kinase cascades. Current Opinion in Cell Biology *8*, *205–215*.

218. **Tsai, E. Y. et al.** (*2000*). A Lipopolysaccharide-Specific Enhancer Complex Involving Ets , Elk-*1* , Sp*1* , and CREB Binding Protein and p*300* Is Recruited to the Tumor Necrosis Factor Alpha Promoter In Vivo. Molecular and Cellular Biology *20*, *6084–6094*.

219. **Valouev, A., Johnson, D. S., Sundquist, A., Medina, C., Anton, E., Batzoglou, S., Myers, R. M., and Sidow, A.** (*2008*). Genome-Wide Analysis of Transcription Factor Binding Sites Based on ChIP-Seq Data. Nature Methods *5*, *829–834*.

220. **Vartiainen, M. K., Guettler, S., Larijani, B., and Treisman, R.** (*2007*). Nuclear actin regulates dynamic subcellular localization and activity of the SRF cofactor MAL. Science *316*, *1749–1752*.

221. **Verdoni, A. M., Ikeda, S., and Ikeda, A.** (*2010*). Serum response factor is essential for the proper development of skin epithelium. Mammalian Genome *21*, *64–76*.

222. **Vermes, I., Haanen, C., Steffens-Nakken, H., and Reutelingsperger, C.** (*1995*). A novel assay for apoptosis. Flow cytometric detection of phosphatidylserine expression on early apoptotic cells using fluorescein labelled Annexin V. Journal of Immunological Methods *184*, *39–51*.

223. **Vickers, E., Kasza, A., and Kurnaz, I.** (*2004*). Ternary complex factor-serum response factor complex-regulated gene activity is required for cellular proliferation and inhibition of apoptotic cell death. Molecular and Cellular Biology *24*, *10340–10351*.

224. **Villunger, A., Michalak, E. M., Coultas, L., Müllauer, F., Böck, G., Ausserlechner, M. J., Adams, J. M., and Strasser, A.** (*2003*). p*53*- and drug-induced apoptotic responses mediated by BH*3*-only proteins puma and noxa. Science *302*, *1036–1038*.

225. **Wang, C., Cao, D., Wang, Q., and Wang, D.-Z.** (*2011*). Synergistic activation of cardiac genes by myocardin and Tbx*5*. PloS One *6*, e*24242*.

226. **Wang, D., Chang, P. S., Wang, Z., Sutherland, L. B., Richardson, J. A., Small, E. M., Krieg, P. a, and Olson, E. N.** (*2001*). Activation of cardiac gene expression by myocardin, a transcriptional cofactor for serum response factor. Cell *105*, *851–862*.

227. **Wang, D.-Z., Li, S., Hockemeyer, D., Sutherland, L. B., Wang, Z., Schratt, G., Richardson, J. A., Nordheim, A., and Olson, E. N.** (*2002*). Potentiation of serum response factor activity by a family of myocardin-related transcription factors. Proceedings of the National Academy of Sciences of the United States of America *99*, *14855–14860*.

228. **Wang, J., Li, A., Wang, Z., Feng, X., Olson, E. N., and Schwartz, R. J.** (*2007*). Myocardin sumoylation transactivates cardiogenic genes in pluripotent *10*T*1/2* fibroblasts. Molecular and Cellular Biology *27*, *622–632*.

229. **Wang, Z., Wang, D., Hockemeyer, D., Mcanally, J., Nordheim, A., and Olson, E. N.** (*2004*). Myocardin and ternary complex factors compete for SRF to control smooth muscle gene expression. Nature *428*, *185–189*.

230. **Wang, Z., Wang, D.-Z., Pipes, G. C., and Olson, E. N.** (*2003*). Myocardin is a master regulator of smooth muscle gene expression. Proceedings of the National Academy of Sciences of the United States of America *100*, *7129–7134*.

231. **Wasylyk, B., Hagman, J., and Gutierrez-Hartmann, A.** (*1998*). Ets transcription factors: nuclear effectors of the Ras-MAP-kinase signaling pathway. Trends in Biochemical Sciences *23*, *213–216*.

232. **Wasylyk, C., Criqui-Filipe, P., and Wasylyk, B.** (*2005*). Sumoylation of the net inhibitory domain (NID) is stimulated by PIAS*1* and has a negative effect on the transcriptional activity of Net. Oncogene *24*, *820–828*.

233. **Wei, K., Che, N., and Chen, F.** (*2007*). Myocardin-related transcription factor B is required for normal mouse vascular development and smooth muscle gene expression. Developmental Dynamics *236*, *416–425*.

234. **Weinhold, B., Schratt, G., Arsenian, S., Berger, J., Kamino, K., Schwarz, H., Rüther, U., and Nordheim, A.** (*2000*). Srf(-/-) ES cells display non-cell-autonomous impairment in mesodermal differentiation. The EMBO Journal *19*, *5835–5844*.

235. **Wimmel, A., Lucibello, F. C., Sewing, A., Adolph, S., and Müller, R.** (*1994*). Inducible acceleration of G*1* progression through tetracycline-regulated expression of human cyclin E. Oncogene *9*, *995–997*.

236. **Wu, W., Shen, X., and Tao, S.** (*2010*). Characteristics of the CArG-SRF binding context in mammalian genomes. Mammalian Genome *21*, *104–113*.

237. **Yakovlev, A. G., Di Giovanni, S., Wang, G., Liu, W., Stoica, B., and Faden, A. I.** (*2004*). BOK and NOXA are essential mediators of p*53*-dependent apoptosis. The Journal of Biological Chemistry *279*, *28367–28374*.

238. **Yan, S. F. et al.** (*1999*). Hypoxia-associated induction of early growth response-*1* gene expression. The Journal of Biological Chemistry *274*, *15030–15040*.

239. **Yang, S.-H., Jaffray, E., Hay, R. T., and Sharrocks, A. D.** (*2003*). Dynamic interplay of the SUMO and ERK pathways in regulating Elk-*1* transcriptional activity. Molecular Cell *12*, *63–74*.

240. **Yoshida, T., Sinha, S., Dandré, F., Wamhoff, B. R., Hoofnagle, M. H., Kremer, B. E., Wang, D.-Z., Olson, E. N., and Owens, G. K.** (*2003*). Myocardin is a key regulator of CArG-dependent transcription of multiple smooth muscle marker genes. Circulation Research *92*, *856–864*.

241. **Zaromytidou, A.-I., Miralles, F., and Treisman, R.** (*2006*). MAL and ternary complex factor use different mechanisms to contact a common surface on the serum response factor DNA-binding domain. Molecular and Cellular Biology *26*, *4134–4148*.

242. **Zhang, S. X., Garcia-Gras, E., Wycuff, D. R., Marriot, S. J., Kadeer, N., Yu, W., Olson, E. N., Garry, D. J., Parmacek, M. S., and Schwartz, R. J.** (*2005*). Identification of direct serum-response factor gene targets during Me*2*SO-induced P*19* cardiac cell differentiation. The Journal of Biological Chemistry *280*, *19115–19126*.

243. **Zhang, X., Pickin, K. a, Bose, R., Jura, N., Cole, P. a, and Kuriyan, J.** (*2007*). Inhibition of the EGF receptor by binding of MIG*6* to an activating kinase domain interface. Nature *450*, *741–744*.

244. **Zheng, H., Wasylyk, C., Ayadi, A., Abecassis, J., Schalken, J. a, Rogatsch, H., Wernert, N., Maira, S.-M., Multon, M.-C., and Wasylyk, B.** (*2003*). The transcription factor Net regulates the angiogenic switch. Genes & Development *17*, *2283–2297*.

245. **Zhou, J., Hu, G., and Herring, B. P.** (*2005*). Smooth Muscle-Specific Genes Are Differentially Sensitive to Inhibition by Elk-*1*. Molecular and Cellular Biology *25*, *9874–9885*.

VII. ABBREVIATION LIST

Acta2 – actin alpha 2, smooth muscle, aorta
AMKL – acute megacaryoblastic leukemia
ANF – atrial natriuretic factor
APS – ammonium persulfate
Arp2/3 complex – actin-related protein-2/3 complex
Bok – BCL2-related ovarian killer
bp – base pair
BSA – bovine serum albumin
CarG box – consensus SRF-binding site (CC(A/T)6GG)
CarG-like element – non- consensus SRF-binding site
cDNA – complementary DNA
ChIP – chromatin immunoprecipitation
CHX – cycloheximide
CMV – cytomegalovirus
Co-IP – co-immunoprecipitation
CSF-1 – colony stimulating factor 1
DIC – differential interference contrast
DMEM – Dulbecco's modified Eagle medium
DMSO – dimethylsulfoxide
DNA – deoxyribonucleic acid
E – embryonic day
EBS – Ets-binding site
eGFP – enhanced green fluorescent protein
EGFR – epidermal growth factor receptor
Egr-1 – early growth response 1 gene
Elk-1 – Ets-like transcription factor 1
ERK – extracellular signal-regulated kinase
FACS – fluorescence activated cell sorting
FBS – fetal bovine serum
FGF – fibroblast growth factor
FUCCI – fluorescent ubiquitination-based cell cycle indicator
G0, G1, S, G2, M – phases of cell cycle
GAPDH - Glyceraldehyde 3-phosphate dehydrogenase
GFP – green fluorescent protein
GPRC – G-protein coupled receptor
HeLa – cervical cancer cell line taken from Henrietta Lacks
HPRT – hypoxanthine phosphoribosyltransferase
HRP– horseradish peroxidase
IEG – immediate early gene(s)
Jasp – jasplakinolide
Kb – kilobase
kDa – kilodalton
KO – knock-out
LIMK – LIM-kinase
LPA – Lysophosphatidic acid
mAG – monomeric Azami Green protein
MAPK – mitogen-activated protein kinase
MDCK – Madin-Darby Canine Kidney cell line
mDia – murine Diaphanous
MEF – mouse embryonic fibroblast
MEf2 – myocyte enhancing factor 2
mKO2 – monomeric Kusabira Orange 2 protein
MPI – Max-Planck Institute
MRTF(s) – myocardin-related trasnscription factor(s)
MYOCD – myocardin
NF-κB – nuclear factor kappa B
NLS – nuclear localization signal
P – postnatal day
PAGE – polyacrylamide gel electrophoresis
Pai-1 – plasminogen activator inhibitor 1
PBS – phosphate buffered saline
PCR – polymerase chain reaction
PDGF – platelet-derived growth factor
PVDF – polyvinylidene fluoride
Rb – retinoblastoma protein
RFP – red fluorescent protein
RFP – red fluorescent protein
RIPA – radioimmunoprecipitation assay buffer
RNA – ribonucleic acid
ROCK – Rho-associated protein kinase
RPEL – actin-binding protein domain with consensus sequence RPxxxEL
SAP – SAF-A/B Acinus PIAS DNA-binding domain
SCAI – suppressor of cancer cell invasion
SDS –sodium dodecyl sulfate
SEM – standard error of the mean
shRNA – small hairpin RNA
SILAC – stable isotope labeling by amino acids in cell culture
siRNA – small interfering RNA
SM – smooth muscle
SM-MHC – smooth muscle myosin heavy chain
SRE – serum response element
SRF – serum response factor
SUMO – small ubiquitin-related modifier
TCF(s) – ternary complex factor(s)
TGF-β – tumor growth factor β
TNF-α– Tumour necrosis factor α
TPA – phorbol ester 12-O-tetradecanoyl-13-acetate
Traf – TNF-receptor-associated factor
UTR – untranslated region
WB – western blot
wt – wild type

VIII. LIST OF PUBLICATIONS

Parts of this dissertation were published in the following peer-reviewed works:

Descot A, Hoffmann R, Shaposhnikov D, Reschke M, Ullrich A, Posern G. 2009. Negative regulation of the EGFR-MAPK cascade by actin-MAL-mediated Mig6/Errfi-1 induction. *Molecular cell* **35**:291–304.

Leitner L, Shaposhnikov D, Descot A, Hoffmann R, Posern G. 2010. Epithelial Protein Lost in Neoplasm alpha (Eplin-alpha) is transcriptionally regulated by G-actin and MAL/MRTF coactivators. *Molecular cancer* **9**:60.

Leitner L, Shaposhnikov D, Mengel A, Descot A, Julien S, Hoffmann R, Posern G. 2011. MAL/MRTF-A controls migration of non-invasive cells by upregulation of cytoskeleton-associated proteins. *Journal of cell science* **124**: 4318-31.

Shaposhnikov D, Descot A, Schilling J, Posern G. 2012. Myocardin-related transcription factor A regulates expression of Bok and Noxa and is involved in apoptotic signaling. *Cell Cycle* **11**:141–150.

Shaposhnikov D, Kuffer C, Storchova Z, Posern G. 2013. Myocardin-related transcription factors are required for the coordinated cell cycle progression (submitted to *Cell Cycle*).

IX. ACKNOWLEDGEMENTS

First, I would like to thank Prof. Dr. Guido Posern for giving me the opportunity to work on this interesting project, for his scientific input, helpful discussions, support and general mentoring throughout my time in his laboratory.

I thank Prof. Dr. Elmar Wahle from the University of Halle who very kindly accepted to be my official supervisor at the University.

The former members of the Posern lab Arnaud Descot, Laura Leitner and Stephan Busche I would like to thank for all the collaborations we undertook and for making the atmosphere in the lab relaxed, but at the same time productive.

I would like to express my gratitude to the members of my advisory committee, Prof. Dr. Peter Becker, Dr. Marc Schmidt-Supprian, Prof. Dr. Gunter Meister and Dr. Zuzana Storchova for their advice and support during my studies.

I thank the members of the M.Mann department of MPI of Biochemistry – Marco Hein-Yannic and Christian Eberl – for the excellent collaboration project and their professional attitude.

Members of Z. Storchova lab, Christian Kuffer and Anastasia Kuznetsova, I would like to thank for helpful discussions and for sharing with me their expertise in live cell imaging.

I would like to thank my practical students Lissa Pincz and Peter Sinner. It was a real pleasure to work with you. Alexander Mengel I would like to thank not only for being an integral part of our lab during his master thesis, but also for excellent badminton matches after work!

Current members of the Posern lab Patricia Eisenach, Julia Weissbach, Franziska Schikora, Falk Pohl, Ulrich Blache, Astrid Vess, Anja Weber, Victoria Schröder I thank for being awesome labmates! Robert Torka and Simone Gusenbauer I thank for making our office at MPI probably the coolest one in the whole institute!

For facilitating my scientific and non-scientific experiences in Munich and Halle, I would like to thank all members, past and present of the Ullrich department of MPI, Daniel Wilson lab and their friends from Gene Center of LMU, and the members of Institut für Physiologische Chemie in Halle.

Last, but not least, I am grateful to my family and Maria Wagner for their continuous support, encouragement and being there for me at all times.

This work was financially supported by the Deutsche Forschungsgemeinschaft (DFG).

Eidesstattliche Erklärung

Hiermit erkläre ich an Eides statt, dass die vorliegende Arbeit selbstständig und nur unter Benutzung der angegebenen Quellen und Hilfsmittel erstellt wurde. Die Stellen, die anderen Werken wörtlich oder sinngemäß entnommen sind, sind als solche kenntlich gemacht. Ich versichere weiterhin, dass die Arbeit in gleicher oder änlicher Form noch keiner anderen Prüfungsbehörde vorgelegen wurde.

Halle (Saale), den 21.04.2013 Dmitry Shaposhnikov

Lebenslauf

Name/Vorname:	**Shaposhnikov Dmitry**
Adresse:	Carl-von-Ossietzky-Straße 16, 06114 Halle (Saale)
Geburtsdatum/Ort:	03 März 1984 in Kaliningrad, UdSSR
Staatsangehörigkeit:	Russische Föderation
Familienstand:	ledig
Email:	dmitry.shaposhnikov@medizin.uni-halle.de

Akademische Ausbildung. Forschungstätigkeit

10.2008 - heute

Doktorand am Max-Planck Institut für Biochemie (Martinsried). Seit 05.2012 - an der Martin-Luther-Universität Halle-Wittenberg, Institut für Physiologische Chemie. **Thema:** The role of myocardin-related transcription factors in proliferation and cell cycle regulation of fibroblast cells".

01.2007 - 05.2008

Gaststudent/Gastwissenschaftler (Aufbaustudium) am Imperial College London, Ovarian Cancer Forschungszentrum. **Thema:** "Molecular mechanisms of action behind a new tumour suppressor gene OPCML"

10.2005 - 01.2007

Doktorand am Forschungsinstitut für Mikrobiologie und Epidemiologie, Minsk, Weißrussland. **Thema:** "Construction and immunological analysis of bacterial ghosts carrying exposed hantaviral nucleocapsid proteins".

05.2005 - 10.2005

Wissenschaftlicher Mitarbeiter am Forschungsinstitut für Mikrobiologie und Epidemiologie, Minsk, Weißrussland.

24.06.2005

Abschluss Diplom in Biologie und Biotechnologie an der Weißrussische Staatlichen Universität, Minsk, Weißrussland (Note: 1.0). Titel der Diplomarbeit: "Immunological analysis of a recombinant peptide composed of repetitive sequences of antigenic determinants of Puumala virus".

09.2000 - 06.2005

Studium an der Weißrussische Staatlichen Universität, Minsk, Weißrussland. Fächer: Biologie, Biotechnologie, Biochemie.

Ausbildung

09.1998 - 06.2000

Abitur am Lyzeum der Weißrussische Staatliche Universität. Leistungkurse: Biologie, Chemie